©Copyright 2012
Shannon Marie Dennis

C. elegans Germline Defense Against Retrotransposons

Shannon Marie Dennis

A dissertation

submitted in partial fulfillment of the

requirements for the degree of

Doctor of Philosophy

University of Washington

2012

Reading Committee:

James R. Priess, Chair

Harmit S. Malik

James H. Thomas

Program Authorized to Offer Degree:

Molecular and Cellular Biology

University of Washington

Abstract

C. elegans Germline Defense Against Retrotransposons

Shannon Marie Dennis

Chair of the Supervisory Committee:
Affiliate Professor James R. Priess
Department of Biology

Nematodes appear to have efficient defenses against the germline activity of retroviruses and retrotransposons, as evidenced by the small number of sequences in their genome derived from such elements. No viruses that infect the *C. elegans* germline have been discovered, nor has the presence of virus-like particles (VLPs) been previously reported in germ cells. Retroelements that infect non-dividing cells must access the nucleus via nuclear pores, and in nematode germ cells the majority of nuclear pores are clustered under ribonucleoprotein particles called P granules. In order to determine how retroelements confront or circumvent P granules, we first searched for strains with germline VLPs. We surveyed 16 wild strains of *C. elegans* and 4 additional *Caenorhabditis* species using electron microscopy. We discovered VLPs in the germlines of *C. japonica* and a few *C. elegans* strains, including the lab wild-type strain N2. Using RNA interference to knock-down candidate retrotransposons, we determined that the *C. elegans* VLPs are the product

of Cer1, a Ty3/Gypsy class LTR retrotransposon. Expression of Cer1 is both temperature- and age-dependent. In conditions where Cer1 is abundantly expressed it contributes to programmed cell deaths that occur normally during germline development. The distribution of germline VLPs differed between *C. japonica* and *C. elegans,* suggesting different strategies for accumulation near the nucleus, were they might encounter free nuclear pores. In *C. japonica,* we found VLPs in clusters near P granules, indicating they may aggregate near P granules to gain nuclear proximity. In *C. elegans,* in contrast, the VLPs only accumulated near the nuclear envelope (NE) in post-pachytene germ cells, where P granule-free nuclear pores are being added to the NE. Additionally, *C. elegans* VLPs show a strong association with microtubules (MTs), and wild-type localization of VLPs is dynein-dependent. We propose that the *C. elegans* VLPs bind to MTs in order to resist cytoplasmic flow and probe for free nuclear pores. The studies described here provide a foundation for using the model *C. elegans* to study host-pathogen interactions between retroelements and germ cells.

TABLE OF CONTENTS

LIST OF FIGURES

LIST OF TABLES

Acknowledgements

I would like to thank my advisor, Jim Priess, for giving me the opportunity to carry out this research project in his laboratory and for his mentorship during my graduate education. I also thank all of the other members of the Priess lab for their input into this project during lab meetings and discussions, and for their friendship over the years. I thank the administrators of my graduate program, and especially Michele Karantsavelos, for all of their hard work supporting graduate students. I thank my funding sources, including the MCB program, an NIH developmental biology pre-doctoral training grant, and HHMI. I would like to give special thanks for my ARCS fellowship, which was supported by the Washington Research Foundation. My final professional thanks go to those who served on my thesis committee for all of their input into this project and mentorship.

On a personal note, I thank my parents and extended family for their encouragement, without which I could not have made it to this point. My husband Lucas has been by my side weathering the ups and downs of my graduate education for the last six years, and I can't thank him enough for keeping me from quitting. My best friend, Jill, needs to be thanked for her constant encouragement and for always believing in me so much that it makes me believe in myself. Thank you.

Dedication

To my daughter, Caileigh

Chapter 1: General Introduction

Viruses, DNA transposons, and retrotransposons pose a threat to genome integrity when they integrate into a host's genome. If these integration events occur in the germline, they can be passed on to subsequent generations. Organisms have therefore evolved genomic defense mechanisms to restrict the activity of viruses and mobile genetic elements, and in many cases there are specific defense mechanisms active in the germline. In this chapter I will first review these defense mechanisms in different organisms, with a particular focus on the small RNA silencing mechanisms. In the second section I will review what is known about the potential role of germline ribonucleoprotein granules in transposon and virus restriction. In the final section I will focus on programmed cell death, and review its role in immune defense as well as its other roles in the germline.

Section I: Genomic Defense By Small RNA Pathways

C. Elegans As A Model For Silencing

Germ cells must rigorously protect their genome to minimize the effect of transposable elements and viruses on the genomes of subsequent generations. The *C. elegans* genome contains several DNA transposons, such as Tc1 and Tc3, whose active germline transposition has been observed in laboratory studies. There are also intact LTR (long terminal repeat) and non-LTR retrotransposons and

retroviruses. The LTR retroelements can be grouped into 19 families called Cer1 through Cer19 (for *C. elegans* retrotransposons)[1]. In general, LTR retrotransposons/retroviruses are similar to well-characterized vertebrate retroviruses as they contain a *gag* gene encoding the structural components to make capsids, and a *pol* gene encoding reverse transcriptase (RT) and integrase (INT) proteins. The sequence homology, presence, and order of the various genes allow LTR retroelements in animals to be grouped into four basic clades, one of which is related to vertebrate retroviruses. Elements in the other three clades, Ty1/Copia, Ty3/Gypsy, and Bel, can either encode envelopes (retroviruses) or lack envelopes (retrotransposons)[2]. Of the 19 Cer families in *C. elegans*, Cer1-Cer6 are members of the Ty3/Gypsy clade, and Cer7 through Cer19 are members of the Bel clade[1]. Although there are several families of retroelements in *C. elegans*, there is usually only one intact member per family. Indeed, less than 1% of *C. elegans* N2 (standard laboratory strain) genome is made of retroelements compared to roughly 40% of the human genome. This fact, in combination with the failure to identify retrotransposition events in the laboratory despite the presence of intact full-length retroelements in the genome, suggests that *C. elegans* has a robust defense against retrotransposons in the germline, though the basis for this restriction is unknown[3].

Small RNA Silencing Pathways

Small RNA pathways involving Argonaute proteins in *C. elegans, Drosophila*, zebrafish, and mice have been implicated in silencing retrotransposons and

viruses[4-9]. In the past few years a complex interaction between viruses and microRNAs (miRNAs) is also emerging, with specific miRNAs restricting or facilitating viral replication and also many viruses being shown to encode their own miRNAs that can control both the virus itself and host mRNAs[10,11] One example of miRNA control of viruses in mammals is attenuation of HIV-1 replication by miR-17 and miR-20, which occurs through their repression of a host cofactor (PCAF) used by the virus to transactivate integrated HIV[12]. MicroRNAs have also been shown to increase the activity of viruses. For example, a human liver-specific miRNA, miR-122, increases replication of Hepatitis C Virus (HCV)[13]. Restriction of several viruses in invertebrates occurs via RNA interference (RNAi), and some viruses encode RNAi inhibitors such as the B2 protein encoded by the insect virus Flock-House Virus. Mutant viruses lacking B2 are sensitive to RNAi, and viral replication is then restored if the RNAi machinery is knocked out[14].

Argonaute proteins in most organisms fall into two sub-groups; The Ago group of Argonaute proteins is involved in RNAi and microRNA (miRNA) pathways, while the Piwi group binds piRNAs (piwi-interacting RNAs). *C. elegans* has both groups of Argonaute proteins, and in addition has a worm-specific Argonaute group (WAGO group)(Figure 1)[15]. Argonaute proteins bind various classes of small RNAs, including small interfering RNAs (siRNAs), miRNAs, and piRNAs. Mature miRNAs and siRNAs interact with Argonaute proteins of the Ago subgroup to form a ribonucleoprotein complex called RISC (RNA-induced Silencing Complex) that functions in post-transcriptional gene silencing. A seed sequence of approximately 5

nucleotides in the 5' end of the small RNA is the most important for target RNA recognition. Perfect complementarity of the seed sequence in a siRNA to an mRNA leads to mRNA degradation, and is the basis for RNAi. Imperfect base-pairing of an miRNA creates a "bulge" with the target that results in translational inhibition and can also cause mRNA destabilization[16].

The RNAi and microRNA (miRNA) pathways both depend upon the activity of the RNAse III enzyme Dicer for small RNA biogenesis. miRNAs start as pri-miRNA transcripts, sometimes containing several miRNAs. These are processed first in the nucleus by the RNAse III enzyme Drosha into ~70mer pre-miRNA hairpins; these are exported via Exportin-5 into the cytoplasm, where they are further cleaved by the RNAse III endonuclease Dicer to make mature ~22mer miRNAs. siRNAs are generated by Dicer-mediated cleavage of longer dsRNAs into 20-25mers. In flies there are two Dicers, each specific to either miRNA or siRNA processing, but in worms and mammals there is only one Dicer. In contrast to miRNAs and siRNAs, piRNAs are generated independent of Dicer. The majority of known piRNAs in Drosophila come from large genomic loci comprised primarily of repetitive elements; the clusters are transcribed as one long transcript, and then processed into piRNAs. The *C. elegans* equivalent of piRNAs are a group of RNAs that are slightly shorter, 21 bases, and are thus called 21-U RNAs. Like piRNAs, the 21-U RNAs have a modified 3' end and are generated independent of the Dicer RNAse III endonuclease. 21-U RNAs originate from a broad group of clustered, but non-

contiguous, genes in *C. elegans*, and each 21-U RNA appears to be transcribed independently in response to a conserved upstream regulatory motif [17,18].

Germline-Specific Silencing of Transposons by piRNA Pathway

Germline-specific silencing of transposable elements (TEs) has been characterized in many animals including nematodes, flies, mammals, and fish. Studies of differences in DNA transposon motility among natural isolates of *C. elegans* determined that all strains have active somatic transposition but some strains, including the common lab strain N2, silence transposons specifically in the germline[19,20]. Screens identified a collection of genes named "mutator" genes; Disrupting these genes increased transposon mobility and thus the frequency of transposon-induced mutations[21]. After the discovery of RNA interference (RNAi), additional screens were done for factors required for RNAi in the soma, germline, or both tissues. The genes identified included many of these same mutator genes [22,23]. Some of these genes were found to be required specifically for RNAi in either the soma or germline. For example, *C. elegans* has multiple RNA-dependent RNA polymerases (RdRPs) that amplify the RNAi signal and are required for effective silencing in the worm[24]. One of these RdRPs, *rrf-1*, is specifically required for somatic silencing, while another, *ego-1*, is required for germline RNAi[25].

PIWI Argonautes and piRNAs in *Drosophila* have the best-studied role in repressing germline expression of retroelements. Retroelements that integrate into

a piRNA locus are transcribed and processed into piRNAs. For example, the *flamenco* locus contains remnants of the *gypsy, ZAM,* and *Idifex* retroelements. piRNAs generated from retroelements in the piRNA loci are complementary to other copies of the same retroelements elsewhere in the genome. There are three Piwi-clade Argonautes in *Drosophila*: Piwi, Ago3, and Aubergine (Aub)[7]. Aub and Ago3 are found exclusively in the germline while Piwi is also found in the follicle cells that surround the germ cells[26-28]. Once a transposon jumps into a piRNA cluster, piRNAs targeting all genomic copies of that transposon are made and amplified via a ping-pong mechanism involving all three piwi homologs. In this way the genome maintains a memory of active transposons and uses this memory to silence them. Additionally, piRNAs and Piwi proteins are loaded into oocytes to silence transposons in the early embryo.

In mouse spermatocytes, piRNAs and Piwi proteins play a similar role in the silencing of ERVs and TEs. Loss of either Mili or Miwi2, which are two of the Piwi homologs in mice, causes increased activity of *Line-1* and *IAP* retrotransposons and results in male sterility due to ensuing problems in spermatogenesis. While some of the mechanistic details of the process differ between flies and mammals, there are many similarities, including the use of a feed-forward ping-pong mechanism to amplify the silencing effect against active retrotransposons[29,30].

The *C. elegans* orthologs of PIWI are PRG-1 and PRG-2, and these proteins bind 21-U RNAs. The DNA transposon Tc3 has been identified as a 21-U RNA target and its transposition increases 100-fold in *prg-1, prg-2* double mutants. However, none of the intact *C. elegans* retroelements are located in the broad groups of 21-U

RNA genes, and sequenced 21-U RNAs do not correspond to the retroelements[17,18]. Thus, a piRNA/PIWI pathway appears to restrict DNA transposons in *C. elegans*, but not retroelements.

Virus Restriction in *C. elegans* by Small RNA Pathways and PCD

The first natural viruses known to infect *Caenorhabdhitis* species were recently identified in a wild isolates of *C. elegans* and *C. briggsae*[31]. The identified viruses, Orsay and Santeuil, are novel nodaviruses that showed species-specific infection. The laboratory wild-type strain, N2, effectively restricted replication of the Orsay virus unless the RNAi pathway was disrupted using mutations in *rde-1* or *rde-4*. The additional identification of virus-derived small interfering RNAs (viRNAs) in infected worms shows that RNAi plays an active role in restriction of natural virus infections in *C. elegans*[31].

Argonaute proteins as well as the programmed cell death (PCD) pathway had been previously implicated in restricting the expression of non-worm viruses that have been introduced artificially into *C. elegans* animals or cultured cells. The viruses used in these studies were Vaccinia Virus (DNA poxvirus), Vesicular Stomatitis Virus (negative-strand RNA virus), and Flock-House Virus (positive-strand RNA virus)[32-36]. There were three main strategies employed to surmount the difficulty of infecting worms with non-worm viruses. The first was infection of cultured primary cells from *C. elegans* embryos with Vesicular Stomatitis Virus, a negative-strand RNA virus[35,36]. While this approach doesn't allow viral replication to be followed in the context of a whole organism, it does allow for genetic studies since the primary cells can be derived from embryos carrying

mutations in genes of interest. Theses studies showed that RNAi restricted the replication of the virus. Another group used Vaccinia Virus, an enveloped DNA poxvirus, to infect adult animals by first permeabilizing the adults with polyethylene glycol (PEG) [32]. While they did observe viral replication and could study genetic interactions with virus replication, the PEG treatment itself killed many of the animals. The authors did, however, demonstrate a role for the PCD pathway in restricting virus replication in this system. The third approach used to study viral replication in *C. elegans* is the expression of Flock-House Virus (FHV) tagged with GFP and introduced into *C. elegans* as a transgene driven from a heat-shock (HS) promoter, which also showed an important role for the RNAi pathway in restriction of viral replication[33]. This system has the most potential for use in genetic screens, and the authors have recently published a second study with a small-scale candidate RNAi feeding screen (about 100 genes, a third of which showed an effect on viral replication)[34].

Section II: Role of Germline RNP Granules in the Restriction of Transposons

The presence of germline-specific granules in a broad spectrum of animal species has been observed for over four decades by electron microscopy [37]. Although studies in different organisms have yielded a variety of names for these granules, including chromatoid bodies, nuage, P granules, polar granules, and intermitochondrial cement, it has become clear that these granules contain many of the same components, which are primarily RNA-binding proteins and RNAs. Many germ granule components are also found in processing bodies (P bodies), which are

found in somatic as well as germ cells and are involved in RNA regulation. Germ plasm including germ granules has been shown to specify the germ cell fate. One major proposed role of these granules is therefore the storage and proper segregation during cell division of mRNAs. However, many proteins found in germ granules suggest that these granules play a more active role in RNA regulation, possibly in addition to a role in RNA storage. Overall the function of the germ granules remains unclear.

Discoveries over the past decade of small RNA-mediated silencing pathways have shed new light on some functions of germ granules. Specific factors involved in small RNA pathways, including the effector Argonaute proteins and target mRNAs, have been found in germ granules and P bodies. Furthermore, small RNA pathways have been shown to play a role in the silencing of transposable elements (TEs) and viruses. The repression of these genomic parasites is critical in the germline to protect germ DNA from changes that will be passed to subsequent generations. As covered in the previous section, there are germline-specific factors for restriction of TEs, and now many of these factors have been shown to accumulate in germ granules. In this section I will summarize recent findings suggesting that one of the functions of germ granules is in the restriction of TEs and viruses.

Transposon Silencing Machinery Is Found in Some Germline Granules

Cytological studies of the subcellular localization of Argonaute proteins and other proteins involved in TE silencing have shown that many of these proteins

localize to germline RNP granules. In *C. elegans,* several Argonaute proteins expressed in the germline have been found in germ granules, including the piwi clade Argonaute PRG-1, which silences the Tc3 DNA transposon, and several WAGO-clade Argonautes, including WAGO-1 and CSR-1[17,38,39].

Studies of the subcellular localization of piRNA pathway components in mouse and fly germlines have led to the identification of new germline RNP granules called pi-bodies. In *Drosophila,* pi-bodies are a part of the germ granule called cytoplasmic nuage, and they contain the piwi proteins Ago3 and Aub and overlap with a subset of the P bodies in the cytoplasm. These RNP granules also contain transposon RNA that is targeted for degradation via the piRNA pathway[40]. In mouse spermatocytes, two different RNP granules have been identified as having piwi pathway components. During embryogenesis there are two piwi homologs expressed in mouse spermatocytes: MILI and MIWI2. MIWI2 is found in distinct granules that are contained within the perinuclear nuage, and the authors call these granules pi-bodies. MILI is found in cytoplasmic granules that have been described as intermitochondrial cement in earlier electron microscopy studies. In addition to MILI these granules contain several P body components, including DCP1, and the authors name these granules pi-P bodies[41,42]. The presence of TE mRNA and proteins known to silence TEs in germ granules strongly suggests that one of the major functions of these granules is the protection of the germline genome from the activity of these genomic parasites. The question remains of what role the formation of these granules itself plays in this process. Also, if only a subset of germ granules contain these silencing components, is there a distinct role for the remainder?

Relationship of Germline Granules to the Germ Nucleus

One key to understanding why proteins and RNAs may localize to these germ granules is the subcellular localization of germ granules. Germ granules in all organisms have perinuclear localization for at least part of the germ cell lifecycle. Germ granules (called P granules) in *C. elegans* are cytoplasmic in mature oocytes and the first four embryonic germ cell divisions. After the fourth division, however, they are found on the nucleus and remain there through gametogenesis in the adult germline. Furthermore, electron microscopy of adult gonads shows that perinuclear P granules are associated with clusters of nuclear pores[43].

One of the major questions remaining in germ granule biology is what function the assembly of these granules has. This is a question that is also relevant to related RNP granules, such as P bodies. The aggregation of P body components into microscopically visible granules is not essential for their functions, including mRNA de-capping, nonsense mediated decay, microRNA-mediated repression, and translation repression during stress [44-47]. It has been argued, however, that these proteins may still be functioning in the context of an RNP granule, but that the granule hasn't aggregated into something large enough to detect by light microscopy [45].

The location of germ granules on the nuclear periphery may facilitate their function in the silencing of TEs. The location over clusters of nuclear pores in *C. elegans,* for example, may force TE mRNA to pass through P granules during nuclear export and therefore come in contact with TE silencing factors in P granules[43,48].

Additionally, retrotransposons undergo part of their replication in the cytoplasm and must re-access the nucleus through nuclear envelope breakdown or nuclear pores in order to cause new integration events. In the *C. elegans* germline the clustering of P granules over the nuclear pores may therefore present a barrier to retrotransposon replication[49]. In mouse germ cells the piRNA pathway also causes the transcriptional silencing of TEs through DNA methylation, which requires piRNA-protein complexes to enter the nucleus. This may be another reason piRNA components are found in perinuclear nuage; In this case, rather than catching things on the way out, the perinuclear localization allows easy access back in to the nucleus[29].

Section III: Programmed Cell Death in the Germline

Programmed cell death (PCD), or apoptosis, is a mechanism by which individual cells eliminate themselves from an organism. This process is often initiated during development to allow for tissue restructuring, such as the apoptosis of cells in the webbing between mammalian fingers during fetal development[50]. Cells can also be triggered to die by apoptosis when something goes wrong, such as an abnormal mitosis or infection by a pathogen. In many organisms there is also active PCD during gametogenesis. This section focuses on programmed germ cell death in *C. elegans*, with some added examples drawn from studies in other organisms. I will first give an overview of the core PCD pathway, followed by a more specific overview of germline PCD. I will then introduce the models for why PCD is occurring

in the germline, including the role of PCD in restricting viruses and transposable elements.

The Mechanism of Programmed Cell Death

Studies in *C. elegans* were pivotal in elucidating the core PCD pathway, which is conserved in mammals (Figure 1.2). This pathway culminates in the activation of a caspase (aspartate-specific cysteine protease) that triggers a cascade of downstream events that break down the cell and mediate its engulfment by neighboring cells (for a review of the downstream steps in *C. elegans* see [51]). In *C. elegans* all PCD is mediated, with few exceptions, by the caspase CED-3. CED-3 is activation occurs through interaction with CED-4/Apaf-1[52]. Both CED-3 and CED-4 proteins are present in most cells, but survival is promoted by CED-9/Bcl-2[53]. CED-9 prevents CED-4 from associating with CED-3, thereby allowing the cell to live until a killing signal is received. During hermaphrodite development 131 somatic cells undergo PCD[54]. In these cases, a developmental cue triggers the transcription of *egl-1*, a BH3-domain containing protein[55]. This pro-apoptotic protein binds to CED-9, disrupting its ability to sequester CED-4. This in turn allows for the association of CED-4 with CED-3, activating the cell death program.

The mechanism by which CED-9 inhibits CED-4 activation of CED-3 remains unclear. In mammalian PCD, pro-apoptotic BH3-domain containing proteins inhibit Bcl-2 family proteins, and this inhibition leads to permeabilization of the mitochondrial membrane and release of cytochrome c; this release leads to the

formation of the apoptosome with Apaf-1 and caspase-9, which in turn causes the activation of downstream caspases[56,57]. In *C. elegans,* mitochondrial fragmentation has been observed in cell deaths[58], and some mitochondrial proteins including AIF and EndoG are released[59]. However, no role for cytochrome c has been revealed, and only weak PCD defects are observed in when those genes are knocked down. Instead it was proposed that CED-9 binds directly to CED-4, sequestering it at the mitochondrial membrane. CED-4 and CED-9 have been shown to bind *in vitro*, and previous studies showed co-localization at the mitochondrial membrane, with accumulation of CED-4 at the nucleus when cell death was initiated[60-62]. The model was that binding of EGl-1/BH3 to CED-9/Bcl-2 disrupted the CED-9/CED-4 binding, allowing CED-4 to traffic to the nucleus and activate CED-3. A new study, however, could not find evidence of *in vivo* co-localization of CED-9 and CED-4, and instead found CED-4 at the nuclear periphery in all cells[63]. This study suggests that the role of *ced-9* in inhibiting *ced-4* may be indirect, similar to its role in mammals. Future studies should reveal whether the CED-9/CED-4 interaction is indeed indirect *in vivo*, and what other proteins might provide the missing link in the cell death pathway.

The Role of PCD During Gametogenesis

PCD of germ cells can play a role in many of the same processes as somatic PCD, including tissue remodeling, removal of damaged or infected cells, and regulation of cell number. The dying cells may also act as nurse cells for the survivors. In the *C. elegans* adult hermaphrodite gonad approximately half of all

germ cells undergo PCD[64]. The hermaphrodite gonad consists of 2 U-shaped arms. The cells divide mitotically at the distal end of each arm, and then progress through Meiosis I as they move proximally. In the last larval stage, L4, the germ cells differentiate into sperm that is stored in the spermatheca, which sits between the gonad and uterus. In adults, germ cells instead differentiate into oocytes, which will be fertilized by the sperm stored in the spermatheca. The gonad is a syncytium, with the germ nuclei on the periphery of the gonad. Each germ nucleus is partially enclosed by plasma membrane but remains connected by large ring channels to the large syncytial core. The ring channel closes when the oocyte matures in the proximal end of the gonad, prior to fertilization. By convention each germ nucleus and its surrounding cytoplasm is referred to as a germ "cell" despite the connection to the common core. Cells die by PCD primarily in the late pachytene zone of the gonad[64].

The Nurse Cell Model

The mature oocytes are much larger than the developing oogonia. This enlargement occurs through 2 main mechanisms. One is the uptake of yolk by endocytosis facilitated by receptors on the plasma membrane[65], and the second is cytoplasmic streaming, which moves materials from the cytoplasmic core into the enlarging oocyte through the ring channel[66]. It has been proposed that the dying cells may act as nurse cells for these enlarging oocytes; RNA and protein made by these cells move into the core and then stream proximally into the enlarging oocytes. Some support for this model comes from a study of oocyte quality in aging animals.

Andux and Ellis found that the quality of oocytes, as determined by assaying embryonic and larval viability, decreases as age increases. Furthermore, they found that this decline in oocyte quality occurs earlier in animals defective in germ cell death - *ced-3* and *ced-4* mutant animals. In addition to a decrease in viability of the progeny, they also found an increase in the number of "small eggs" which could represent either breakdown of oocytes/eggs or small oocytes[67]. These data are consistent with a model of limited resources. The cell death that occurs in wild-type animals allows mature oocytes to be loaded with the full resources needed for embryonic development. If those cells don't die then less resources are available and oocytes start to get less loaded into them, leading to the small eggs and decrease in embryo and larva viability. It is important here to note that progeny from young animals, even cell death defective animals, do not suffer from these oocyte quality issues. Interestingly, while these physiological deaths are regulated by the core PCD machinery including *ced-9, ced-4,* and *ced-3*, they do not require the BH3 protein *egl-1*[64].

DNA Damage Induced Germline PCD

In addition to this potential role in a nurse cell system in the gonad, germline PCD in *C. elegans* functions to remove nuclei with DNA damage. This PCD is usually triggered by checkpoints in Meiosis, and can be clearly seen in the lab if the worm is exposed to an insult such as gamma radiation[68]. This results in massive PCD in the gonad. In contrast to physiological germ PCD, but similar to the somatic cell deaths that occur during development, this PCD is mediated by the transcriptional

regulation of *egl-1*/BH3 and a related BH3-domain gene, *ced-13*(Figure 1.2)[64,69]. These pro-apoptotic activators inhibit the activity of *ced-9*/Bcl-2, allowing CED-4/Apaf-1 and CED-3/caspase to become active. The activation of *egl-1* transcription in response to DNA damage is regulated by the *C. elegans* p53 homolog, *cep-1*[70]. Regardless of where the DNA damage occurs in the gonad, the cells always die in the same region. This may be due to restriction of some necessary cell death machinery to that region such as activated MAPK, which in turn regulates expression of *cep-1*/p53[71].

If a worm lives a normal healthy life then the only reason DNA damage-induced PCD would occur in the germline is the occasional error in meiosis. A wide variety of insults or circumstances can trigger additional cell deaths. As mentioned above, UV-irradiation causes DNA damage that triggers germ PCD. Other stresses that lead to germline PCD include osmotic stress, heat-shock and pathogen infection (e.g. *Salmonella typhimurium*). For a more extensive review of this stress-induced germline PCD see [72]. Another situation that leads to increased PCD in the adult germline is starvation. One specific example of this is the adult reproductive diapause. This is a special life-stage that animals enter into if they are in starved and crowded conditions during the appropriate window in the last larval stage (L4)[73]. Instead of becoming full adults these animals arrest as a small adult with just 2 embryos, one fertilized from each gonad arm. Worms can remain in this state for at least 30 days, during which time their germline shrinks down to about approximately 35 nuclei per gonad arm. The other cells die by PCD. This shrinking of the germline through PCD is proposed to be a preservation strategy to

redistribute the resources in the germline to maintain the soma and remaining germ stem cells. Worms kept in this state for 30 days can recover when placed on food again and live out a full adult lifespan. The germline grows back to a normal size and oogenesis resumes. While the mature sperm do not survive in the spermatheca for this duration, if new sperm is added by mating with males, the resulting embryos are viable[73]. While this is an extreme example, it may further demonstrate a role for germline PCD in maintaining the correct balance of resources for the germline.

PCD in Response to Viruses and Transposons

A virus infection places a certain amount of stress on a cell and triggers innate immune responses that can include PCD. To date no foreign viruses have been discovered that can naturally infect the *C. elegans* germline, but in artificial virus infection systems of somatic *C. elegans* cells, PCD has been found to restrict viral replication[32]. This is consistent with viral restriction systems in mammals (reviewed in [74]). In mammals, PCD is triggered in response to virus infections by both adaptive immune responses and cell-autonomous responses. A cell that has an active virus infection will display viral peptides on its cell surface. This cell will then be recognized by T lymphocytes and be triggered to die by PCD, thereby eliminating the infected cell from the population and restricting further replication of the virus. The cell-autonomous response can be triggered by the disruption the virus causes to cellular metabolism. In particular it has been shown that many viruses trigger cell cycle entry in order to increase their own replication. They often trigger the cell cycle without also sending the necessary anti-apoptotic survival signals to the cell.

The cell can then recognize this division as aberrant and undergo p53-dependent PCD[74].

In addition to foreign viruses, an organism is faced with the endogenous mobile genetic elements that can become active, as described in previous sections. Evidence that the activity of retrotransposons can cause DNA damage and subsequent PCD comes from studies of the LINE-1 (L1) non-LTR retrotransposon in human cells. First, it was shown that cell lines have increased PCD when L1 becomes highly active; this increased PCD is not seen if the cells lack intact p53[75]. It was then demonstrated that high activity of L1 causes a high amount of double-stranded breaks (DSBs)[76,77]. This suggests that the increased cell death seen when L1 is active is at least in part the direct result of the DSBs, which occur as part of the retrotransposition process. Interestingly, there is some evidence that genotoxic stress can lead to increased activity of L1, in part by allowing L1 to take advantage of existing DSBs in order to integrate more efficiently (reviewed in [78]). The success of L1 retrotransposition might therefore rely on the correct balance of activity so that it can create or capitalize on DSBs without triggering the host cell to die by PCD.

Germline PCD in Response to Silencing Mechanisms

A recent study in *C. elegans* demonstrated a role for RNA interference (RNAi) and a related phenomenon, co-suppression, in triggering germline PCD[79]. RNA interference involves the production of small RNAs that target the RNAi silencing

machinery to mRNAs with matching sequences, leading to the degradation of those target mRNAs. RNAi also results in the epigenetic silencing of the corresponding locus by recruiting chromatin factors associated with repressed transcription. Co-suppression occurs when highly repetitive DNA sequences are present in many organisms including plants and *C. elegans.* One circumstance where co-suppression occurs in *C. elegans* is when a plasmid encoding a germline-expressed gene is injected into worms. The result is an extra-chromosomal transgenic array with a high-copy number of the gene. This repetitive DNA is very efficiently silenced in the germline, although such transgenes can escape total silencing in somatic cells. In addition to the silencing of the transgene, silencing is also observed for the endogenous germline gene, leading what would otherwise be an overexpression experiment to instead mimic a knockdown phenotype. The co-suppression and RNAi pathways in *C. elegans* share some but not all components, indicating that they are related but not identical phenomena[80].

The recent study by Adamo *et al.* demonstrated that both co-suppression and RNAi targeting germline-expressed genes leads to increased PCD in the gonad[79]. They further demonstrated that this increase in PCD is dependent on *cep-1*/p53, indicating that it could be occurring through the DNA-damage-induced PCD pathway. Indeed, they find a concomitant increase in the number of RAD-51 foci, an indicator of DSBs. The primary endogenous function of both co-suppression and RNAi is thought to be the silencing of mobile genetic elements and invading viruses. This new study suggests that in addition to silencing the expression of these genome

invaders, co-suppression and RNAi pathways may lead to PCD in cells with the highest expression levels, possibly culling those high-expressing cells from the population.

Further evidence that suggests a role for transposon activity in inducing germline PCD comes from studies in zebrafish of a Piwi homolog. As mentioned above, Piwi proteins are a subclass of the Argonaute gene family, which are essential components of small RNA silencing pathways. Piwi proteins are primarily expressed in the germline, and this has been established in diverse organisms including mammals, zebrafish, drosophila, and *C. elegans*[7,18,81-83]. In all of these organisms they have been shown to silence at least some transposons; Removal of Piwi proteins causes an increase in germline transposon activity. In addition to their role in silencing transposons, piwi proteins have roles in germline stem cell maintenance and normal germ cell development. In the study of a piwi homolog in zebrafish, Ziwi, an increase in PCD was observed when Ziwi was removed. This correlated with an increase in transposon activity, but it remains to be determined whether the PCD was a direct result of transposon activity or a different role of Ziwi in germline developmental processes[83].

The Role of PCD in Genome Defense

The importance of restricting mobile genetics elements and virus infections in the germline is well established. The relative role that PCD plays in this restriction, however, remains unclear. The germline poses a unique problem in many ways. One reason for this is the necessity of DSBs for crossovers in meiosis. Different cell types in a multicellular organism have different sensitivities to PCD

induction. In *C. elegans,* for example, PCD is not triggered in the male germline or somatic tissues of either sex. Susceptibility to apoptosis also changes as germ cells progress through meiosis. PCD does not occur in the distal region of the gonad where mitosis and early meiotic steps are occurring. PCD is instead restricted to the more proximal region of the gonad[64]. Are cells in this region primed like T cells to die readily if they become actively attacked by viruses or transposons? The recent work by Adamo *et al.* demonstrates that two genome defense mechanisms, RNAi and co-suppression, can lead to DSBs and PCD[79]. Many questions stem from this result. What is the mechanism causing the DSBs? Can this PCD and DSBs be observed when transposons are active? The latter question may require the development of new tools, since many known strains with increased transposon activity have mutations in the co-suppression or RNAi pathways, which may or may not influence the ability of the germ cells to die in response to the transposon activity.

Aim of My Dissertation Research

In the work described in the following chapters my aim was to uncover the mechanisms by which *C. elegans* protects its germline from the activity of retroelements. The first aim was to identify a strain with an active retroelement to study. The second aim was to characterize this retroelement and determine the role of small RNA pathways in silencing it. An additional aim was to uncover any role that perinuclear P granules might play in retroelement biology, potentially as an obstacle to their entry into the nucleus. These aims are addressed in chapter 2.

Chapter 3 describes my work showing that the identified retrotransposon causes germ cell death in the *C. elegans* germline.

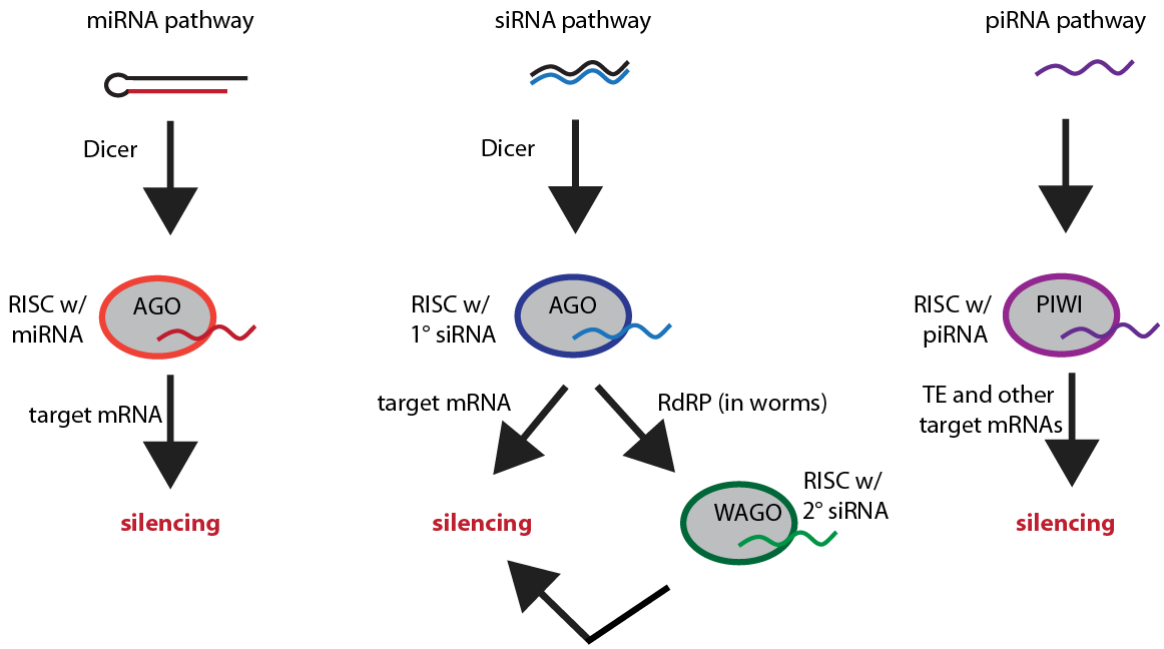

Figure 1.1. Brief Overview of Small RNA Pathways in Animals.
There are 3 major small RNA pathways in animals, involving miRNAs, siRNAs, and piRNAs. The miRNA and siRNA pathways both require Dicer for processing of the hairpin precursor miRNA or dsRNA trigger, respectively. The processed small RNA then binds to an Argonaute protein from the Ago clade in an RNA-Induced Silencing Complex (RISC) in order to silence targets. In worms there is an additional amplification step in the siRNA pathway, whereby 1° siRNAs are amplified by RNA-dependent RNA polymerases (RdRPs) into 2° siRNAs. The 2° siRNAs form RISC with secondary Argonaute proteins, which are from the WAGO, or Worm-specific Argonaute, clade. The piRNA pathway, in contrast to the others, does not require Dicer for small RNA processing. The piRNAs are bound by Argonaute proteins from the PIWI clade, and primarily mediate silencing of transposable elements (TE).

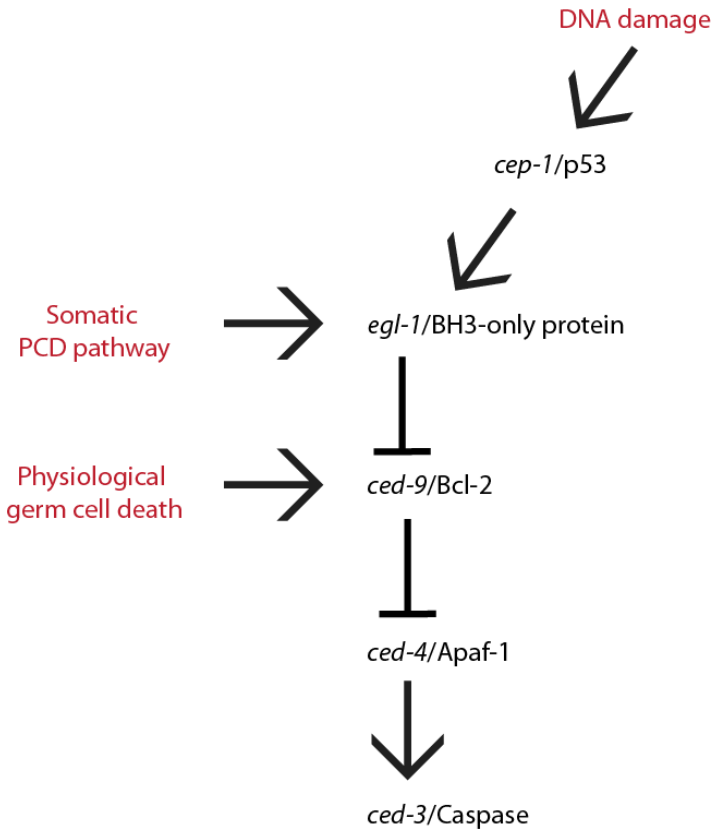

Figure 1.2. Programmed Cell Death Pathway in *C. elegans* Germline.
This schematic shows a simplified version of the PCD pathway. The core PCD pathway involves the caspase *ced-3*, which interacts with the Apaf-1 homolog *ced-4. ced-4* is inhibited by the anti-apoptotic Bcl-2 homolog, *ced-9.* In cell deaths that occur during somatic development and cell deaths that are induced by DNA damage or certain stresses in the gonad, the BH3-domain containing pro-apoptotic gene *egl-1* inhibits *ced-9* in order to initiate the core PCD pathway. DNA damage-induced cell deaths additionally act through the p53 homolog, *cep-1*, upstream of *egl-1.* In contrast, the physiological germ cell deaths do not require the activity of *egl-1,* and the upstream activation of these deaths remains unclear. Modified from [84].

Chapter 2: *C. elegans* Germ Cells Show Temperature and Age-Dependent Expression of *Cer1*, a Gypsy/Ty3-Related Retrotransposon

NOTE ON CHAPTER 2: This work was published in PLoS Pathogens.

Citation: Dennis S, Sheth U, Feldman JL, English KA, Priess JR (2012) *C. elegans* Germ Cells Show Temperature and Age-Dependent Expression of *Cer1*, a Gypsy/Ty3-Related Retrotransposon. PLoS Pathog 8(3): e1002591. doi:10.1371/journal.ppat.1002591

Abstract

Virus-like particles (VLPs) have not been observed in *Caenorhabditis* germ cells, although nematode genomes contain low numbers of retrotransposon and retroviral sequences. We used electron microscopy to search for VLPs in various wild strains of *Caenorhabditis*, and observed very rare candidate VLPs in some strains, including the standard laboratory strain of *C. elegans*, N2. We identified the N2 VLPs as capsids produced by *Cer1*, a retrotransposon in the Gypsy/Ty3 family of retroviruses/retrotransposons. *Cer1* expression is age and temperature dependent, with abundant expression at 15°C and no detectable expression at 25°C, explaining how VLPs escaped detection in previous studies. Similar age and temperature-dependent expression of *Cer1* retrotransposons was observed for several other wild strains, indicating that these properties are common, if not integral, features of this retroelement. Retrotransposons, in contrast to DNA transposons, have a cytoplasmic stage in replication, and those that infect non-dividing cells must pass their genomic material through nuclear pores. In most *C. elegans* germ cells, nuclear pores are largely covered by germline-specific organelles called P granules. Our results suggest that *Cer1* capsids target meiotic germ cells exiting pachytene, when free nuclear pores are added to the nuclear envelope and existing P granules begin to be removed. In pachytene germ cells, *Cer1* capsids concentrate away from nuclei on a subset of microtubules that are exceptionally resistant to microtubule inhibitors; the capsids can aggregate these stable microtubules in older adults, which exhibit a temperature-dependent decrease in egg viability. When germ cells

exit pachytene, the stable microtubules disappear and capsids redistribute close to nuclei that have P granule-free nuclear pores. This redistribution is microtubule dependent, suggesting that capsids that are released from stable microtubules transfer onto new, dynamic microtubules to track toward nuclei. These studies introduce *C. elegans* as a model to study the interplay between retroelements and germ cell biology.

Author Summary

Retrotransposons and retroviruses pose enormous threats to animal and plants because of their ability to insert into host genes. Retroelements that replicate in germ cells can, if left unchecked, expand exponentially in the host genome. *C. elegans* has proven to be an exceptional model system for studying many facets of cell and molecular biology, and the genome contains both retrotransposon and retroviral sequences. However, no virus-like particles have been observed in *C. elegans* germ cells. We show here that *Cer1*, an endogenous Gypsy/Ty3 class retrotransposon, is expressed at very high levels in *C. elegans* germ cells, but escaped detection in previous studies because its expression is both temperature and age dependent. These studies reveal new aspects of microtubule regulation in *C. elegans* that the retroelement appears to exploit to navigate the germ cell cytoplasm, and demonstrate the power of *C. elegans* for studying host/pathogen interactions in germ cell biology.

Introduction

DNA transposons, retrotransposons, and retroviruses that are expressed in germ cells have tremendous potential to damage the genome by creating novel insertions that are transmitted vertically to host progeny. Because DNA transposons replicate by an excision and reintegration mechanism ("cut and paste"), replication of an endogenous element does not necessarily increase copy number [85]. Retrotransposons, however, replicate by first transcribing genomic RNAs that are later reverse transcribed for integration ("copy-and paste"), and endogenous elements thus have the potential to increase their copy numbers exponentially if left unchecked [85,86]. Accordingly, animal and plant genomes typically contain far more copies of retrotransposons than of DNA transposons. For example, retrotransposons constitute about 40% and 75% of the human and *Zea mays* genomes, respectively, while DNA transposons contribute 3% and 8.6% [87,88]. In striking contrast, retrotransposons constitute only 0.6% of the *C. elegans* genome, while DNA transposons make up about 12% [3,89,90]. Although the *C. elegans* genome contains about 20 distinct families of long terminal repeat (LTR) retrotransposons and retroviruses, each family consists of only one or a few members [91]. Thus, retroelements enter the nematode genome at some frequency, but show comparatively little expansion. No viruses or Virus-Like Particles (VLPs) have ever been reported in the germ cells of *C. elegans* or other *Caenorhabditis* species, and experiments designed to identify spontaneous germline mutations in *C. elegans* yielded only novel insertions by DNA transposons [92,93]. Indeed, *C.*

elegans has long been considered an inadequate model organism to study natural virus-host interactions, although recent studies have shown that it is possible to artificially infect nematodes or nematode cell lines with promiscuous viruses, and a natural virus that infects intestinal cells has been identified [31-33,35,36].

A fundamental difference between DNA transposons and retroelements is that DNA transposons undergo their replication cycle entirely within the nucleus, while retrotransposons and retroviruses that infect non-dividing cells must transport their genetic material across nuclear pores. Non-LTR retrotransposons replicate by first producing a genomic RNA that is exported to the cytoplasm. This mRNA forms a ribonucleoprotein particle (RNP) that is imported back to the nucleus for reverse transcription and integration [94]. LTR retrotransposons closely resemble retroviruses, and encode similar GAG proteins (capsid, nucleocapsid) and POL proteins (protease, reverse transcriptase, ribonuclease H, integrase). Like retroviruses, LTR retrotransposons synthesize and export a genomic RNA that combines with capsid and nucleocapsid proteins to form VLPs. Some retroviruses require nuclear envelope breakdown to target host chromosomes, while others such as human immunodeficiency virus (HIV) infect non-dividing cells via entry through nuclear pores [95]. For example, nuclear entry of the HIV pre-integration complex involves the host nucleoporins NUP153 and RANBP2, and the karyopherin Transportin-3 [96,97]. The HIV Vpr protein can interact directly with FG-repeat (phenylalanine glycine) nucleoporins, and these interactions appear necessary for

the pre-integration complex to be imported across nuclear pores and into the nucleus.

In *Caenorhabditis* germ cells, nuclear pores are intimately connected with large, germline-specific granules called P granules [43]. Many animals from nematodes to mammals contain distinctive granules in their germ cells that are not found in somatic cells; these granules can be either cytoplasmic or associated with nuclei, and their presence, localization, and morphology can change during germ cell development [98,99]. However, in contrast to most examples of germ granules in other animals, P granules are found in *Caenorhabditis* germ cells throughout the life cycle, and are nearly always perinuclear [98,99]. Moreover P granules cover at least 75% of the nuclear pores on most germ nuclei in the gonad [43]. Like nuclear pores, P granules contain multiple FG-repeat proteins, and can block the passive diffusion of molecules above 40 kDa [48,100]. Thus, most molecules entering nematode germ nuclei must first traffic through 200-400 nm P granules before they reach the 50 nm nuclear pores. Specific import and export pathways involving FG-repeat nucleoporins are required to move most materials through nuclear pores, and we have proposed that related pathways involving FG-repeat P granule proteins might be necessary to traffic materials through the much larger P granules [48,101].

C. elegans P granules consist of diverse molecules involved in mRNA metabolism [99], and have been shown to transiently intercept nascent mRNA in adult germ cells [48]. Thus, P granule localization over nuclear pores likely is important for

regulatory proteins and RNAs within P granules to survey nascent mRNA before that mRNA is released into the large, syncytial cytoplasm of the gonad. However, we are interested in the possibility that P granule localization might secondarily restrict retroelements that, unlike DNA transposons, must access nuclear pores to complete their replication cycle. If so, nematode retroelements might require strategies to penetrate or bypass P granules. To begin a study of the cell biology of retroelements in nematode germ cells, we first searched for wild strains with VLPs in germ cells. We found VLPs in the germ cells of *C. japonica*, where they appear to form, or accumulate, directly on P granules. We also discovered that several strains of *C. elegans* have VLPs, including the standard laboratory strain N2, but only when adults are cultured at temperatures below 25°C. We show that the *C. elegans* VLPs are products of an endogenous, Gypsy/Ty3 class retrotransposon called *Cer1* (*C. elegans* retrotransposon 1) *Cer1* capsids are first detected near meiotic germ cells in early pachytene, but accumulate around nuclei only in late pachytene/diplotene when new nuclear pores are added that are not associated with P granules. We propose that *Cer1* capsids target this specific population of germ nuclei by exploiting changes in the stability of germ cell microtubules.

Results

Background

Each arm of the *C. elegans* adult hermaphrodite gonad resembles a U-shaped cylinder, with approximately 1000 germ nuclei near the periphery (Figure 2.1A) [102]. Most germ nuclei are incompletely cellularized by plasma membranes; the apical plasma membrane has a small opening, called the ring channel, that connects with a large, shared region of gonad cytoplasm called the core (Figure 2.1B). All images shown in this study are either longitudinal, optical sections taken through the center of the core (central plane) or taken slightly interior to the apical surface (super-apical plane; Figure 2.1A, B). The basal plasma membrane contacts either extracellular matrix, or somatic sheath cells that partially surround the gonad. Although most of the gonad is a syncytium, by convention a nucleus and the surrounding cytoplasm extending up to the ring channel is referred to as a germ "cell". Cells at the distal end of the gonad divide mitotically, and their descendants enter successive stages of meiosis and oogenesis as they progress toward the opposite, or proximal, end of the gonad. Actin-dependent, cytoplasmic flow transports materials along the gonad core, toward and into enlarging oogonia [66]. When oogonia reach their full size, their ring channels close to form cellularized oocytes. Dense populations of microtubules are present throughout the gonad, both within germ cells and in the gonad core. Pachytene nuclei are surrounded by a basket of microtubules ("basket microtubules") that extend from the basal and lateral membranes, through the ring channel, and into the gonad core (Figure 2.1B) [66,103]. By electron microscopy, other microtubules we call core microtubules

appear to extend from the core plasma membrane into the super-apical zone, or into deeper regions of the core, without entering germ cells (data not shown). Additional anatomical and physiological features of the gonad that are noteworthy as potential obstacles, or opportunities, for retroelements targeting germ cell chromosomes are summarized in Figure 2.1C.

Germline VLPs in the N2 laboratory strain are the product of the *Cer1* retrotransposon

Electron microscopy was used to screen for candidate VLPs in the adult gonads of 21 *Caenorhabditis* strains. These included both *elegans* and non-*elegans* species, and both hermaphroditic and male/female strains (Table 2.1, and Materials and Methods). Representative germ cells were analyzed from mitosis through all stages of meiosis, up to the formation of cellularized oocytes; over 17,000 germ cells were scored in the initial survey, and all candidate VLPs were photographed. In these studies, we observed multiple examples of two types of atypical, spherical bodies we considered possible VLPs; two additional nuclear and cytoplasmic bodies were observed in some strains, but these occurred in less than 0.1% of germ cells and were not analyzed further.

The first type of VLP was observed only in *C. japonica*. These VLPs are about 80 nm in diameter, covered by fine spikes, and have variable, highly electron-dense cores (Figure 2.1D). The *C. japonica* VLPs were found in all female and male gonads examined (n >30 for each), and were present in 16-19% of total germ cells

beginning in the mid-pachytene region (Table 2.1). From this region through early oogenesis, essentially all VLPs were adjacent to P granules (Figure 2.1E and Supplemental Figure S2.1A-S2.1C). The VLPs were present in grape-like clusters that generally increased in size with germ cell development. In oogonia, where P granules detach from the nucleus, the VLP clusters were in the cytoplasm and appeared separated from P granules (data not shown). Very few or no VLPs were detected in mature oocytes or in early embryonic cells. However, morphologically similar VLPs appeared about midway through embryogenesis in several types of differentiating somatic cells, including hypodermis (skin), muscles, and intestinal cells, where the VLPs often were closely associated with microtubules (Supplemental Figure S2.1D-S2.1F).

The second type of VLP was found in germ cells of four wild strains of *C. elegans* and, surprisingly, the standard laboratory strain, N2 (Table 2.1). We confirmed the presence of N2 VLPs in (1) worms derived from bleached eggs, indicating that the VLPs are endogenous, (2) in a newly obtained stock of the N2 reference strain from the *Caenorhabditis* Genetics Center, and (3) in a low passage "ancestral" stock of the original N2 isolate (Table 2.1, http://www.cbs.umn.edu/CGC). Similar to the *C. japonica* VLPs, the *C. elegans* VLPs are about 80 nm in diameter and covered with fine spikes. The interiors of some VLPs contain one or two electron-dense bodies that resemble curved rods and likely correspond to the genetic material (Figure 2.1F). More commonly, small electron-dense foci are visible in the interior that might represent sectional views of the rods, or distinct stages of maturation or

compaction. In contrast to *C. japonica*, the *C. elegans* VLPs were not observed in adult male gonads or in fourth larval stage (L4) hermaphrodite gonads, and were not observed in any embryonic cells (Table 2.1 and data not shown). The *C. elegans* VLPs were present at much lower abundance than the *C. japonica* VLPs: More than 95% of the *C. elegans* germ cells examined lacked VLPs, and the few positive cells typically contained only one or two VLPs.

We began our analysis on the *C. elegans* VLPs, despite their low abundance, because of the numerous advantages of *C. elegans* for genetic and molecular experiments. To facilitate the analysis, we first asked whether we could increase the number of VLPs through physiological stress (heat, starvation), or by eliminating various pathways (RNAi, cell death) and cell types (coelomocytes) that might have the potential to repress or remove VLPs (Table 2.2). None of these conditions caused a marked increase in VLPs, although there was a modest and reproducible increase in *alg-1(RNAi); alg-2(ok304)* animals defective in the microRNA pathway (Table 2.2). We next attempted to use RNAi to identify the source of the VLPs, beginning with the several families of *Cer* elements in the *C. elegans* genome (Table 2.2). We observed no decrease in VLP numbers with dsRNA directed against the retrotransposons *Cer2*, *Cer3*, *Cer4*, *Cer5*, *Cer6*, or against the endogenous retrovirus *Cer1*3. In contrast, dsRNA against the retrotransposon *Cer1* eliminated all VLPs, strongly suggesting that the VLPs are *Cer1* capsids.

Cer1 is an 8.8 kb LTR retrotransposon in the Gypsy/Ty3 family of retroviruses/retrotransposons (Figure 2.2A) [104]. *Cer1* has a single, long open reading frame with the potential to encode a GAG- and POL-containing polyprotein [1]. The N2, laboratory strain of *C. elegans* contains one, apparently intact, copy of *Cer1*, and three LTR fragments [91]. The *Cer1* insertion in N2 disrupts *plg-1*, a mucin-like gene that is required for the formation of the copulatory plug in mated adults; wild *C. elegans* strains are polymorphic for this insertion [105]. The 5' and 3' LTRs of *Cer1* are identical, which can indicate a recent insertion as both LTRs are generated from a single template during retrotransposon replication [106]. However, there is no evidence that *Cer1* remains active in N2: No spontaneous mutations have been shown to result from the transposition of *Cer1*, or of any other *Cer* element [92,93], and no mRNAs that can encode essential GAG or RT proteins from *Cer1* have been identified in any of several *C. elegans* cDNA and EST (Expressed Sequence Tag) projects (compiled at the Wormbase web site, *http://www.wormbase.org*, release WS227, 2011). Finally, *Cer1* was reported to lack an obvious Primer Binding Site (PBS) [91]. A PBS is critical for replication, and typically is found near the 5' LTR; the complementary 3' end of a specific host tRNA binds the PBS to prime minus-strand DNA synthesis. However, in a search of the tRNA database GtRNAdb [107] we found that the sequence TGGGGGCCGAACCG, which is directly adjacent to the *Cer1* 5'LTR, is complementary to the 3' end of *C. elegans* tRNA-Pro(TGG) (Supplemental Figure S2.2). The identical sequence was conserved in a group of *C. japonica* LTR retrotransposons we identified independently in best reciprocal BLAST searches with the *Cer1* GAG sequence

(Supplemental Figure S2.2). In a search of the *C. elegans* genome for additional copies of the presumptive PBS, we discovered LTRs and protein coding fragments from a larger, now extinct family of *Cer1*-like retrotransposons (Supplemental Figure S2.2). Although those LTRs and the *C. japonica* LTRs are highly diverged from *Cer1,* each contains one or more predicted binding sites for the *C. elegans* E2F transcription factor, EFL-1 (Supplemental Figure S2.2) [108]. In preliminary studies, we found that a transgene containing the 5'LTR of *Cer1* and partial coding sequences linked to GFP (Green Fluorescent Protein) was expressed in germ cells, but was expressed in somatic cells instead of germ cells when the predicted E2F binding site GGCGCGAA was mutated to GGGCCGAA (our unpublished results).

Temperature dependence of *Cer1* GAG expression

Because GAG proteins are the main structural components of retroviral and retrotransposon capsids, we generated a monoclonal antibody (αGAG) against the predicted *Cer1* GAG protein. αGAG stained small, uniform puncta in N2 gonads (Figure 2.2B-D), but showed no staining in *Cer1*(*RNAi*) gonads, or in gonads from the CB4856 Hawaiian strain of *C. elegans.* This strain also lacks the *Cer1* sequence [105] and lacks VLPs by electron microscopy (Table 2.1, Table 2.3, and data not shown). Similarly, αGAG did not stain gonads from N2 adult males or L4 hermaphrodites that lack VLPs by electron microscopy (Table 2.3). On Western blots of total worm proteins, αGAG stained a single band of about 82 kDa, compared to a predicted GAG size of 83-86 kDa (Figure 2.2E). This protein is much smaller than the size of the predicted *Cer1* polyprotein, suggesting that the polyprotein is cleaved after

synthesis. Unexpectedly, in the course of these experiments we discovered that GAG expression was strongly dependent on culture temperature and adult age. Worms grown at 25°C showed no detectable GAG expression by immunostaining or by Western analysis (Figure 2.2B, 2.2E and Table 2.3). GAG was expressed at low and variable levels in adults cultured at 20-23°C, but was expressed at much higher levels in 15°C adults. Moreover, GAG expression could be either induced, or repressed, by shifting adult animals between 15°C (ON) and 25°C (OFF; Figure 2.2B-D, Table 2.3). Because our initial survey of *Caenorhabditis* wild strains, and of N2-derived mutant strains, was performed on 1 day old (day 1) adults raised at standard culture temperatures of 20-23°C, we repeated electron microscopy on day 1 and day 3 N2 adults grown at 15°C. We found that VLPs (hereafter designated as *Cer1* capsids) were much more abundant at 15°C than observed previously at higher temperatures (see below). We have not yet been able to determine if the *C. japonica* VLPs have similar temperature sensitivity: Abundant VLPs were observed in four separate *C. japonica* cultures grown over a 4 month interval in the first stages of this study. However, we observed only a few VLPs in more recent preparations, suggesting that expression is subject to silencing.

Culture temperatures of 27°C and above are stressful or lethal for *C. elegans*, and even 25°C can activate variable, low-level expression of some heat shock reporters in some somatic tissues (our unpublished results). To determine whether the lack of *Cer1* expression at 25°C resulted from activation of the heat shock pathway, we examined *hsf-1(sy441)* mutants defective in the heat shock regulator HSF-1 [109].

Similar to wild-type adults, the *hsf-1(sy441)* mutants expressed GAG at 15°C, but not 25°C. Conversely, osmotic stress from culture media containing 350 mM NaCl is sufficient to activate a heat shock response at low temperature (see [110] and references therein), but was unable to repress GAG expression at 15°C (Table 2.3). To determine whether temperature affected *Cer1* mRNA expression, Northern analysis was performed on poly(A)-selected RNA from adult hermaphrodites cultured at either 15°C or 25°C, using probes specific for three regions spanning the *Cer1* coding region (Figure 2.2A and 2.2F). These results showed that a *Cer1* transcript of about 2.4 kb is produced at both 15°C and 25°C, but that a large transcript of about 8 kb is detectable only at 15°C. We next sequenced RNAs that were amplified by RT-PCR using primers for various *Cer1*-specific sequences, and an additional primer specific for SL1 (Spliced Leader 1); SL1 is a 22 nt trans-spliced leader sequence found on about 60% of *C. elegans* mRNAs (Figure 2.2A and Materials and Methods) [111]. We found that the 8 and 2.4 kb mRNAs correspond to the sequences diagrammed in Figure 2.2A; the 2.4 kb message is spliced and is identical to the sole *Cer1* mRNA identified previously in *C. elegans* EST and cDNA projects (Wormbase web site, *http://www.wormbase.org*, release WS227, 2011). These results show that *Cer1* capsids are not detectable at 25°C because the 8 kb mRNA that encodes the GAG and POL proteins is not detectable at that temperature.

The spliced 2.4 kb mRNA can encode a novel, approximately 60 kDa protein that includes discontinuous, but in-frame, peptide sequences shared with the N-terminus of GAG (Figure 2.2A). The spliced mRNA utilizes *Cer1* sequences that conform to

consensus acceptor and donor intron splice sites for *C. elegans* (Supplemental Figure S2.3) [112]. This splicing pattern is likely to be a general feature of the *Cer1* family, as *Cer1*-related retrotransposons in both *C. remanei* and *C. japonica* contain consensus splice acceptor and donor sequences at similar positions (our unpublished results). We detected the spliced mRNA with, and without, the SL1 leader at both 15°C and 25°C (Figure 2.2A, 2.2F and data not shown). In contrast, the 8 kb message did not appear to be spliced, and was not trans-spliced at the site utilized by SL1; it could not be amplified with an SL1-specific primer, but was amplified with primers either 5' or 3' of the SL1 site (see legend to Figure 2.2A). Thus, capsid production at 15°C requires that multiple, consensus splice sites within *Cer1* are skipped in order to generate the 8 kb mRNA that encodes GAG and POL.

We next performed in situ hybridization on fixed gonads to examine the spatial and temporal expression of the 8 kb mRNA, using probes specific for either *rt* or *gag* (diagrammed in Figure 2.2A). At 15°C, *gag*-containing RNA was first detectable in the early pachytene region of the gonad, but was not detected in somatic tissues such as the intestine (Figure 2.2G, 2.2I). The gonad expression correlates with the onset of GAG immunostaining (Figure 2.2D), with the first appearance of VLPs by electron microscopy (Supplemental Figure S2.1G), and is similar to the onset of EFL-1/E2F expression [113]. Fluorescence In Situ Hybridization (FISH) further showed that the RNA was enriched in the super-apical zone of the gonad core, with relatively little RNA in the cytoplasm surrounding germ nuclei (Figure 2.2J). Interestingly, both alkaline phosphatase and FISH detection protocols showed RNA

containing *gag* and *rt* concentrated in a pair of nuclear dots (Figure 2.2G, 2.2J and Figure 2.2K). No nuclear dots were observed in CB4856 worms that lack *Cer1*, and only one nuclear dot was observed in N2/CB4856 heterozygotes that have one copy of *Cer1* (Figure 2.2L and data not shown). These results suggest that the double dots in N2 represent RNA at or near the site of *Cer1* insertion on the paired, homologous chromosomes. Similar nuclear dots were detected in N2 gonads at 25°C that otherwise lack the *gag*-containing mRNA (Figure 2.2H). These results suggest that *gag*-containing RNA is transcribed at 25°C, but fails to accumulate in the cytoplasm. Finally, we wanted to determine whether the temperature-dependence of GAG expression was unique to the N2 copy of *Cer1*, or was a more general characteristic of *Cer1* retrotransposons. Using available data on the pattern of *Cer1* insertion in various wild *C. elegans* strains [105], we immunostained 15 wild isolates that have the N2 pattern of *Cer1* insertion in the *plg*-1 gene, and 15 strains with *Cer1* inserted elsewhere in the genome. 21 of the 30 strains contained immunoreactive GAG particles at 15°C that closely resembled the N2 staining pattern, but none contained GAG particles at 25°C (Table 2.4).

Cer1 capsid localization in germ cells

Essentially all of the immunostaining results for GAG-containing particles described here correlate with *Cer1* capsid localization determined by electron microscopy. Therefore, we refer to the immunostained, GAG-containing particles simply as *Cer1* capsids. In support of this designation, biochemical studies to be described elsewhere show that the GAG protein detected on Western blots of worm extracts

purifies with a sedimentation profile typical of viruses or capsids (our unpublished results). In overview, *Cer1* capsids first appear in early- to mid-pachytene, where they localize almost exclusively in the super-apical region of the gonad core, outside of the germ cell proper and away from nuclei (Figure 2.3A). By electron microscopy, capsids are present in small groups that are closely associated with rough endoplasmic reticulum (Supplemental Figure S2.1G), but capsids later appear more dispersed and associated with microtubules (Figure 2.4A, B). Capsids remain largely confined to the gonad core throughout the mid-pachytene region, but during late pachytene/diplotene most capsids accumulate around, or at the base of, germ nuclei (Figure 2.3A and Figure 2.4C-2.4E; see also Figure 2.5E).

In oogonia and early oocytes, most capsids are concentrated in large, crescent-shaped aggregates that are adjacent to the nuclear envelope (Figure 2.3A and Figure 2.4F). In mature oocytes, capsids disperse throughout the cytoplasm and most disappear (data not shown). The small population of capsids that persist in newly fertilized embryos exhibit two additional localization patterns: When fertilization initiates the first of two meiotic divisions of the maternal chromosomes, capsids localize equally to both poles of the meiosis I spindle (Figure 2.3B, 2.3C). This spindle rotates perpendicular to the anterior surface of the embryo, and during division half of the maternal chromosomes are extruded from of the embryo as the first polar body; capsids at the anterior spindle pole are similarly extruded into the polar body (Figure 2.3D). During these stages, additional capsids localize in small foci distributed across the periphery of the embryo (arrowheads in Figure 2.3C).

This peripheral localization occurs at about the same time as much larger cortical granules move to the surface and are exocytosed to form an extra-embryonic layer [114]. The peripheral capsids are not visible at later stages, suggesting that some of these are externalized and/or degraded. Very few or no capsids persist into cleavage-stage embryos, and any remaining capsids show no enrichment in the embryonic germ cell precursors (asterisk in Figure 2.3D). Previous studies showed that cytoplasmic dynein and dynein-associated proteins localize to both poles of the meiosis I spindle and to foci at the periphery of the newly fertilized embryo [115], similar to the localization of *Cer1* capsids. We found that each of two temperature-sensitive alleles of *dhc-1*/dynein resulted in variable and markedly reduced levels of capsid staining throughout the gonad, even at the permissive temperature for both mutations (Figure 2.3E, quantified in Table 2.3). We do not yet know from biochemical experiments whether dynein is directly associated with capsids, but we did not observe significant colocalization of DHC-1/dynein and *Cer1* capsids in gonads by immunostaining (data not shown).

Capsids accumulate progressively with adult age

We found that capsid accumulation requires oogenesis but not spermatogenesis (Table 2.3), and is strongly dependent on adult age. For the latter analysis, we cultured hermaphrodites in the constant presence of males, as oogenesis arrests in the absence of sperm. By the second day of adulthood (day 2 adults) and increasing thereafter, many gonads contain huge numbers of capsids organized into linear arrays that resemble wavy lines, or tangles of wavy lines (Figure 2.5A-2.5D, and

Supplemental Figure S2.4A, S2.4B). Co-staining for HIM-4/hemicentin, which localizes by the apical membrane [116], showed that the tips of the wavy lines occasionally and partially enter germ cells through the ring channels (Figure 2.5B). However, the vast majority of capsids localize in the core, outside of germ cells and away from nuclei, similar to capsids in younger adult gonads (Figure 2.4B and Figure 2.5A-2.5D). The abundance of capsids, and the presence and size of the lines and tangles, varies considerably for germ cells that are at the same developmental stage, but at different positions in the gonad core (double arrow in Figure 2.5D).

Both young and older adults show a marked shift in capsid distribution as germ cells begin to exit pachytene, in the pachytene/diplotene region: Nearly all of the lines and tangles of capsids disappear from the core, and large numbers of capsids redistribute into germ cells and around nuclei (Figure 2.4E, and Figure 2.5E-2.5G). In normal development, the late pachytene/diplotene nuclei enlarge and add new nuclear pores that are not covered by P granules; all P granules are eventually shed from germ nuclei during subsequent oogenesis [43,98]. Thus, capsids in both young and older adults only accumulate around germ nuclei with available, P granule-free nuclear pores. Electron microscopy, and co-staining for capsids and P granules, showed that most capsids do not accumulate directly on P granules (Figure 2.4D, and Figure 2.5H), although a few capsids are found within P granules at this stage (Supplemental Figure S2.1H). Instead, most capsids are located near and between P granules, and appear directly associated with microtubules (Figure 2.4C, 2.4E and Figure 2.5H).

Changes in *Cer1* capsid localization parallel changes in stable microtubules

Several observations suggested that microtubules are involved in capsid localization. First, we found that about 30% of capsids scored in randomly selected electron micrographs appeared to contact one or more microtubules (n= 180/560 capsids, Figure 2.4A, 2.4C). As microtubules that don't present clear cross-sectional or longitudinal profiles in micrographs are difficult to score, this percentage likely underestimates the association. Second, aggregates of large numbers of capsids and microtubules were visible in electron micrographs of day 3 and older adults that resembled the wavy lines and tangles detected by immunostaining (Supplemental Figure S2.4A, S2.4B). Finally, the localization of capsids in newly fertilized embryos closely resembles that of cytoplasmic dynein, as described above. Despite the above correlations, the distribution of most capsids in immunostained gonads bears little resemblance to the distribution of microtubules: Microtubules are highly abundant throughout the gonad (Figure 2.6A), while capsids are concentrated in much smaller regions (Figure 2.6B, 2.6C).

To determine whether capsid localization was dependent on microtubules, we treated gonads with the inhibitors nocodazole or colcemid. Cytoplasm normally flows proximally through the gonad core, transporting materials toward and into enlarging oocytes, but bypasses the late-pachytene/diplotene germ cells where capsids accumulate [66]. Flow is actin-, but not microtubule- dependent, and can carry transport large, inert beads a distance of nearly half the length of the gonad in

only 25-30 minutes [66]. Thus, we anticipated that if microtubules normally anchor the capsids against flow, the capsids would flush proximally in inhibitor-treated gonads. Instead, the inhibitors caused little if any change in the distribution of capsids throughout the early- to mid-pachytene region, including the wavy lines and tangles of capsids present in older adults (data not shown and see below).

The nocodazole concentration used for those experiments (10 μg/ml; 1 hr) was the same used in previous studies on gonad microtubules [103]. However, we discovered that a large subset of microtubules was not depolymerized by that treatment, or even higher doses of nocodazole (40 μg/ml; 2 hrs). For our subsequent analysis, we chose a standard dose of 10 μg/ml nocodazole for 30 minutes, and we refer to microtubules that resist depolymerization under these conditions as 'stable' microtubules. We found that this dose of nocodazole effectively depolymerized dynamic microtubules in the spindles of mitotic germ cells in the distal gonad (Figure 2.6E, 2.6F), and depolymerized dynamic microtubules in the most mature oocytes (Figure 2.6D, 2.6H) [117]. In contrast, large numbers of stable microtubules persisted in the early- to mid-pachytene region, where they were concentrated along the super-apical zone of the gonad core (Figure 2.6D, 2.6G). A subset of the stable microtubules could be traced into germ cells, indicating that some of these are basket microtubules (Figure 2.1B, Figure 2.6G, and data not shown). *Cer1* was not the source of microtubule stability, as gonads in each of the following types of animals that lack *Cer1* capsids contained stable microtubules: L4 hermaphrodites, adult males, adult hermaphrodites at 25°C, and

adult hermaphrodites treated with *Cer1*(dsRNA) at 15°C (n=30-75 gonads scored for each, data not shown). In addition, stable microtubules were observed in the gonads of a hybrid strain we constructed where the intact *plg-1* gene from CB4856 was introgressed into N2 to replace *Cer1* (see Figure 2.7B below); we refer to these N2-derived animals that lack *Cer1* as *Cer1(-).*

To determine the relationship with *Cer1* capsids, we examined stable microtubules (after nocodazole treatment) in wild-type and *Cer1(-)* animals that were grown as adults for 1 to 6 days at 15°C in the presence of males. We found a striking correspondence between the localization of capsids and the stable subset of microtubules in adults at all ages, and in all regions of the gonad. The following describes our results for the mid-pachytene region, where nearly all capsids localize to the core (Figure 2.7A-2.7E). In control experiments, the pattern of total microtubules (stable plus labile) in untreated, day 1-6 wild-type gonads appeared identical to the pattern in untreated, age-matched *Cer1(-)* gonads (Figure 2.6B, Figure 2.7A, and data not shown). The pattern of stable microtubules in day 1-2 wild-type gonads (Figure 2.6G) closely resembled that in day 1-6 *Cer1(-)* gonads (Figure 2.7B, and data not shown); in both types of gonads, the stable microtubules were enriched in a uniform layer along the superapical zone of the core. Beginning on day 3, however, the wild-type gonads often contained aggregates of stable microtubules (Figure 2.7C, 2.7F). The percentage of gonads with aggregates, and the number of aggregates per gonad, both increased with adult age, such that most wild-type gonads contained at least one aggregate by day 6 (Figure 2.7H). Remarkably,

essentially all capsids throughout the mid-pachytene region were localized on stable microtubules, and capsids were particularly concentrated in the aggregates (Figure 2.7C, 2.7F). While the stable microtubules in *Cer1(-)* gonads had a relatively uniform thickness (Fig. 2.7D), the capsid-bearing stable microtubules in wild-type gonads varied markedly in thickness, suggesting they were bundled (Fig. 2.7E). Together, these several results show that stable microtubules exist independent of *Cer1* capsids, but that capsids appear to cause an age-dependent aggregation of the stable microtubules. The microtubule aggregates are not apparent in untreated wild-type gonads immunostained for tubulin, presumably because of the high density of total microtubules. However, the presence of microtubule aggregates in untreated gonads is confirmed directly by electron microscopy (Supplemental Figure S2.4A, S2.4B), and indirectly by the localization of capsids (Figure 2.5C, 2.5D).

The largest aggregates of stable microtubules and capsids appear to bridge across the entire diameter of the gonad core, and are often adjacent to regions nearly devoid of stable microtubules (arrowhead in Figure 2.7C). Thus, the aggregates might grow by stripping stable microtubules from neighboring regions. If the function of the stable microtubules is to maintain gonad architecture, as we consider likely, we wondered whether the aggregates might impact fertility. We compared age-matched wild-type and *Cer1(-)* adults over each of 7 days at 15°C, but did not observe a significant difference in the number of dead eggs laid (n >20,000 total eggs for each strain; Figure 2.7G). We next cultured both strains at 15°C until day 3, to pre-load the wild-type gonads with capsids, then shifted the adults to 25°C and

examined the eggs laid over the next 24 hour period. The wild-type, shifted adults produced significantly more dead eggs, and had slightly less total progeny, than the *Cer1(-)* adults (Figure 2.7I, 2.7J). Thus, under the moderate stress of 25°C, wild-type animals pre-loaded with capsids appear to be less fertile than *Cer1(-)* adults.

Cer1 capsids traffic toward nuclei in association with dynamic or labile microtubules

Stable microtubules are present in the gonad core throughout the early to mid-pachytene region, but disappear abruptly as germ cells exit pachytene (Figure 2.6D, 2.6G, and Figure 2.8A). Similarly, the giant aggregates of stable microtubules in older adults nearly always disappear by late pachytene/diplotene: From over 160 nocodazole-treated gonads examined, only one contained a giant aggregate of stable microtubules and capsids in this region (arrow in Figure 2.8B). Thus, stable microtubules appear to break down, or become destabilized, at the same stage that capsids move out of the core and into germ cells (Figure 2.5E). We found that nocodazole treatment sharply reduced the number of capsids in late-pachytene/diplotene germ cells (compare Figure 2.8A with Figure 2.5G). Thus, the movement of capsids into germ cells is dependent on microtubules, but these microtubules are not resistant to nocodazole.

The stable microtubules disappear in late pachytene/diplotene germ cells, but reappear in late oogonia and immature oocytes where they are concentrated in a focus near the nuclear envelope (arrow in Figure 2.6H and in Figure 2.8D; compare

with the untreated oocyte in Figure 2.8C). This focus of stable microtubules colocalizes with the nuclear-associated crescent of capsids (Figure 2.8D, see also Figure 2.4F). Similar crescents of capsids exist in untreated, earlier oogonia that contain few or no stable microtubules (Figure 2.3A, and Figure 2.6D). These latter crescents are disrupted by microtubule inhibitors (arrowhead in Figure 2.8B). Together, these results suggest that (1) a focus of labile microtubules develops on or near the nuclear envelope after germ cells exit pachytene, (2) that microtubules in the focus gradually stabilize as oogonia develop into immature oocytes, and (3) that capsids accumulate at the focus before and after microtubule stabilization. Finally, the stable microtubules disappear and the capsids disperse in mature oocytes (Figure 2.6D, 2.6H). Most capsids eventually disappear in mature oocytes, but at fertilization the remaining capsids aggregate at the meiosis I spindle as described above. We conclude that capsids are associated with microtubules throughout the gonad and in fertilized eggs, and that the various patterns of capsid localization reflect changes in microtubule stability and patterning.

Discussion

Temperature-dependence of *Cer1* expression

Nematode germ cells, like those in other animals, presumably have multiple layers of defense against transposons. For example, studies primarily from *Drosophila* and mice have provided an elegant model for how germ cells recognize and silence transposons: If replicating transposons integrate into chromosomal traps called piRNA clusters, it primes the synthesis of small, anti-sense RNAs (piRNAs) that can

target both the original transposon and closely-related transposons [81,118]. Thus, novel transposons entering a naïve host have limited windows of opportunity to replicate before the silencing machinery identifies them. To exploit this window, nematode retrotransposons likely require strategies to traffic through, or bypass, both nuclear pores and P granules.

VLPs have not been reported previously in *C. elegans* germ cells, and only a few were observed in our initial electron microscopic survey of several wild strains. However, we showed that the expression of *Cer1*, a Gypsy/Ty3 retrotransposon, is temperature sensitive, such that very few VLPs are present at typical culture temperatures of 20°C to 23°C. Because previous analyses of spontaneous mutations in *C. elegans* were done at 20°C, it will be important in future studies to re-evaluate whether *Cer1* is capable of transposition in the N2 strain using mated, older adults cultured at 15°C. Temperature-dependent expression appears to be a widespread feature of *Cer1* retrotransposons, as a similar dependence was seen in multiple wild strains with different *Cer1* insertion sites. There are several possible rationales why *Cer1* expression is elevated at low temperatures, the simplest being that 15°C best approximates the average temperature of *C. elegans* in its natural environment. For example, average annual soil temperatures recorded 10 cm below the surface at sites in Florida, Montana, Oregon, Michigan, Tennessee, Arizona, Alaska were 22.5, 12.1, 12.8, 8.2, 15.7, 19.5, and 0.8°C, respectively [119]. In addition, our temperature-shift experiments on older N2 adults suggest that expression at 25°C might exacerbate phenotypes associated with capsid accumulation.

Cer1 capsids cannot form at 25°C because GAG and POL proteins are not expressed at that temperature. *Cer1* produces an apparently unspliced 8 kb mRNA that can encode GAG and POL proteins as a single polypeptide, and a spliced 2.4 kb mRNA that encodes a novel protein. The 2.4 kb mRNA is abundant at both 15°C and 25°C, however, the 8 kb mRNA only accumulates in the cytoplasm at 15°C. It does not appear that small RNA pathways prevent the cytoplasmic accumulation the 8 kb mRNA, as all of the mutants tested to date lack capsids at 25°C, similar to wild-type animals.

Splicing is essential for most cellular mRNAs to be exported from the nucleus. However, retrotransposon and retroviral replication requires export of a non-spliced, genomic RNA. Retroviruses can achieve this by structural motifs in the genomic RNA that bind host export factors directly, or by first producing proteins from spliced mRNAs that facilitate the subsequent export of non-spliced, genomic RNA. For example, the HIV Rev protein is the product of a spliced mRNA, and binds to the host export factor CRM-1 as well as to a structured motif (the Rev-response element) in the HIV genomic RNA [120,121]. The 8 kb *Cer1* mRNA is about the same size as the predicted *Cer1* genomic RNA, and thus might serve a dual function as genomic RNA, or at least face similar challenges in nuclear export. Because the novel protein encoded by *Cer1* shares some peptide sequences with GAG, and one of the expected functions of GAG is to bind and package the genomic RNA, we

speculate that this novel protein might similarly bind the 8kb RNA and regulate its splicing or export.

Cer1 capsids appear to target meiotic germ cells

The localization pattern of *Cer1* capsids described here for the N2 strain appears very similar to that in other wild strains that express *Cer1*. Thus, this pattern is likely to be relevant for considering how *Cer1* accesses germ cell chromatin. *Cer1* does not appear to bypass P granules and the nuclear envelope by targeting dividing cells in larvae or adults: *Cer1* is not expressed in L4 or earlier larvae, where all germ cells divide mitotically, and *Cer1* is not expressed in the mitotic niche of adult hermaphrodite or male gonads. We found that *Cer1* and *Cer1*-related retrotransposons conserve at least one predicted E2F binding site in their LTRs, and that this site appears important for germline expression. E2F activator proteins have well-studied roles in promoting the mitotic cell cycle in mammals and *Drosophila*, and DNA tumor viruses de-repress E2F protein complexes to drive S-phase DNA synthesis [122]. However, *C. elegans* EFL-1/E2F does not appear to function in mitosis, and instead regulates germ cell expression of numerous genes that control oogenesis and early embryogenesis [108]. Indeed, the present network of EFL-1/E2F-regulated genes in *C. elegans* germ cells might have expanded by the past transposition of *Cer1* family members, much as endogenous retroviruses appear to have seeded p53 binding sites in the human genome [123].

If *Cer1* has not evolved to target mitotic germ cells in adult or larval gonads, it might instead target the mitotic germ cell precursors in early embryos; these precursors have rapid cycle times of only 15-25 minutes, compared to 16-24 hours for adult germ cells [54,124]. For this strategy, however, it would seem counterproductive for *Cer1* capsids to bind microtubules. If capsids simply did not bind microtubules, they would be transported passively into oocytes by actin-dependent cytoplasmic streaming, and at fertilization would be further transported directly into the embryonic germ cell precursors by a second wave of actin-dependent cytoplasmic flow [66,125]. Instead, the anchoring of *Cer1* capsids to stable microtubules in the gonad core prevents many, if not most, capsids from ever reaching embryos produced by self-fertilization: Each arm of the hermaphrodite gonad can produce about 1000 oocytes, but only produces about 150 sperm. Thus, adults run out of sperm and can no longer self-fertilize at about the same time that peak numbers of capsids accumulate in the gonad core.

Most capsids in both *C. elegans* and *C. japonica* disappear in mature oocytes, suggestive of host defenses that prevent capsids from entering embryonic cells. For example, oocyte cytoplasm might contain specific proteases that have evolved to recognize, and degrade, capsids. As second possibility is that oocyte cytoplasm triggers the disassembly of capsids. The oocyte cytoplasm contains a very high level of FG-repeat nucleoporins such as NPP-9/RanBP2/Nup358 [48], which presumably is necessary to support the assembly of nuclear pores during the rapid proliferation of early embryonic cells. In addition, oocytes contain high levels of FG-repeat P

granule proteins that likely contribute to the dynamic growth, shrinkage and fusion behaviors of detached, cytoplasmic P granules [126]. If *Cer1* capsids, like HIV capsids, target FG-repeat proteins on the nuclear pores, large quantities of such proteins in the cytoplasm might effectively become decoys that trigger premature capsid disintegration.

While *Cer1* capsids are not enriched in any mitotic germ cell population, they are expressed abundantly throughout the pachytene stage of meiosis. However, the vast majority of capsids remain in the gonad core until germ cells begin to exit pachytene, when most capsids transfer into germ cells and near nuclei. As germ cells exit pachytene, they begin to increase in size and eventually become large oocytes. There is a concomitant increase in nuclear size, with the addition of nuclear pores that lack P granules and the gradual removal of existing P granules. Thus, capsids converge on germ nuclei when large numbers of P granule-free nuclear pores first become available. Such a strategy would likely provide only a narrow window of time for nuclear entry and integration, as the post-pachytene germ cells cease transcription and hypercompact their chromatin as they differentiate into oocytes (Figure 2.1C).

Navigating the *C. elegans* gonad by changes in microtubule patterning and stability.

By electron microscopy, we detected *C. japonica* VLPs in the early- to mid-pachytene region, similar to *Cer1* capsids in *C. elegans* gonads. However, the *C. japonica* VLPs

first appear, and then remain, on P granules. As newly exported mRNA traffics directly through P granules [48], this localization might be an efficient strategy for capsid proteins to capture and package viral RNA. In addition, P granule localization maintains capsids by the nuclear envelope, potentially allowing a constant surveillance for free nuclear pores. In contrast, *Cer1* capsids in *C. elegans* appear to traffic toward nuclei from initial positions in the gonad core. Particles the size of the 80 nm *Cer1* capsids are not expected to move appreciably without some type of force-generating machinery; studies in other systems have shown that dextran particles greater than 20 nm are essentially immobile in cytoplasm (see [127] and references therein). Actin-dependent streaming moves cytoplasm through the core of the gonad and into late oogonia, but does not appear to transport cytoplasm into the earlier germ cells that show perinuclear accumulation of capsids [66]. We found that *Cer1* capsids are associated with microtubules in all regions of the gonad, suggesting that changes in the microtubule cytoskeleton underlie changes in capsid localization. For example, *Cer1* capsids are dispersed uniformly throughout the cytoplasm of mature oocytes just prior to fertilization. At fertilization, however, the microtubule cytoskeleton reorganizes to form the meiotic spindle and capsids converge at both poles of the spindle.

Viruses often exploit the microtubule cytoskeleton to locate host nuclei [128,129]. In many cell types, microtubule minus ends are anchored by the centrosome, which functions as the major microtubule-organizing center (MTOC). Because the centrosome is often adjacent to the nucleus, viruses can traffic from the cell

periphery toward the nucleus by hijacking minus-end directed microtubule motor proteins; upon release from the microtubule, the virus has a high probability of encountering a nuclear pore. For example, herpes simplex virus, HIV-1, and adenovirus each use the minus-end directed motor protein dynein to navigate host cells [128,129]. *C. elegans* gonads contain dense populations of microtubules that include subpopulations we term basket microtubules and core microtubules. However, the centrosome appears to lose its MTOC function once germ cells exit mitosis, and the centrosome itself is eliminated during oogenesis [103]. Instead, the germ cell plasma membrane appears to function as an MTOC for basket microtubules [103], and we consider it likely that the core plasma membrane acts as an MTOC for core microtubules. Animal cells typically have dynamic microtubules ($t_{1/2}$ = ~10 minutes) as well as long-lived, stable microtubules ($t_{1/2}$ > 1 hour) [130]. In the *C. elegans* gonad, we showed that some basket and core microtubules appear exceptionally resistant to concentrations of microtubule inhibitors that rapidly depolymerize known, dynamic populations of microtubules, such as those in mitotic germ cells and in the most mature oocytes. Because capsids appear to accumulate over time on the stable microtubules, we argue that these same microtubules are long-lived in vivo.

We propose a "load-release-transfer" mechanism as a working model for how *Cer1* capsids concentrate near post-pachytene germ nuclei (Figure 2.9). First, capsids that form in the early- to mid-pachytene region load onto surrounding microtubules in the core. Capsids might initially associate equally with dynamic and stable

microtubules, but over time would accumulate on the long-lived, stable microtubules. Early to mid-pachytene germ cells are small with relatively little cytoplasm, but microtubules extending from these cells into the core represent a much larger, cognate surface for capsid accumulation. Cytoplasmic dynein is required for normal levels of capsid accumulation in the core, but we do not yet know whether dynein mediates capsid binding to microtubules, or whether capsids can traffic on the stable microtubules.

The number of capsids loaded onto stable microtubules increases as germ cells progress through pachytene, often resulting in the bundling or aggregation of stable microtubules in older adults. We consider it likely that the stable microtubules provide the architectural framework for the gonad core throughout the pachytene region, and must be destabilized for germ cells to increase in size as they exit pachytene. The abrupt change in microtubule stability releases the accumulated capsids into a relatively small region of core cytoplasm. There, many capsids transfer to dynamic microtubules, and move into germ cells, before being swept proximally by flow. The transferred capsids might traffic toward nuclei in association with microtubule motor proteins, or by microtubule dynamics. Although we have not yet determined the polarity of microtubules in this region, it seems likely that many are nucleated at or near the nuclear envelope and could concentrate capsids: Microtubules in general are enriched by the nuclear envelope of those cells, and a focus of stable microtubules develops close to the envelope where capsids accumulate. Thus, we hypothesize that a new, nuclear-associated

MTOC forms as cells exit pachytene, and microtubules associated with this site gradually stabilize as germ cells mature into oogonia. This MTOC is not associated with the centrosome per se, which is eliminated during oogenesis, but might be associated with a remnant of the centrosome or with centrosome-derived proteins.

The present study demonstrates that the genetics and cell biology of *C. elegans*, one of the best-understood models for animal development, can be used to study host-pathogen interactions between retroelements and germ cells. Because viruses necessarily rely heavily on host functions, their analysis has provided significant insights into host biology in many systems. Here, our analysis uncovered stage-dependent changes in the microtubule cytoskeleton of *C. elegans* germ cells, posed new questions about how microtubule stability is established and regulated, and showed that capsid localization can be used as a proxy for the distribution of stable microtubules. Further dissection of *Cer1* expression should provide insights into RNA splicing and export in germ cells, EFL-1/E2F-regulated transcription, and inform strategies for building *Cer1*-based vectors for temperature-inducible, germ cell-specific gene expression. Although the various small RNA pathways do not silence *Cer1* expression in the N2 strain at 15°C, we anticipate that analysis of *Cer1*-containing wild strains that lack GAG expression should reveal how this element is targeted for silencing in wild populations.

Materials and Methods

RNA analysis

For Northern analysis, synchronous hermaphrodites grown from bleached eggs were grown at 20°C until the L4 stage, then either shifted to 15°C or 25°C for 48 hours. About 1 ml of packed adults from each culture was rinsed in PBS twice, then resuspended and homogenized in Trizol (Invitrogen), followed by treatment with DNAse and RNA precipitation as per the manufacturer's instructions. The RNA was checked for purity by running samples on agarose gels. PolyA-containing RNA was selected using an Oligotex mRNA midi Kit (Qiagen) following the kit protocol. Probes were prepared using Amersham Ready-to-Go DNA labeling beads-dCTP (Amersham), and unincorporated nucleotides were removed with NucAway Spin Columns (Ambion), both following product protocols. RNA blotting and hybridization followed published protocols [131], except with the suggested alternate buffer [Prehybridization/hybridization: 7% SDS, 0.5 M NaHPO45, 1mM EDTA; wash #1: 5% SDS, 40 mM NaHPO4, 1mM EDTA; wash #2: 1%SDS, 40 mM NaHPO4, 1mM EDTA]. Nylon membrane was used for blotting (BioRad) as per the manufacturer's protocol. For RT PCR, cDNAs were generated using SuperScript One-Step RT PCR (Invitrogen) and Platinum Taq (Invitrogen). Products were gel purified using QiaQuick Gel Extraction Kit (Qiagen) and sequenced by the FHCRC Genomics Resource. The following primer sequences were used for the analysis summarized in Figure 2.2A: SL1(5'-GTTTAATTACCCAAGTTTGAG-3'), KE409F(5'-CGCCTTTGAGTTTGCAATCGTTT-3'), KE402F(5'-AAATCTGAAGAATGGAGGTGAACGAGGGACAGGATA-3'), KE411F (5'-TTGGATAGTGGTGCTAGTATTTC-3'), KE413F(5'-GACTTCGTCATTGACACCTTATC-3'),

KE416R(5’-TCCGATTTCACCATTAGCAAAC-3’), KE401BR(5’-ATAACACCTCAAAGCCTCCTG-3’), KE415R(5’-GATAAGGTGTCAATGACGAAGTC-3’), KE402CR(5’-TTCAAAGAAACAGGCAGAGCG-3’).

The *in situ* procedure was modified from the protocol of G. Broitman-Maduro and M. Maduro (http://www.faculty.ucr.edu/~mmaduro/) as previously described [48]. DIG-labeled ssRNA probes were made by in vitro transcription using DIG RNA Labeling Kit (Roche), using as template a PCR product amplified from genomic DNA with the following primer sequences: *rt* probe (5'-AGGTGATTGGGAAAGGAGAG-3', 5'-GCGATTGTAGCGTTGCTTCA-3'), *gag* probe (5'-TCCCAGGTCCAGACGAATAG-3', 5'-GCTCTCTCGAGATATTCTGAG-3')

RNAi experiments

Unless noted otherwise, RNAi experiments used worms cultured at 20-23°C and dsRNA feeding strains from the Ahringer library as described [132]. Third larval stage (L3) *alg-2(ok304)* animals were fed on *alg-1*(F48F7.1 dsRNA) until adulthood. For analysis of *Cer* elements, N2 worms were fed on dsRNA-expressing bacteria for 3 generations before analysis of adults using the following library strains: *Cer1* (F44E2.2 dsRNA), *Cer4* (T23E7.1 dsRNA), and *Cer5* (T03F1.4 dsRNA). Sequences from the remaining *Cer* elements were PCR amplified from genomic DNA using the following primer pairs then cloned into feeding vector pPD129.36 as described

[133]: *Cer2* (5'-GGACGAGCTTATCGTGTTCC-3', 5'-CAACTCAACGAGCCATCTCC-3'), *Cer3* (5'-ATGAGAGAGCTCAGTTACAAGC-3', 5'-GGTTCTACTAGTATAAGCTATCG-3'), *Cer6* (5'-ATGACGGTTAAGGGTCGAGTT-3', 5'-CGATGAATCCCAGAAACGAGAT-3'), *Cer13* (5'-TCTTTCAAGGCATCTCAGCG-3', 5'-AACCTCGGTCCAATTGATCC-3' plus 5'-TTCTCAACAGCGTCTCCATCG-3', 5'-CAGCTGTCCGATCTGTTTCAC-3'.

Immunocytochemistry and microscopy

The following antibodies were used: αTubulin (1:1 YL1/2 and YOL3/4; Abcam), αPGL-1 [134], αHIM-4 [135]. αGAG was generated in the FHCRC Hybridoma Production Facility using bacterially expressed, GST-tagged GAG following published protocols [136]. GAG protein-coding sequences from nucleotide positions 1789-2748 were fused in frame at the C-terminus of GST using pGEX-6P-1 (Amersham), and purified from Rosetta (DE3) pLyS cells (Novagen). Approximately 500 hybridoma colonies were identified that screened positively against GST-GAG by the ELISA screening test. Cell line P3E9 (αGAG) was obtained by re-screening all of the positive hybridoma cell supernatants by indirect immunofluorescence microscopy of fixed wild-type and *Cer1(RNAi)* gonads.

Inhibitor experiments

Worms were collected in drops of M9 buffer [137] on a taped microscope slide and rinsed in three or more changes of M9 to clear bacteria, then rinsed in two changes of gonad culture media (GCM: 50% Leibovitz L-15 medium (GIBCO), 10% Fetal Calf Serum (GIBCO), 5.6% sucrose, 2mM $MgCL_2$). Slides containing 20-30 worms in a

drop of GCM were placed on a precooled dissecting microscope stage at 8-10°C; cooling was used to slow animal movements to facilitate dissection. Worms were cut immediately with a scalpel blade, just behind the pharynx to release the gonad, and the slides were removed to room temperature; the elapsed time on the cooled stage did not exceed 2 minutes. An equal volume of 15°C GCM was added that contained 2X nocodazole (Sigma) plus 1 mM levamisole (Sigma) in GCM. Nocodazole was diluted fresh each time from a 5 mg/ml stock in dimethylsulfoxide kept at -20°C. The levamisole was added after dissection to prevent damage to the gonad from the contraction of attached muscles during incubation with the inhibitor. The slide with gonads plus inhibitor was placed on a pre-cooled block at 15°C, and transferred to a 15°C incubator for the designated time.

Fixation, immunostaining, and microscopy

MeOH fixation was used for images shown in Figure 2.3 and for experiments listed in Tables 2.3 and 2.4 as follows. Worms were dissected on microscope slides in a small drop of M9 buffer and covered with a coverslip. The slide was frozen on dry ice, the coverslips removed, and the slide immersed in –20°C MeOH (5 minutes) before rinsing in three changes of PBS for 5 minutes each. Slides were incubated with antibody overnight at 4°C. A two step formaldehyde fixation [138] was modified for experiments to simultaneously localize *Cer1* GAG and microtubules as follows. Worms were dissected as for the nocodazole experiments above, except that gonad buffer (GB: 75 mM HEPES (6.9), 1.2% sucrose, 40 mM NaCl, 5 mM KCL, 2 mM MgCL2, 1 mM EGTA) was substituted for GCM. After dissection, an equal

volume of fixation buffer #1 [6% formaldehyde, 75 mM HEPES (6.9), 40 mM NaCl, 5 mM KCL, 2 mM MgCL2, 1 mM EGTA] was added for 2 minutes, then two equal volumes of fixation buffer #2 [3% formaldehyde, 30 mM Sodium Borate (11), 2 mM MgCl2] were added briefly before removing the combined fixative and adding fixation buffer #2 for 7 minutes. The gonads were rinsed briefly with PBS, permeabilized in PBS plus 0.3% Triton X-100 (Sigma) for 10 minutes, then rinsed several times in PBS and immunostained overnight at 4°C.

Widefield images (Figure 2.2B-2.2D, Figure 2.3A-2.3E) were acquired with a Nikon Eclipse 90i upright microscope using 40x (Plan Fluor, 1.4 NA) and 60x (Plan Apo VC, 1.4 NA) lenses and a Retiga-4000DC camera (QImaging). Images were exported to Adobe Photoshop for cropping, reorientation, and contrast and brightness adjustments. All other images were acquired with a DeltaVision microscope and processed using deconvolution software (Applied Precision). All images shown are single plane, except for Figure 2.5A and Figure 2.5E, which are two plane (0.2 μm) projections to visualize ring channels.

For electron microscopy, L4 hermaphrodites grown at 20°C-23°C were selected and allowed to develop to young adults for 24-48 hours. For male/female strains, L4 females were collected and mated with males. Gonads were dissected from 40-60 adults, then fixed with glutaraldehdye and osmium tetroxide and processed for electron microscopy as described [43]. Grids were viewed with a JEOL JEM-1230 transmission electron microscope. To avoid scoring individual germ cells and

gonads more than once in the initial survey, each gonad was numbered and scored in a single, representative thin section through the middle of the core. Germ cells typically were examined at 4,000X to 6,000X, and candidate VLPs were photographed at 8,000X with a Gatan UltraScan 1000 CCD camera. For each sample, germ cells were examined in the distal, mitotic region, and at all stages of meiosis through oogenesis. The gonad core contains large numbers of vesicles of various shapes that might be confused with VLPs, however the cytoplasm around germ nuclei is relatively devoid of organelles. Thus, quantitation was performed only on germ "cells" up to the ring channel, although the core was inspected in many gonads.

Acknowledgements

We thank Jacqualyn Burnson and Jason Pitt for expert technical assistance, Jeff Molk, Jeff Rasmussen and Maxine Linial for advice, and Karen Bennett, Marie-Anne Felix, Bob Horvitz, Karin Kiontke, Craig Mello, Erich Schwarz, James Thomas, and William Wadsworth for strains or reagents. Some of the nematode strains used in this work were provided by the Caenorhabditis Genetic Center, which is funded by the NIH National Center for Research Resources (NCRR).

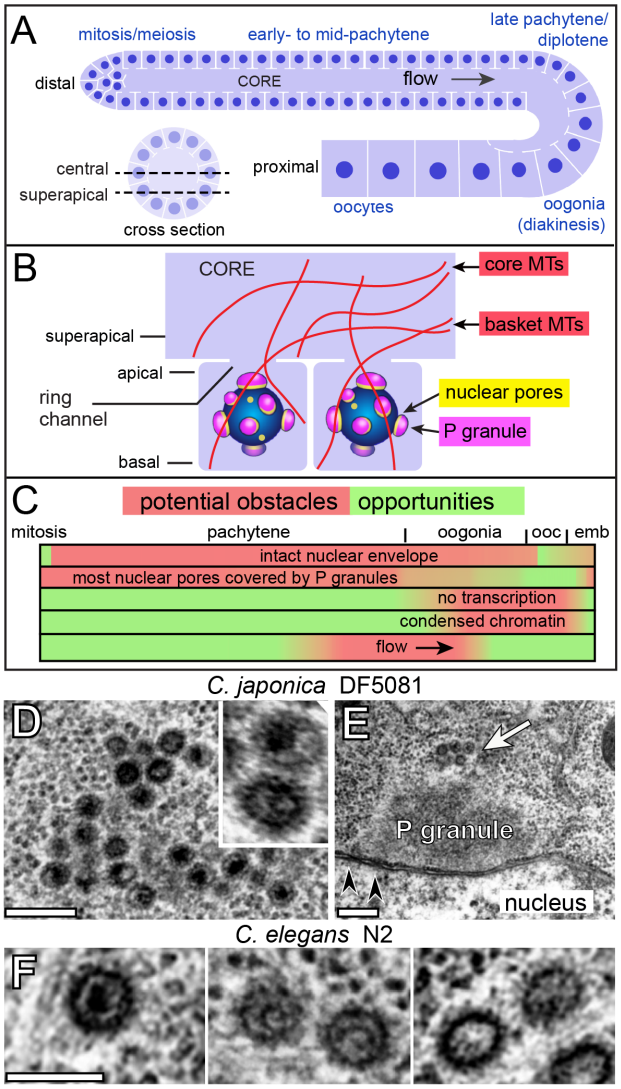

Figure 2.1. Nematode gonads contain VLPs.
(A) Diagrams of longitudinal and cross sections through one arm of the adult hermaphrodite gonad with germ nuclei indicated in dark blue; somatic sheath cells that surround the gonad are not shown. Optical sectioning planes referred to in this paper are indicated in the cross-section (dashed lines). During development, germ cells move from the distal (mitotic) end of the gonad toward the proximal end, where they differentiate as oocytes. (B) Enlarged diagram of two germ cells with ring channels opening to the gonad core. Basket and core microtubules (MTs) are drawn in red. (C) Linear representation of germ cell development. Red shading indicates region-specific conditions in germ cells that might impede viral replication. These include the state of the nuclear envelope [139], P granules [98], transcription [140], chromatin [141], and cytoplasmic flow [66]; ooc= oocytes, emb= embryos. (D-E) Electron micrographs of *C. japonica* VLPs. Low magnification in panel E shows a small cluster of VLPs (arrow) on top of a P granule; arrowheads indicate examples of nuclear pores. See also Supplemental Figure S2.1A-S2.1C). (F) *C. elegans* VLPs showing variation in internal electron density; note curved, rod-like bodies within the VLPs in the middle panel. Scale bars: D (0.2 µm), E (0.5 µm), F (0.1 µm).

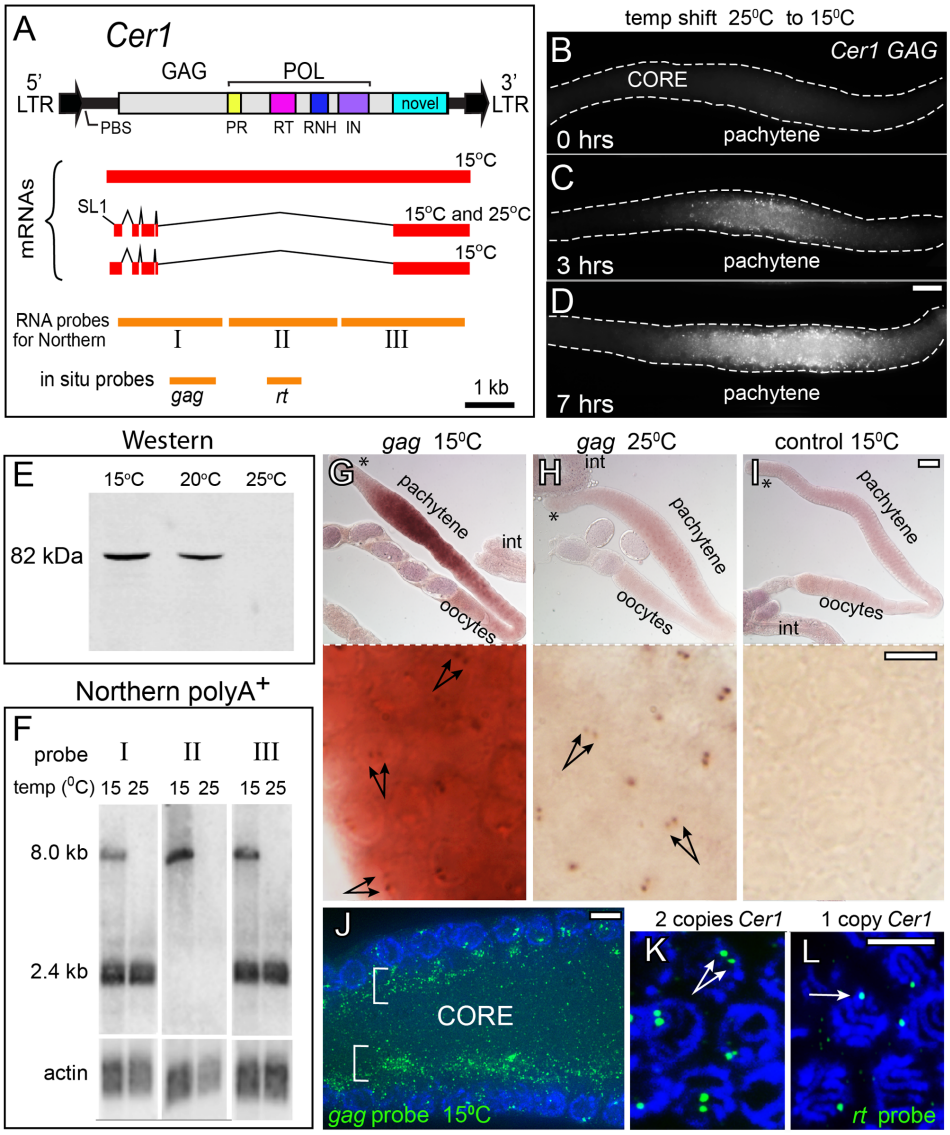

Figure 2.2. *Cer1* GAG expression is temperature dependent.
(A) Diagram of the *Cer1* retrotransposon, mRNA products confirmed by sequencing in this study, and the locations of probes used for Northern and in situ experiments. Colored boxes within POL correspond to homology regions for Protease (PR), Reverse Transcriptase (RT), Ribonuclease H (RNH), and Integrase (IN) as described [1]. mRNAs beginning 5' to the splice acceptor used for SL1 trans-splicing were demonstrated by RT-PCR using primer pairs KE409F, KE416R and KE409F, KE401BR (Materials and Methods). (B-D) Gonads immunostained with αGAG; gonads were dissected from day 1 adults raised at 25°C, then shifted to 15°C for the times indicated. (E) Western blot of total proteins from adults grown at either 15°C, 20°C, or 25°C; blots were stained with αGAG. (F) Northern blots of poly(A)$^+$-selected RNA from adults grown at either 15°C or 25°C; blots were hybridized with probes (I-III) as diagrammed in panel A. Normalization relative to a control actin probe showed that the difference in signal between 15°C and 25°C is at least tenfold for the 8 kb band. (G-I) RNA in situ hybridization (alkaline phosphatase detection) of gonads and intestines (int) from adults cultured at the indicated temperatures, using probes for sense or antisense (control) *gag*-containing mRNA; each asterisk indicates the distal, mitotic region of the gonad. Bottom panels are higher magnifications of the same gonads showing *gag*-containing RNA concentrated in paired, nuclear dots (double arrows). (J) Fluorescence in situ hybridization (FISH) of a 15°C gonad using the *gag*-specific probe (green); the image shows a longitudinal, optical section through the gonad core.

Note that RNA is concentrated in the superapical region of the core (brackets), and in paired dots within nuclei (blue, DAPI). (K-L) High magnification of FISH with the *rt*-specific probe; images show two nuclear dots in wild-type germ cells (panel K, two copies of *Cer1*) and one dot in nuclei from N2/CB4856 heterozygotes (panel L, one copy of *Cer1*); control CB4856 homozygotes which lack *Cer1* show no staining (data not shown).
Scale bars: B-D (20 μm); G-I (20 μm), inserts (5 μm); J-L(5 μm)

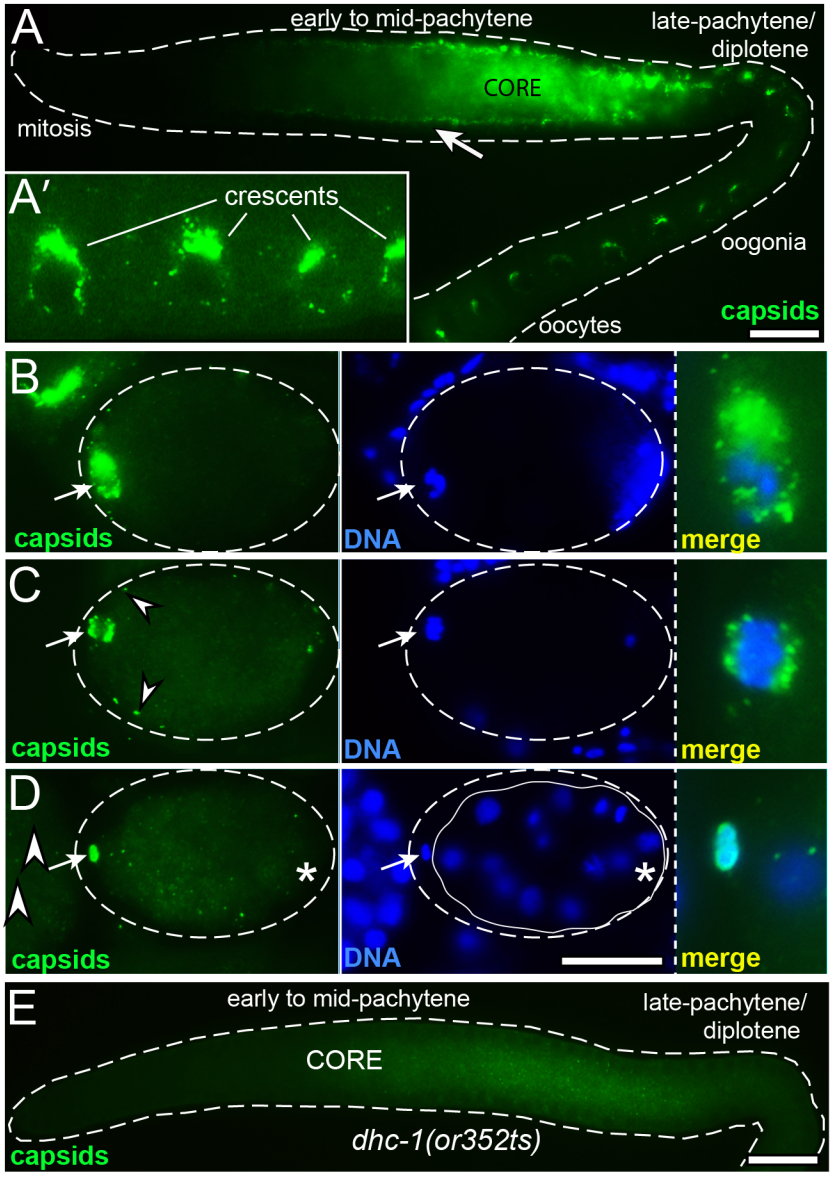

Figure 2.3. *Cer1* capsids show stage-specific changes in localization.
(A) Low magnification, wide-field image of a gonad from a 15°C adult, immunostained with αGAG to detect *Cer1* capsids (green). Note that capsids in the mid-pachytene region are enriched along the superapical zone of the core (compare with 2.2J), rather than within germ cells at the periphery (arrow). (A') High magnification showing the crescent-shaped aggregates of capsids by oogonia nuclei. (B,C) Newly fertilized eggs showing the maternal chromosomes at diakinesis (B), and at metaphase of the meiosis I division (C). Arrows point to concentrations of capsids associated with the meiosis I spindle, and arrowheads indicate small foci of capsids at the periphery. The examples shown for these images contain unusually high numbers of capsids; most eggs show the same localization pattern but with fewer capsids, and many fertilized eggs contain no detectable capsids. (D) 28-cell stage embryo; the arrow points to capsids within the first polar body. The asterisk is below the germ cell precursor, showing that capsids do not concentrate in this cell. The eggshell is outlined in panels B-C (dashed line), and the cellular boundary of the 28-cell embryo is indicated in panel D (white line). (E) Capsid localization in a *dhc-1*/dynein mutant; this gonad was scored as "+" in Table 2.3. Scale bars: A-E (20 μm).

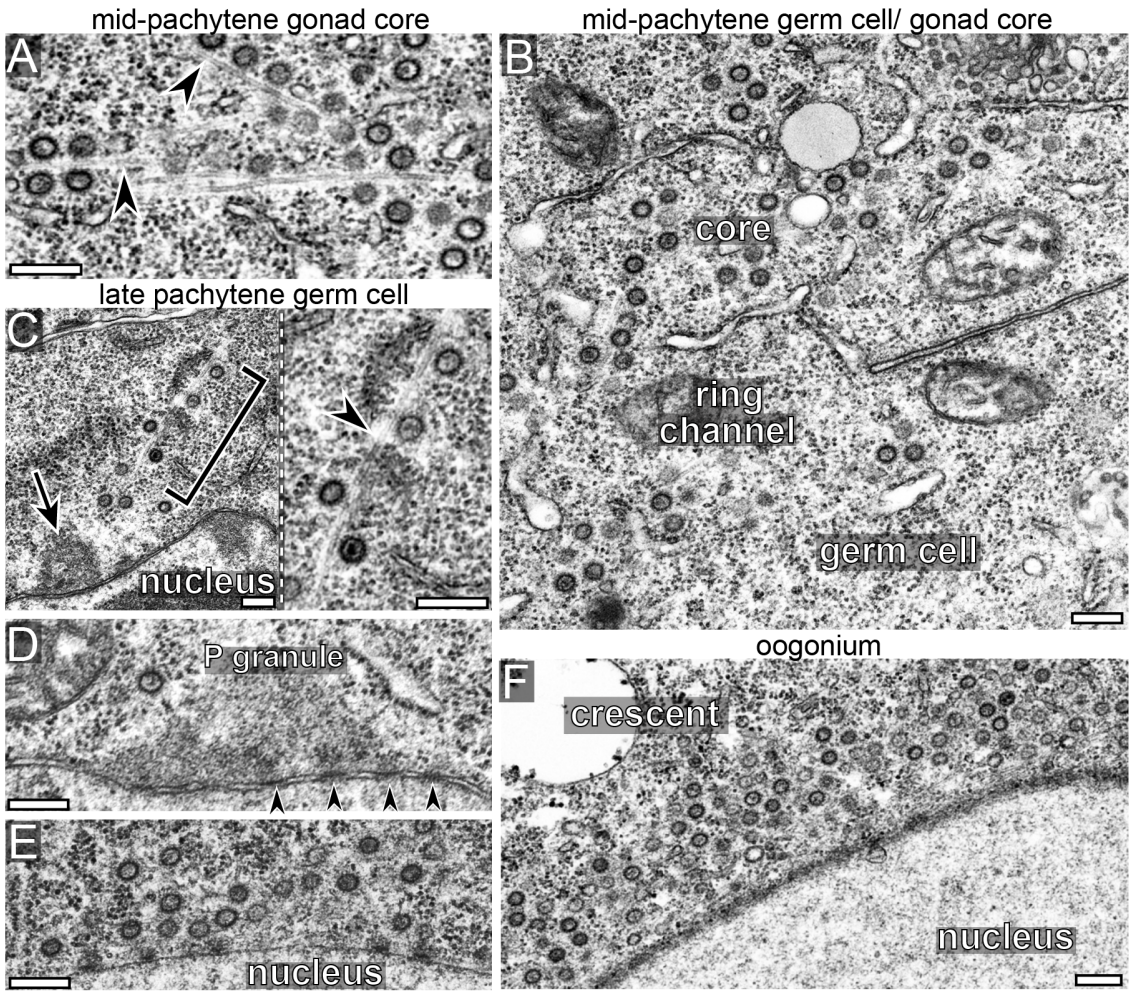

Figure 2.4. *Cer1* capsids localize on microtubules.

(A-F) Electron microscopy of gonads from 15°C adults; regions of the gonad are as indicated at the top of the panels. Capsids localize predominantly to the core in the mid-pachytene region, but concentrate near nuclei in late-pachytene germ cells (C-E) and in oogonia (F). Note that many capsids localize with microtubules (arrowheads) both in the core (panel A) and in germ cells (panel C). P granules are visible in panels C (arrow) and in panel D; arrowheads in panel D indicate examples of nuclear pores. (E) Cluster of capsids near the nucleus of an early oogonium. (F) A "crescent" of capsids by an oogonium nucleus; there are at least 64 capsids and numerous microtubules visible at higher magnifications of this single thin section (data not shown). Scale bars: A-F (0.2 μm).

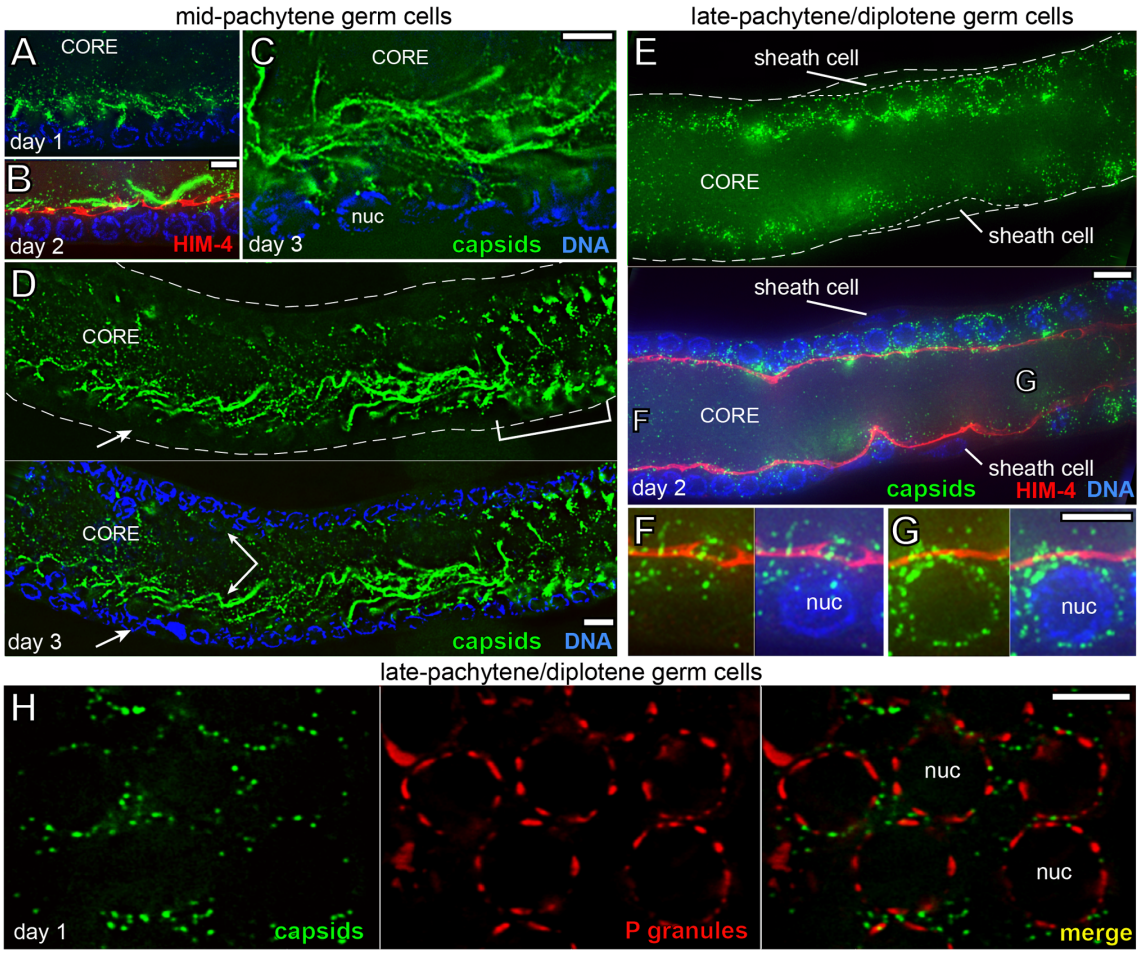

Figure 2.5. Capsids accumulate in the mid-pachytene gonad core as adults age at 15°C.

(A-D) Longitudinal, optical sections through gonads showing increased accumulation of capsids (green) with adult age, as indicated. The gonad in panel B is immunostained for HIM-4/hemicentin (red) to visualize the apical membrane (see Figure 2.1B). Note that capsids localize predominately in the core, outside the ring channel and away from nuclei (blue, DAPI). (C) Capsids grouped in wavy lines and tangles of lines in the mid-pachytene region of a day 3 adult. (D) Low magnification of the mid-pachytene region. Note variation in capsid abundance between the two sides of the gonad core (double-headed arrow), and that the wavy lines of capsids disappear as germ cells move proximally into late pachytene (bracketed region). (E-G) The late-pachytene/diplotene region, stained and imaged as for panel B; two of the somatic sheath cells that surround the gonad are visible in this image. Germ cells from regions F and G are shown at high magnification, oriented as in Figure 2.1B. An optical rotation of a similar region of the gonad is shown in Supplemental Movie S1. (H) Optical section through germ nuclei in the late-pachytene/diplotene region showing capsids (green) and P granules (red, αPGL-1). Note that capsids localize close to the nuclear envelope, but most are not directly on, or within, P granules. Electron micrographs of capsids within P granules are shown in Supplemental Figure S2.1H. Scale bars: A-C, F-H (5 μm), D-E (10 μm).

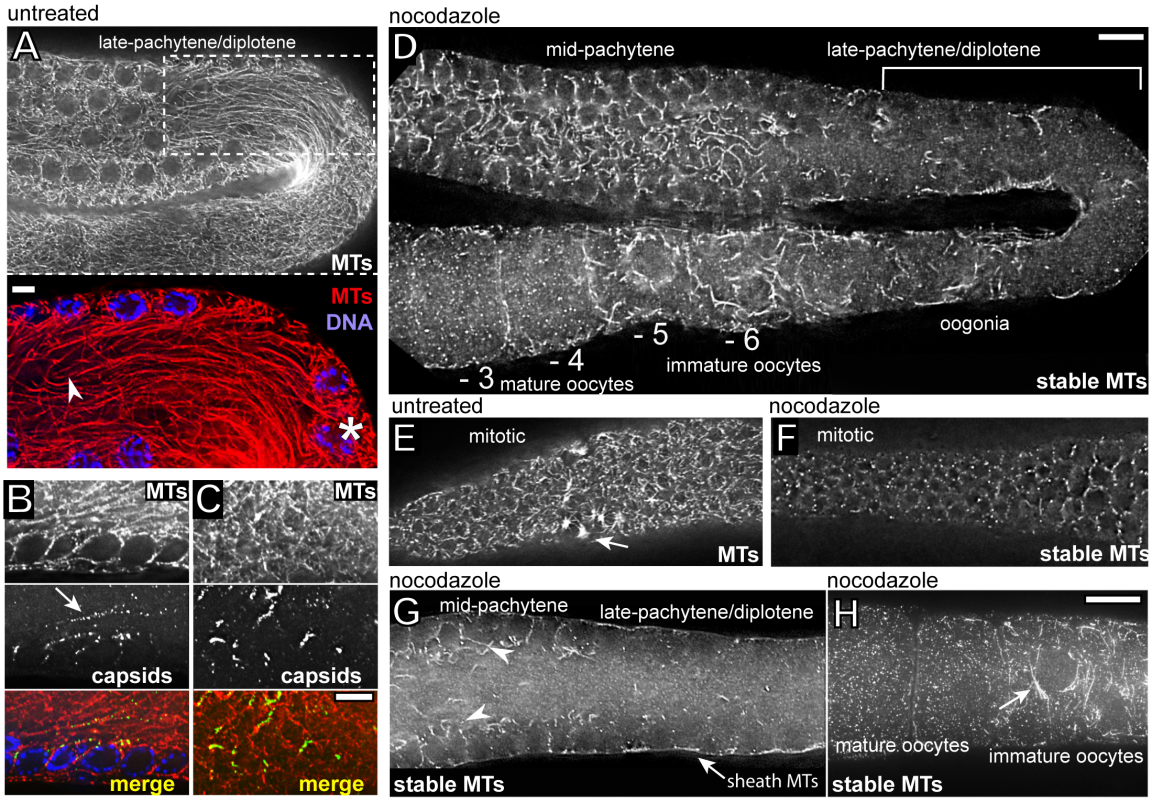

Figure 2.6. A subset of microtubules in the mid-pachytene region are inhibitor-resistant, or stable.

(A) Optical section through the superapical plane of an untreated day 1 adult gonad showing the dense network of long microtubules (see Figure 2.1A for section orientation). The inset shows a high magnification of the dashed box, with an arrowhead marking the end of a single microtubule traced from the indicated germ cell (asterisk). (B,C) Optical sections through the central planes of untreated, day 1 adult gonads; the gonads are immunostained for both microtubules and *Cer1* capsids. Note that capsids are concentrated in linear or irregular shapes, while the microtubules are distributed uniformly. (D) Optical section through the superapical plane of a day 1 adult gonad treated with nocodazole; the bracketed region is the same late-pachytene/diplotene region, and the same optical plane, as for the untreated gonad in panel A. Note that most microtubules have disappeared from this region after nocodazole treatment, in contrast to the numerous "stable" microtubules that remain in the mid-pachytene region. (E,F) Microtubules in the distal, mitotic regions of gonads before (E) and after (F) nocodazole treatment. The arrow in panel E indicates an example of a mitotic spindle. Most of the brightest spots of tubulin visible in panel F co-localize with centrosomes (data not shown). (G) Optical section through the central plane of a nocodazole-treated gonad. This sectional view combined with that in panel D illustrates that most of the stable microtubules in the mid-pachytene region are in the superapical zone of the core (arrowheads). Note that most of the microtubules in the late-pachytene/diplotene germ cells have depolymerized; stable microtubules that appear at the periphery of the gonad (arrow) are outside of germ cells and within the thin cell bodies of somatic sheath cells. (H) Stable microtubules in nocodazole-treated oocytes; the oocytes advance in age right to left (see Figure 2.1A). Note the focus of stable microtubules (arrow) near the oocyte nucleus, and the abrupt disappearance of all stable microtubules in the more mature oocyte to the left; compare with oocyte progression panel D, where numbers indicate oocyte position relative to ovulation.

Scale bars: A-C (5 µm), D-H (10 µm).

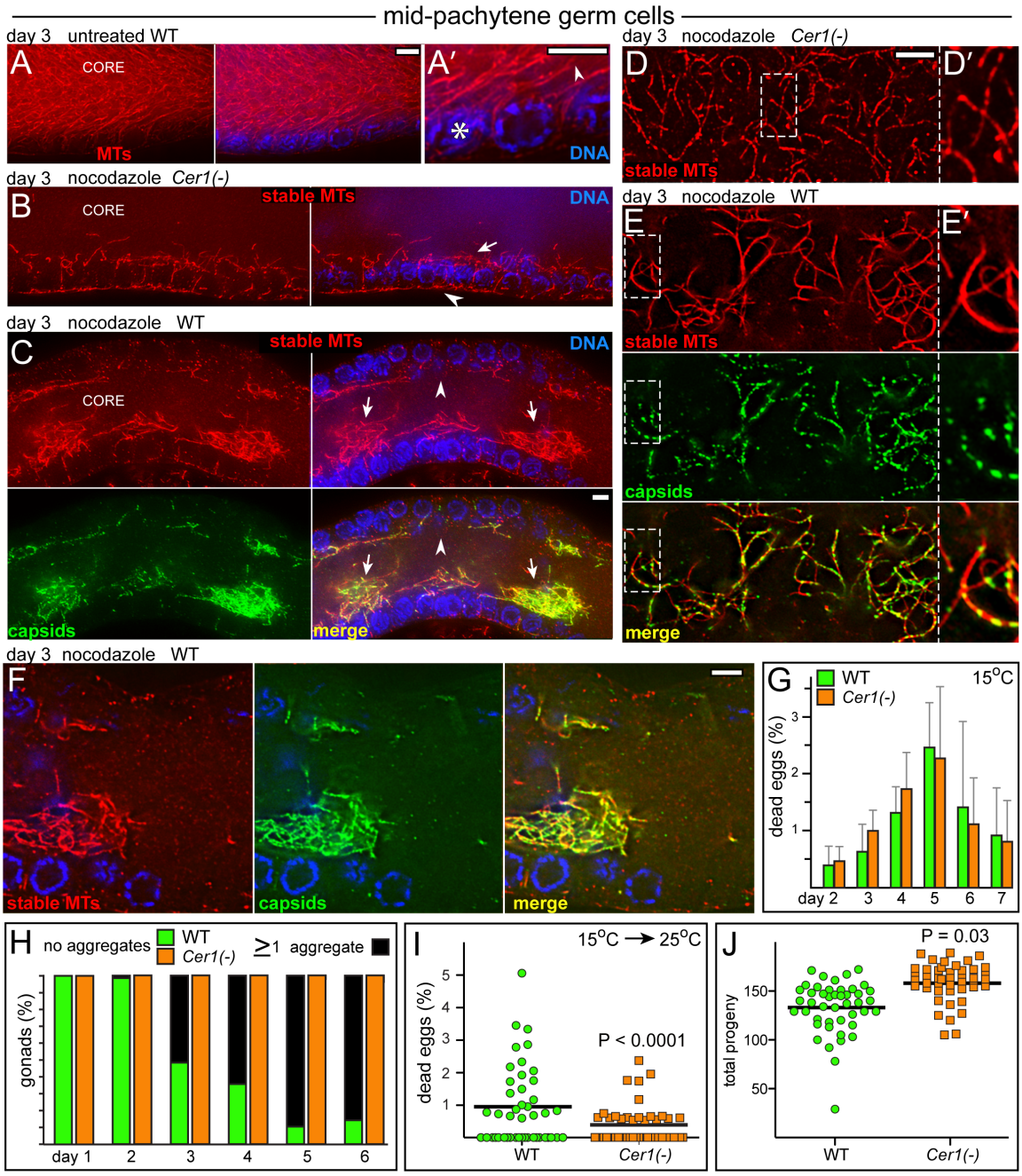

Figure 2.7. *Cer1* capsids accumulate on stable microtubules in the mid-pachytene region.

(A-F) All images are of the mid-pachytene region of day 3 adult gonads. Panels A-C and F show central optical planes, and panels D,E show superapical optical planes. (A) Untreated wild-type gonad, showing the dense population of total microtubules in the core; panel A' indicates a basket microtubule (arrowhead) traced back to the germ cell of origin (asterisk). (B) Stable microtubules in a nocodazole-treated, Cer1(-) gonad. Most of the core microtubules have depolymerized, and the stable microtubules that remain are enriched in the superapical zone (arrow); the arrowhead points to stable microtubules in sheath cells. Stable microtubules in a nocodazole-treated, wild-type gonad. Note the multiple aggregates of stable microtubules (arrows) and the neighboring regions devoid of microtubules (arrowhead). Note also that capsids are strongly concentrated in the microtubule aggregates (see also panel D below). (D-E) Images of stable microtubules as in panels B and C,

respectively, but viewed from a superapical plane. Note the thick and irregular staining of the wild-type stable microtubules, and their association with *Cer1* capsids. Panels at right are high magnifications of the dashed, boxed regions at left. (F) High magnification image of an aggregate from the gonad shown in panel C. Note the abrupt loss of stable microtubules, and most capsids, to the right of the panel as germ cells exit pachytene (see also Figure 2.8B). (G) Quantitation showing mean and standard deviation in the number of dead eggs laid by wild-type and *Cer1(-)* adults grown for the indicated number of days at 15°C. This analysis was performed on 20-25 separate pools of 5 adults each that were cultured in the constant presence of males to maintain ovulation. Brood sizes remained comparable up to day 5 (WT= 437 +/- 57 total progeny, *Cer1(-)* = 442 +/- 83), after which some adults in both sets stopped laying eggs. (H) Percentage of gonads without aggregates of stable microtubules in wild-type (green) and *Cer1(-)* (orange) animals as a function of adult age. Note that nearly all wild-type gonads contain 1 or more aggregates by day 5. (I, J) Analysis of dead eggs and total progeny produced within 24 hours after shifting 3 day adults from 15°C to 25°C. Dead eggs were scored in panel I only if they were approximately normal size. The wild-type adults also produced significantly more small, "partial" eggs than *Cer1(-)* [WT= 2.9%+/- 0.4 partial eggs, *Cer1(-)* = 1.6% +/- 0.2; P<.0001]. Scale bars: A-F (5 μm).

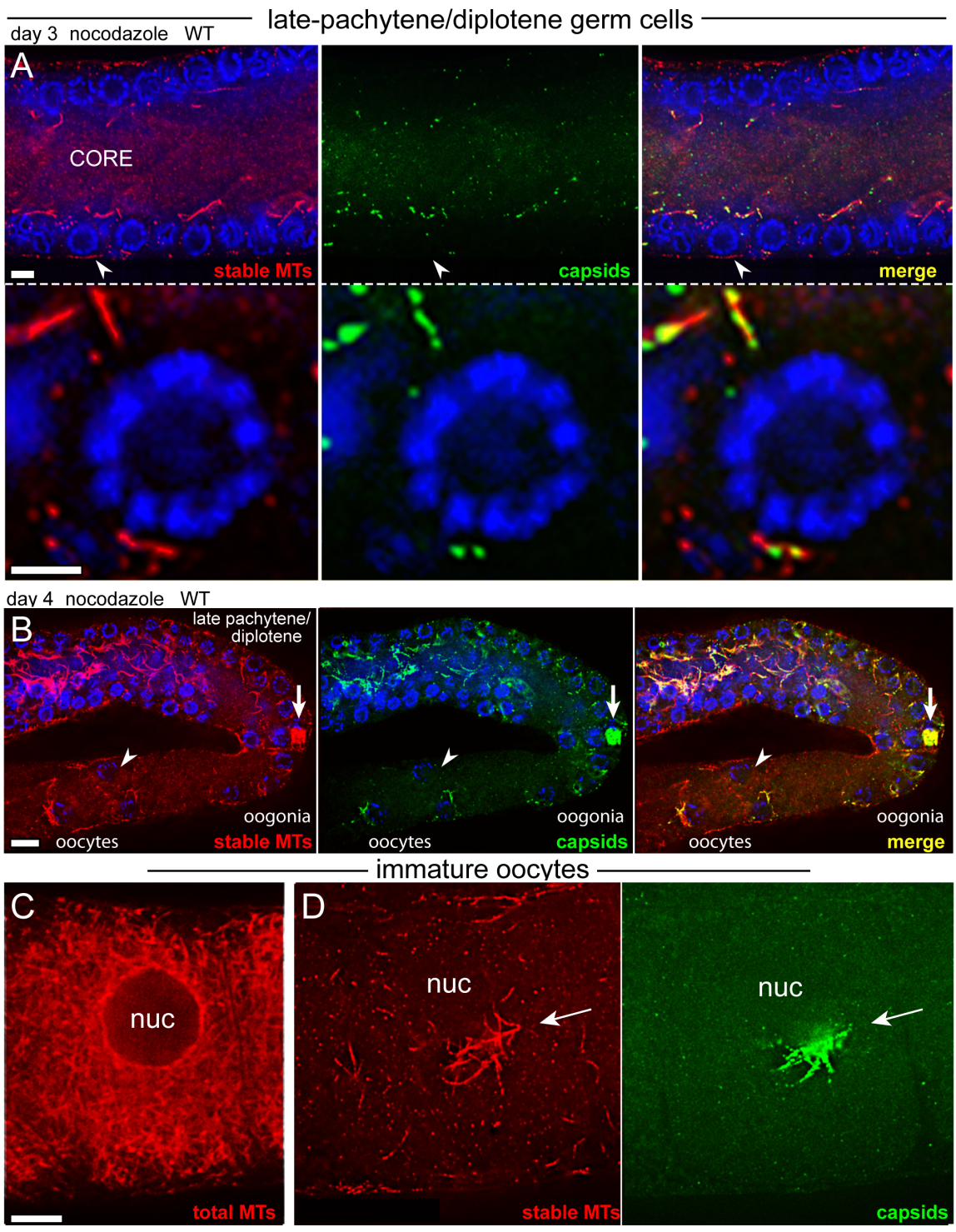

Figure 2.8. Capsid localization near late-pachytene nuclei requires inhibitor-sensitive microtubules.

(A) Late-pachytene/diplotene region of a nocodazole-treated, day 3 wild-type gonad showing the near absence of stable microtubules and capsids; the arrowhead indicates a germ cell shown a higher magnification in the lower panels. Compare these images with the abundant microtubules and capsids in the same region of untreated gonads (Figure 2.6A, boxed region, and Figure 2.5G, respectively). (B) Low magnification image of a nocodazole-treated, day 4 wild-type gonad, oriented

as in Figure 2.6D. Note the rare example of a large aggregate of stable microtubules and capsids in an early oogonium. Because oogonia in this region begin to receive cytoplasmic flow from the gonad core, it is possible that this focus broke off from the mid-pachytene region, rather than surviving the normal developmental progression through late pachytene. Note also that many of the oogonia and early oocytes lack crescents of capsids (arrowhead; compare with Figure 2.3A), and the few crescents of capsids co-localize with stable microtubules. (C) Untreated, wild-type oocyte showing enrichment of microtubules near the nuclear envelope. (D) Nocodazole-treated, wild-type oocyte showing a focus of stable microtubules and a crescent of capsids. Oocytes shown in both panels occupied the -5 position in the ovulation sequence. Scale bars: A (5 μm), B (10 μm), C (8 μm).

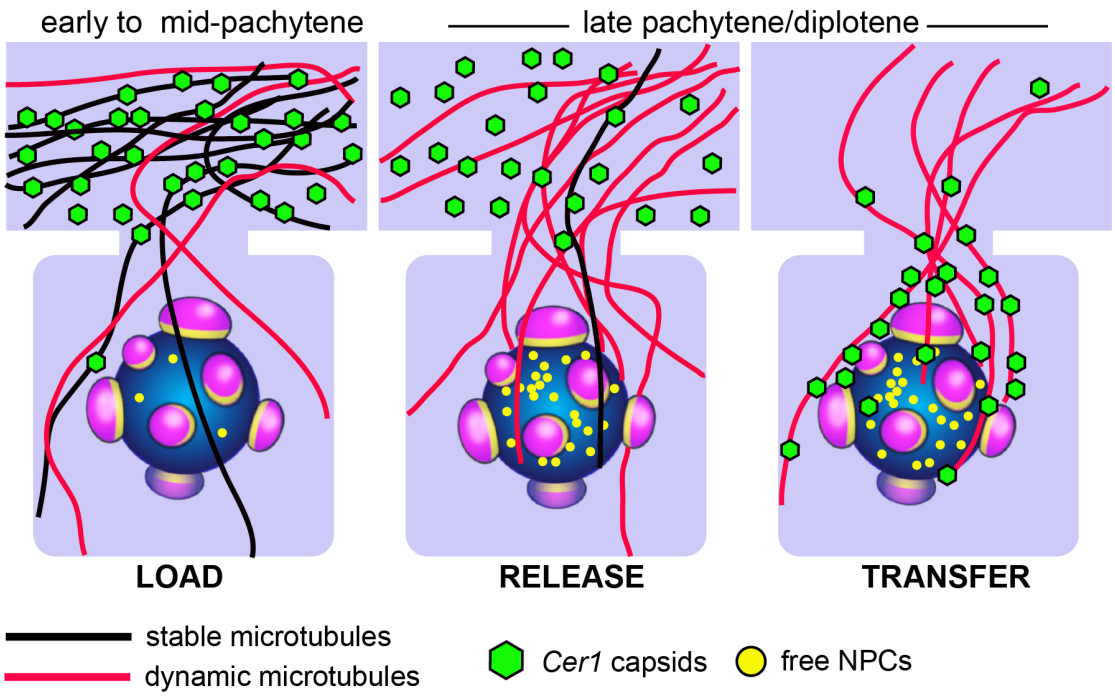

Figure 2.9. Load-Release-Transfer model for capsid traffic toward late-pachytene/diplotene nuclei.

Cartoon of capsids and microtubules as germ cells progress into late pachytene/diplotene. Capsids that had accumulated on stable microtubules (black) in the core (top) are released as these microtubules depolymerize. The released capsids transfer to surrounding labile, or dynamic, microtubules (red) and traffic into germ cells. In an alternative model, capsids could remain on the original microtubule as it becomes destabilized. Traffic could involve microtubule dynamics, or microtubule motor proteins.

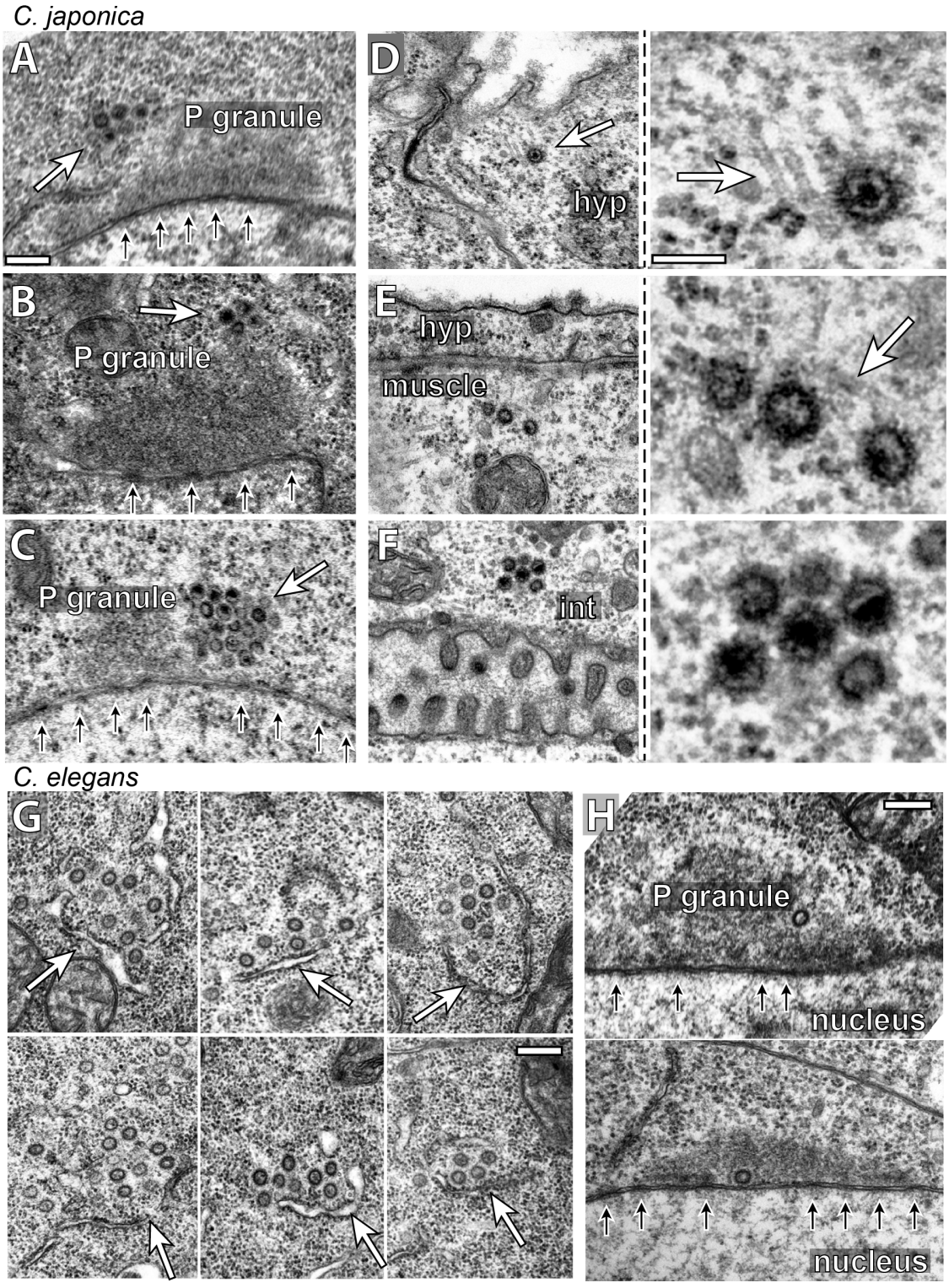

Supplemental Figure S2.1. *C. japonica* VLPs are associated with P granules in adult gonads, and microtubules in somatic cells.

Electron micrographs of VLPs in *C. japonica* (A-F) and *C. elegans* (G-H). *C. japonica* images show VLPs (white arrows) clustered on P granules in an adult female (A), and in adult males (B and C); small black arrows indicate nuclear pores. (D-F) *C. japonica* embryos showing VLPs in differentiating

somatic tissues: hypodermis (hyp, panel D), muscle (panel E), and intestine (int, panel F). Insets show higher magnification examples of embryonic VLPs; note association with microtubules in panels D and E (arrows). (G) Examples of *C. elegans* VLPs when they are first detected in the early- to mid-pachytene core of the gonad. Capsids typically appear in small, non-contiguous groups associated with rough endoplasmic reticulum (arrows). (H) Examples of capsids within P granules in late pachytene germ cells; arrows indicate nuclear pores. Scale bars = 0.2 μm.

Supplemental Figure S2.2. *Cer1*-family LTRs contain predicted binding sites for EFL-1/E2F.

Alignment of 5' LTR and PBS sequences from (1) the N2 copy of *Cer1*, (2) a member of a now extinct, *Cer1*-like family of retrotransposons in N2 (cosmid C03F11), and (3) a *Cer1*-like retrotransposon in the *C. japonica* genome (Contig10639; *C. japonica*-7.0.1, http://genome.wustl.edu). Shaded nucleotides are present in two or more LTRs. Boxed regions indicate predicted E2F/EFL-1 binding sites (G/C)GCG(G/C)GAA [108] , polyA-addition sites, and a possible Primer Binding Site (PBS) 3' to the LTR. The sequence TGG (underlined) at the start of the PBS is not complementary to the 3' end of the *C. elegans* tRNA-Pro gene, but the complementary triplet CCA is added posttranscriptionally to the 3' terminus of eukaryotic tRNAs. Fragments from additional members of the extinct family of *Cer1-like* retrotransposons are found in the following N2 clones: C18A11, C18H2, C24H12, F07G6, F11A5, F16B12, F28B4, F28H6, F40E3, F54G2, T05E8, T22F7, Y20C6A, Y39B6A, Y59E1A, Y67D8C, Y69A2AR, Y71G12B, Y751H4A, Y82E9BL, ZC513, and ZC53 (*http://www.wormbase.org*, release

WS227, 2011). For example, a family member inserted in the N2 gene F54G2.1 contains a partial 5' LTR, the PBS, and sequences that can encode a *Cer1*-like GAG and protease.

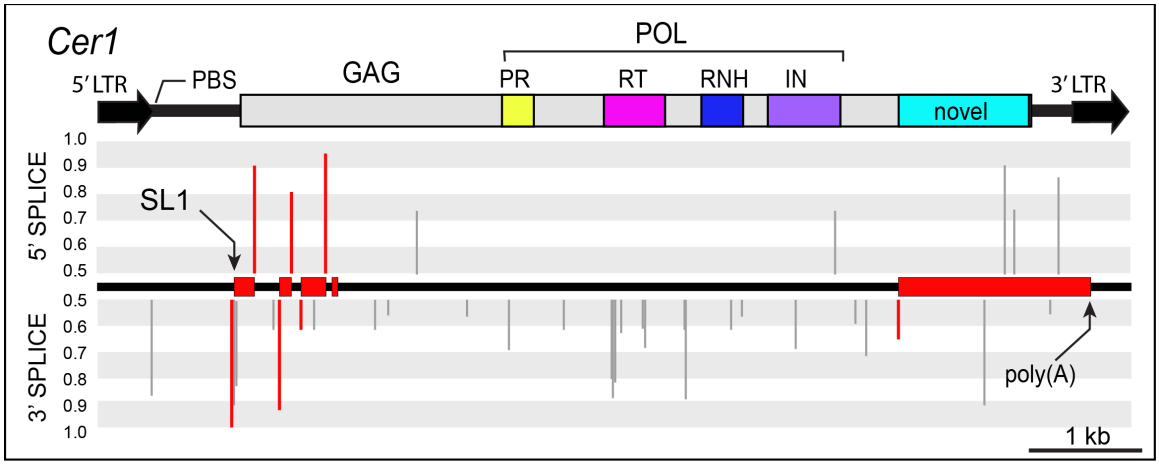

Supplemental Figure S2.3. Generation of the 8 kb *Cer1* mRNA requires skipping *C. elegans* consensus splice sites.

The central black bar represents the *Cer1* sequence (diagrammed at top). Vertical lines above and below the bar indicate candidate 5' or 3' intron splice sites, respectively; the height of each line indicates the *C. elegans* splice site prediction score (scale 0.5 to 1.0) using NetGene2 [http://www.cbs.dtu.dk/services/NetGene2] [73,142]. Vertical lines colored red are the sites used to generate the spliced, 2.4 kb *Cer1* mRNA at 15°C and 25°C (this study). The red boxes represent exon sequences in the 2.4 kb mRNA, and the sites of SL1 trans-splicing and poly(A) addition are indicated by arrows. Note that most of splice sites utilized conform well with *C. elegans* consensus sequences, and must be skipped to generate the 8 kb *Cer1* mRNA. The intron splice sites that generate the fourth exon (3' site = attcag and 5' site = gtgag) are less common and fall below the 0.5 score illustrated, but are present in other spliced introns in *C. elegans* [112].

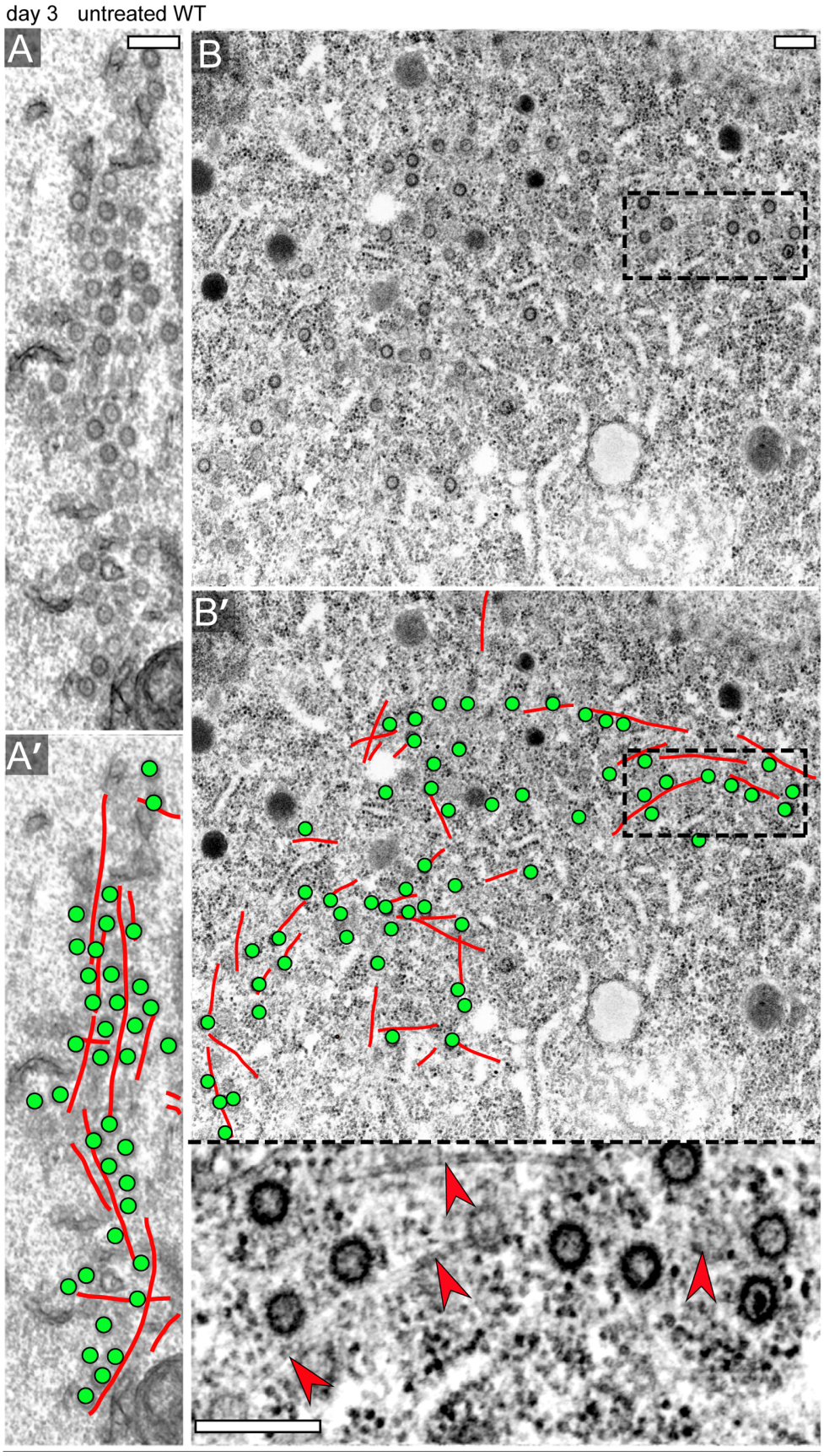
day 3 untreated WT
A
B
B′
A′

Supplemental Figure S2.4. Aggregates of capsids and microtubules are present in day 3 and older, wild-type adults.

(A-B'). Electron micrographs showing aggregates of capsids and microtubules that resemble the wavy lines of capsids (A) and tangles of wavy lines (B) observed by immunofluorescence; compare with Figure 2.5C and 2.7C, respectively. Capsids and microtubules visible in these and/or the adjacent thin sections (not shown) are colored in panels A' and B'. The inset in panel B shows capsids and microtubules (arrowheads) in the boxed region at higher magnification. Scale bar = 0.15 μm (A, B)

TABLE 2.1 Electron microscopy of VLPs in *Caenorhabditis*

Strain (20-23°C)	Locality	VLP-positive germ cells (%)	Germ cells scored
C.e N2 (lab stock) "Wild type"	Bristol, England	3.9	563
C.e N2 Reference	Bristol, England	6.0	941
C.e N2 Reference males	Bristol, England	0.0	955
C.e N2 (ancestral)	Bristol, England	3.9	933
C.e CB4853	Altadena, CA	0.0	586
C.e CB4854	Altadena, CA	0.0	774
C.e CB4555	Pasadena, CA	0.0	681
C.e CB4858	Pasadena, CA	0.0	915
C.e DH424	El Prieto Canyon, CA	0.0	808
C.e CB4856	Hawaii	0.0	1172
C.e KR314	Vancouver, Canada	4.6	326
C.e JU322	Merlet, France	3.7	406
C.e JU263	Le Blanc, Indre, France	0.0	871
C.e RW7000	Bergerac, France	0.0	745
C.e CB4851	Bergerac, France	0.0	620
C.e AB1	Adelaide, Australia	0.0	629
C.e JU258	Ribeiro Frio, Madeira	0.0	745
C.e MY2	Mecklenbeck, Germany	0.9	544
C.e RC301	Frieburg, Germany	0.0	889
C. brenneri PB2801	Costa Rica	0.0	610
C. briggsae AF16	Ahmedabad, India	0.0	657
C. japonica DF5081	Takeo, Japan	19.3	530
C. japonica DF5081 males	Takeo, Japan	16.2	378
C. remanei EM464	Brooklyn, NY	0.0	630
C. remanei SB146	Freiburg, Germany	0.0	561

TABLE 2.2 Electron microscopy of VLPs in *C. elegans* strains

Genotype or Condition (20-23°C)	Strain	Defective Protein or Pathway	VLP-positive germ cells (%)	Germ cells scored
control	N2		3.9	563
spontaneous steriles	N2		0.0	334
heat shock: 34°C for 45 min, 4hr recovery	N2		2.4	430
adr-1(gv6); adr-2(gv42)	BB4	RNA editing; [143]	0.8	777
dcr-1(ok247)	BB1	Dicer; [144]	0.5	743
rde-1(ne300);ced-1(e1735);ced-3(n717)	JJ2230	defective in RNAi and cell death pathways; increases titer of viruses in infected cultured cells; [32,33,35,36]	4.0	155
rde-1(ne300);ced-1(e1735);ced-3(n717) day 5 adults	JJ2230	defective in RNAi and cell death pathways; increases titer of viruses in infected cultured cells; [32,33,35,36]	0.6	997
ppw-1(pk2505)	NL2550	defective in germline RNAi; [145]	0.0	968
prg-1(n4357); prg-2(n4358)	MT14769	Piwi proteins; mutants defective in transposon silencing; [18,146],	0.0	356
kgb-1(um3);kgb-2(km16)	KB7	P granule regulation; [147]	0.2	553
alg-1(RNAi); alg-2(ok304)	WM53	microRNA pathway; [148]	8.0	510
MAGO12	WM191	mutations in each of 12 Argonaute proteins, RNAi defective; [149]	5.5	604
unc-119(ed3); arIs37; cdIs32[pcc1::DT-A(E148D); unc-119(+) pmyo2::GFP]	NP17	no coelomocytes; [150]	6.7	134
Cer1(RNAi)	N2	LTR retrotransposon; [91]	0.0	1213
Cer2(RNAi)	N2	LTR retrotransposon; [91]	5.9	669
Cer3(RNAi)	N2	LTR retrotransposon; [91]	5.5	599
Cer4(RNAi)	N2	LTR retrotransposon; [91]	3.8	739
Cer5(RNAi)	N2	LTR retrotransposon; [91]	6.3	642
Cer6(RNAi)	N2	LTR retrotransposon; [91]	5.1	622
Cer13(RNAi)	N2	LTR retrovirus; [91]	2.6	728

TABLE 2.3 *Cer1* GAG particles detected by immunostaining

Genotype, strain, or condition	Defective protein or pathway	Culture temp (°C)	Stage	Shift temp (°C)	Duration of shift (hrs)	GAG particles (range)	Gonads scored
CB4856		15	A			-	>>100
CB4856		25	A			-	>>100
WT		15	A			+, +++	>>100
WT		20	A			-, +	70
WT		25	A			-	>>100
WT		15	L4			-	23
WT		20	L4			-	15
WT		25	L4			-	44
WT male		15	A			-	18
WT male		25	A			-	18
WT		15	L4	25	21	-	62
WT		15	A	25	21	-	41
WT		15	A	25	10	+	49
WT		25	A	15	10	+, +++	50
fem-1(hc15ts)	spermatogenesis	25	L4	15	24	+, +++	11
hsf-1(sy441)	heat shock [109]	15	A			+, ++	14
hsf-1(sy441)	heat shock [109]	15	L4	25	21	-	15
hsf-1(sy441)	heat shock [109]	15	A	25	21	-	21
WT, 350 mM NaCl	osmotic stress [110]	15	A			+, +++	12
dhc-1(or352ts)	dynein [115]	15	A			- (50%), + (30%), ++ (20%)	20
dhc-1(or283ts)	dynein [115]	15	A			- (26%), + (42%), ++ (32%)	19
dhc-1(or283ts)	dynein [115]	15	A	25	1	- (40%), + (28%), ++(32%)	25
dhc-1(or283ts)	dynein [115]	15	A	25	2	- (52%), + (17%) , ++ (31%)	23
dhc-1(or283ts)	dynein [115]	15	A	25	21	- (98%) + (2%)	41
alg-2(ok304); alg-1(RNAi)	microRNA pathway, [148]	25	A			-	26
ergo-1(tm1860)	endogenous siRNAs, [149]	20	A			+	39
ergo-1(tm1860)	endogenous siRNAs, [149]	25	A			-	24
WM126	mutations in 6 Argonautes, [149]	25	A			-	26
WM191	mutations in 12 Argonautes, [149]	20	L4	25	25	-	>20
WM191	mutations in 12 Argonautes, [149]	25	A			-	>20

TABLE 2.4 *Cer1* GAG particles in *C. elegans* wild strains

Strains	GAG Particles		*Cer1*[a]	*Cer1 insertion in plg-1*[a]
	15°C	25°C		
AB1, CB3191, CB4507, CB4555, CB4851, CB4932, DH424, EG4346, JU311, JU440, JU361, JU394, LSJ1, N2, PX176, TR388	yes	no	present	*yes*
ED3040, JU345, JU395, JU1171, KR314, PB306	yes	no	present	no
CB4854, CB4856, ED3072, JU262, JU263, JU322, JU360, JU362, JU363, JU438, JU1088, MY1, PB303, PX174, RC301	no	no	absent	NA
AB2, CB4853, CB4855, CB4858, ED3005, ED3077, JU258, MY2, MY14	no	no	present	no

[a]Data from [105]

Chapter 3: Cer1, a Ty3/Gypsy Class LTR Retrotransposon, Causes Germ Cell Death in *C. Elegans*

Introduction

Programmed cell death (PCD), or apoptosis, is a mechanism by which unneeded, damaged or infected cells eliminate themselves from an organism during processes including development, gametogenesis, and immune defense[151]. In the immune system it acts to prevent the spread of pathogens. In mammals, PCD is triggered in response to virus infections by both adaptive immune responses and cell-autonomous responses[74]. A cell that has an active virus infection will display viral peptides on its cell surface. This cell with then be recognized by T lymphocytes and be triggered to die by PCD, thereby eliminating the infected cell from the population and restricting further replication of the virus[152]. The cell-autonomous response, on the other hand, can be triggered by the disruption the virus causes to cellular metabolism. In particular it has been shown that many viruses trigger cell cycle entry in order to increase their own replication. They often trigger the cell cycle without also sending the necessary anti-apoptotic survival signals to the cell. The cell can then recognize this division as aberrant and undergo p53-dependent PCD[74]. p53 is a tumor-suppressor with a critical role in DNA-damage induced PCD.

In addition to foreign viruses, organisms face the threat of endogenous mobile genetic elements, such as retrotransposons, that can become active. Evidence that the activity of retrotransposons can cause DNA damage and subsequent PCD comes from studies of the LINE-1 (L1) non-LTR retrotransposon in human cells. First, it was shown that cell lines have increased PCD when L1 becomes highly active; this increased PCD is not seen if the cells lack intact p53[75]. It was then demonstrated that high activity of L1 causes a high amount of double-stranded breaks (DSBs)[76,77]. This suggests that the increased cell death seen when L1 is active is at least in part the direct result of the DSBs, which occur as part of the retrotransposition process. Restriction of mobile genetic elements is particularly important in the germline, where their activity can cause mutational changes in subsequent progeny. Organisms have therefore evolved germline-specific restriction mechanisms to protect themselves from the activity of these genome invaders.

One important component of germline antiviral defense involves RNA silencing mechanisms, which have recently been linked to germline PCD in *C. elegans*. RNA interference (RNAi) targeting germline genes and a related phenomenon, co-suppression, both increase the amount of germline PCD[79]. This increase in PCD is dependent on *cep-1*/p53, indicating that it could be occurring through the DNA-damage-induced PCD pathway (for an overview of the PCD pathway, see Figure 1.2). Consistent with this model, there is a concomitant increase in the number of RAD-51 foci, an indicator of DSBs. While this recent study showed

this PCD effect for endogenous germline genes being targeted by RNAi, it raises the possibility that the same will hold true in the context of antiviral and transposon defense; In addition to silencing the expression of these genome invaders, co-suppression and RNAi pathways may lead to PCD in cells with the highest expression levels, possibly culling those high-expressing cells from the population.

The recent discovery of a retrotransposon that is abundantly expressed in the germline of the laboratory wild-type strain (N2) of *C. elegans* allows for the first analysis of the role of PCD in restricting retrotransposons in the *C. elegans* germline[49]. The innate immune system is conserved in *C. elegans*, and studies in this model were central in elucidating the core PCD pathway as well as the antiviral defense process of RNA interference. While cell culture experiments have shown a role for PCD in virus restriction in *C. elegans* somatic cells[32], and L1 has been shown to cause PCD in cell culture[75], we now have the opportunity to determine what role PCD plays in restricting an endogenous retrotransposon in the germline of an intact organism. This could further provide insight into the mechanism of PCD induction in the germline. Cer1 (*C. elegans* retrotransposon 1) is a Ty3/Gypsy class LTR retrotransposon. Its expression is temperature-sensitive and is most abundant in the same region of the gonad where cell deaths occur[49,64]. In this study, we analyzed the effect that Cer1 has on cell death in the *C. elegans* germline. We found that in the situations where Cer1 is most abundantly expressed, its removal results in a significant decrease in number of germ cell deaths. Our data indicate that in studies of N2 at low temperature 15-20% of the cell deaths occurring are caused by

the presence of Cer1.

Results

Cer1 Virus-Like Particles Are Abundant In Some Cell Corpses

During a survey of *C. elegans* gonads by electron microscopy, we detected several cell corpses with abundant Virus-Like Particles (VLPs) (Figure 3.1A). We previously showed that there are no VLPs in the germline of Cer1(-) strains or Cer1(RNAi) treated animals, and can thus infer that the VLPs in these corpses are the product of the Cer1 retrotransposon[49]. Furthermore, in animals deficient in the engulfment of cell corpses (*ced-1(e1735)*) we found corpses with abundant Cer1 as detected by immunostaining with a monoclonal antibody targeting Cer1 GAG (αGAG). Some persistent corpses in these animals accumulate in the proximal end of the gonad, away from the region where Cer1 is most abundant. This makes it straightforward to detect whether or not a corpse has high levels of αGAG staining. The Cer1 abundance was detected in some but not all of these persistent corpses (Figure 3.1B).

These abundant Cer1 VLPs in cell corpses could indicate that high levels of Cer1 in a cell induce the cell to undergo programmed cell death. Alternatively, the cell might have had abundant VLPs but underwent PCD for unrelated reasons, and the shrinking cytoplasm during the cell death process concentrated the VLPs. A third alternative is that cells undergoing PCD might take up VLPs from the syncytial

gonad core, due to the association of Cer1 VLPs with microtubules. In order to determine if Cer1 was indeed causing germ cell death, we quantified cell deaths in the presence and absence of Cer1.

***Cer1* removal by RNA interference decreases the number of germ cell deaths.**

There are several parallels between the expression of Cer1 and the incidence of germline PCD. Cer1 is not expressed and germline PCD does not occur in males or larvae. In adult hermaphrodites both the amount of Cer1 protein and the number of germ cell deaths occurring increase with adult age. We began our analysis of cell death with hermaphrodites 2 days into adulthood at 15°C. At this time-point there is a significant amount of Cer1 protein in the gonad and also still plenty of hermaphrodite sperm, the loss of which would affect ovulation rates and transcription in the gonad. We compared animals grown on Cer1(RNAi) feeding bacteria to animals grown on an empty vector control or RNAi targeting *pos-1,* an abundantly expressed germline gene. Cer1 protein was abundant in empty vector and *pos-1*(RNAi) treated animals and absent in Cer1(RNAi) animals (data not shown).

We quantified germ cell deaths by identifying germ nuclei that had lost perinuclear accumulation of a P granule component, PGL-1 (Figure 3.2). P granules are germline-specific ribonucleoprotein granules that are located over clusters of nuclear pores in the region of the gonad where cell death occurs[43,64]. During germ cell death, perinuclear accumulation of some constitutive P granule

components is lost [48]. To verify that the cells we were scoring as deaths via this method represented cells undergoing PCD, we quantified the number of such events in worms deficient in PCD, using a strong loss-of-function allele of the *ced-3* caspase. We detected a mean of 0.1 cell deaths per gonad arm in *ced-3(n717)* hermaphrodites (n=24), consistent with previously published results quantifying germ cell deaths via Nomarski microscopy [64]. We conclude that the events we identify by loss of perinuclear PGL-1 represent germline PCD.

The number of germ cell deaths was significantly lower in Cer1(RNAi) treated animals than in either control condition (Figure 3.3A), suggesting that Cer1 contributes to germ cell deaths occurring in the N2 germline at low temperatures. The amount of Cer1 capsid protein detected in the germline is temperature dependent[49]. We tested for a difference in quantity of cell deaths at 20°C, where there is an intermediate amount of Cer1 capsid present, and 25°C, where Cer1 capsid protein is absent. At 20°C there was a slight decrease in the number of cell deaths when Cer1 was removed by RNAi (Figure 3.3B), consistent with the lower abundance of Cer1 at this temperature. At 25°C there is no difference in the number of cell deaths between Cer1(RNAi) treated gonads and the empty vector control (Figure 3.3C), consistent with the fact that neither population has Cer1 capsid present at this temperature. These results suggest that Cer1 is causing germ cell death when it is abundantly expressed.

Cer1 Knockout Decreases the Number of Germ Cell Deaths at 72 but not 48 Hours Post-L4

During the course of these studies it was published that RNAi targeting germline-expressed genes increases the amount of germ cell death[79]. To eliminate the potential caveats of the RNAi-based results, we retested the effect Cer1 has on cell death using a hybrid strain lacking Cer1 (hereafter Cer1(-)[49]). Briefly, this strain was constructed by introgressing the Cer1(-) strain CB4856 into the N2 strain. The N2 strain does additionally have 3 Cer1 solo LTRs elsewhere in the genome, but these do not have coding sequence for Cer1 proteins[91].

We quantified the number of germ cell deaths in *ced-1(e1735)*;*Cer1(-)* animals 2 days into adulthood at 15°C. Surprisingly, we detected no difference in the number of cell deaths in Cer1(-) versus Cer1(+) animals at this time-point (Figure 3.4). We reasoned that the developmental age of the animals and the expression of Cer1 might be different on the RNAi plates, which contained antibiotics and a different strain of bacteria, compared to the standard growth plates we were using for this experiment. Since the amount of Cer1 increases with adult age, we expect Cer1 presence to have a greater effect on cell deaths in older animals. We therefore assayed animals 3 days into adulthood at 15°C. In these experiments we detected a significant decrease in the number of germ cell deaths in Cer1(-) animals (Figure 3.5).

Discussion

We found that the presence of Cer1 causes as much as 20% of the germ cell deaths that occur in the N2 laboratory strain of *C. elegans* under certain conditions. These conditions correlate with conditions where Cer1 protein is most abundant: low temperature several days into adulthood.

Both the removal of Cer1 mRNA by RNAi and the removal of Cer1 coding sequence by introgression of a wild strain showed the same effect of Cer1 on germ cell deaths. The adult age of the animal required to see this effect, however, differed between the two conditions. The RNAi experiments have several caveats, some of which may contribute to this difference: (1) incomplete or variable knock-down can occur, (2) increased germ cell death occurs when germline genes are targeted by RNAi, and (3) we have observed differences in growth rates for worms on RNAi feeding plates. The use of the Cer1(-) strain bypasses all of these issues, but there is potential that other polymorphisms in the strain were carried along with the Cer1(-) allele, and these might have an impact on germ cell deaths. The extent of back-crossing of this strain to N2 and the correlation with the RNAi results, however, lead us to conclude that the primary cause of the effect on germ cell death that we see in both cases is due directly to Cer1.

How is Cer1 causing cell death? To date no new Cer1 integration events have been reported in the laboratory. It is possible that Cer1 is integrating and causing DNA

damage in the process, which in turn triggers the target cell to die. Studies in cell death defective animals at low temperatures might therefore be able to identify Cer1 integration events. If Cer1 triggers cell death through a DNA damage response, then we would expect these deaths to depend on both the pro-apoptotic BH3-domain gene *egl-1* and the *C. elegans* p53 homolog *cep-1*(See Figure 1.2).

Cer1 could also be triggering cell death without integration. The germ cell deaths occurring in normal laboratory condition in the N2 strain have been proposed to serve a nurse cell purpose. The gonad is a syncytium with the germ nuclei connected to the core by large ring channels. Actin-dependent cytoplasmic flow moves materials from the core into the maturing and enlarging proximal oocytes. In mutants defective in germ cell death there is a decrease in the quality of oocytes in aging animals. It is proposed that there are limited resources for maturing oocytes, resulting in a decrease in the size and quality of eggs over time. Cell death reduces the amount of competition for those resources. Expression of Cer1 mRNA and proteins may put an additional strain on the available resources, and more cells are therefore triggered to undergo PCD in order to balance out this deficiency. Previous studies indicated that the presence of Cer1 does not affect the quality of oocytes in aging animals[49], but this may change in animals defective in PCD.

Cer1 associates with microtubules and in older animals causes aggregation of microtubules, and large clusters of microtubules and Cer1 capsids have been observed in these animals[49]. It is possible that this disruption to the cytoskeletal architecture of the gonad might be a contributing factor to the increased germ cell

death. The large clusters of microtubules and capsids can break off, and may cause cellular damage in the process.

How might Cer1 silencing and programmed cell death be related to the RNAi and co-suppression induction of apoptosis? Previous studies of Cer1 indicated that mutations in the RNAi pathways do not cause an increase in VLP number, but this does not preclude the possibility that there is active silencing of Cer1 at the transcriptional level that is not 100% effective and does not represent the rate-limiting step for capsid production. If silencing mechanisms do act on the Cer1 locus then it is possible that when a germ cell crosses a threshold of Cer1 RNA expression, DSBs are induced by the silencing machinery and cause that cell to undergo PCD. Since the silencing-induced PCD pathway requires the previously mentioned *cep-1/*p53 as well as *rde-2*, testing for Cer1-induced PCD in these mutants will be the next step towards identifying the genetic pathway involved.

This study shows that *C. elegans* can be used as a model to study the role of PCD in restricting retrotransposons in the germline. The conservation of the PCD pathway and antiviral defense systems such as RNAi between *C. elegans* and mammals means that future studies in this system can provide valuable insight for a range of organisms.

Materials and Methods

Strains

Nematodes were cultured and manipulated genetically as previously described[137]. Except for the RNAi experiments, worms were fed the standard *E. coli* feeding strain OP50. The following strains and alleles were used: N2, CB3203 [*ced-1(e1735)I*]; JJ2233 [*ced-1(e1735)I; Cer1(-)III*]. Cer1(-) strain construction: We backcrossed strain CB4856 to the N2 strain eight times. We followed the intact *plg-1* gene (and therefore absence of Cer1) by PCR during each cross. The resulting strain therefore contains mostly N2 genetic background but lacks an intact copy of Cer1. The N2 strain does additionally have 3 Cer1 solo LTRs elsewhere in the genome, but these do not have coding sequence for Cer1 proteins[91]. We do not detect any Cer1 capsid in the germline of this strain by immunostaining (data not shown).

Quantification of Germ Cell Death, Immunocytochemistry, and Microscopy

Worms were raised at 20°C until the L4 stage and then picked to fresh plates and shifted to either 15°C, 20°C or 25°C for either 40, 48 or 72 hours as indicated in the results. A two step formaldehyde fixation[138] was modified for experiments to simultaneously localize *Cer1* GAG, PGL-1, and NPP-9 as follows: Worms were dissected on microscope slides in a small drop of gonad buffer (GB: 75 mM HEPES (6.9), 1.2% sucrose, 40 mM NaCl, 5 mM KCL, 2 mM MgCL2, 1 mM EGTA). After dissection, an equal volume of fixation buffer #1 [6% formaldehyde, 75 mM HEPES

(6.9), 40 mM NaCl, 5 mM KCL, 2 mM MgCL2, 1 mM EGTA] was added for 2 minutes, then removed and replaced with fixation buffer #2 [3% formaldehyde, 30 mM Sodium Borate (11), 2 mM MgCl2] for 7 minutes. The gonads were permeabilized in PBS plus 0.3% Triton X-100 (Sigma) for 10 minutes, then rinsed several times in PBS and immunostained overnight at 4°C. Antibodies used: αPGL-1[134], αNPP-9[48], and αCer1 GAG[49].

Widefield images were acquired with a Nikon Eclipse 90i upright microscope using a 40× (Plan Fluor, 1.4 NA) lens and a Retiga-4000DC camera (QImaging). Images were exported to Adobe Photoshop for cropping, reorientation, and contrast and brightness adjustments.

RNA interference and Electron Microscopy

For RNAi experiments worms were cultured on the following dsRNA feeding strains from the Ahringer library as described[132]: *Cer1* (F44E2.2 dsRNA) and *pos-1*. The empty vector control used feeding vector pPD129.36[133]. RNAi feeding plates contained 50μg/ml carbenicillin and 10μg/ml tetracycline.

Electron microscopy was performed as described in [49].

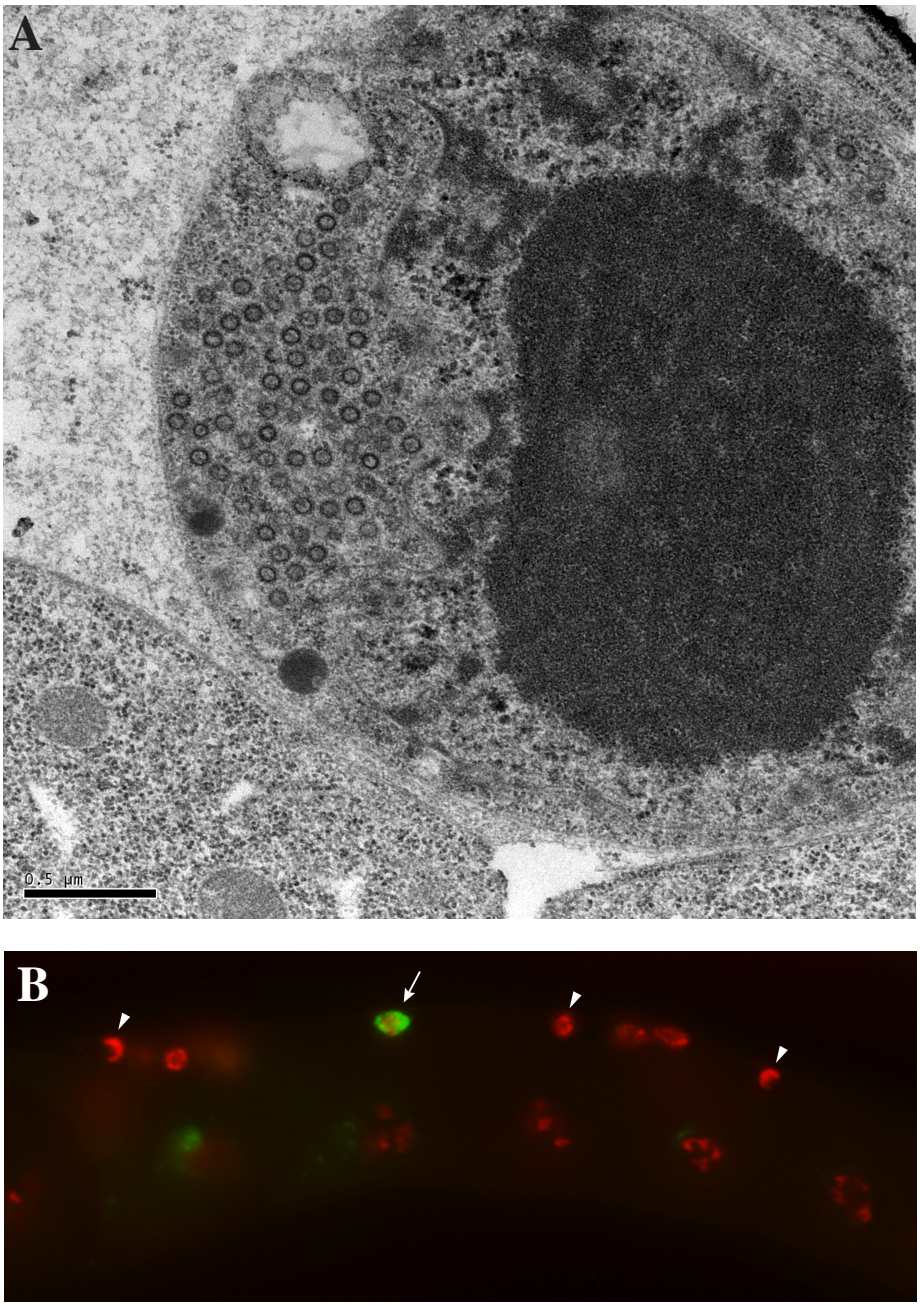

Figure 3.1. Some Cell Corpses Have Abundant Cer1 VLPs.
(A) Electron micrograph showing an example of a germ cell that is undergoing programmed cell death, as evidenced by the nuclear morphology. Note the abundant VLPs in the remaining cytoplasm of this cell. Scale bar: 0.5 µm. This electron micrograph image was taken by James R. Priess. (B) Proximal arm of a *ced-1(e1735)* adult hermaphrodite gonad arm immunostained with αGAG (green) and DAPI (red). Some persistent corpses have abundant Cer1 GAG protein (arrow) while others do not (arrowheads).

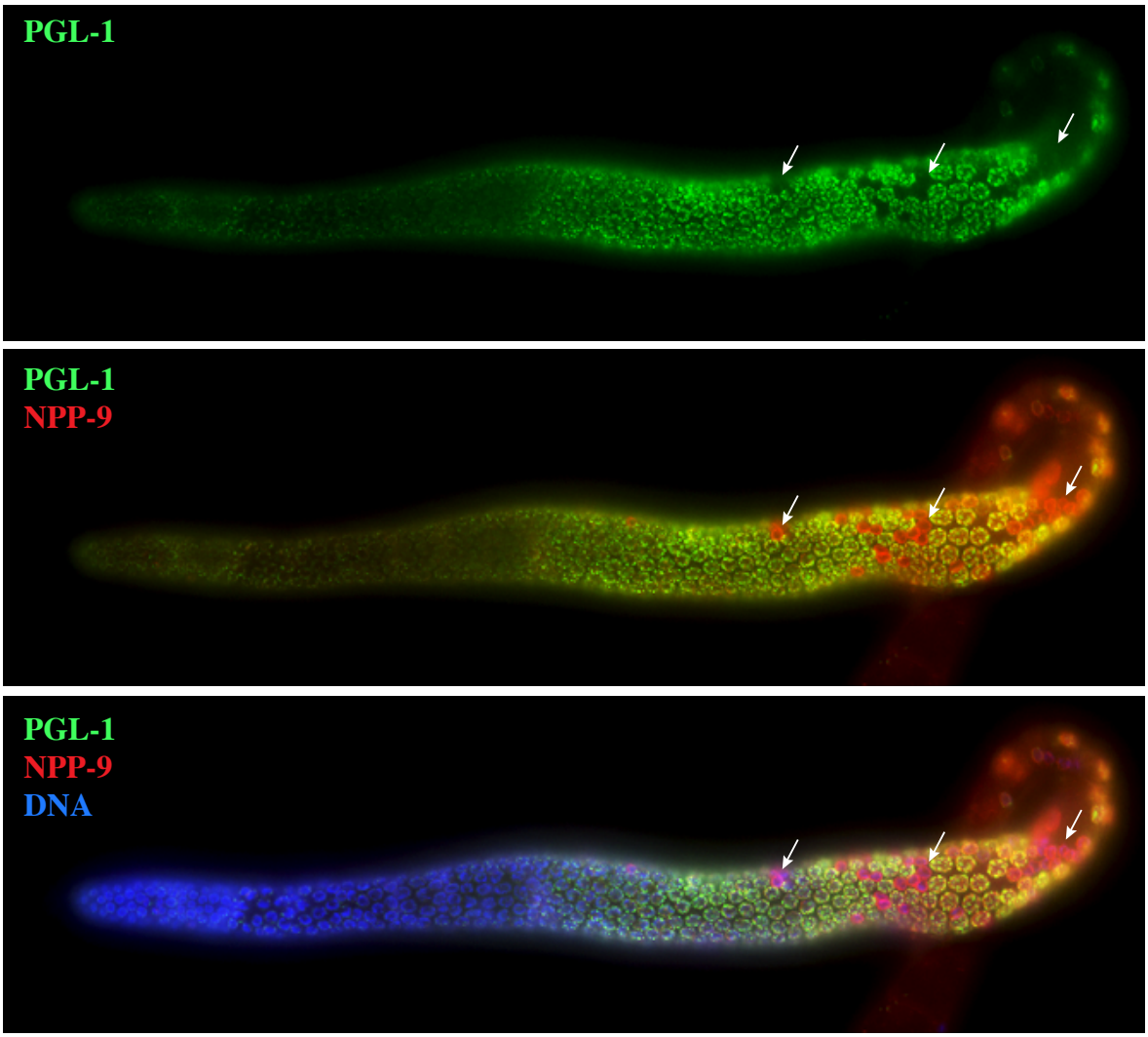

Figure 3.2. Loss of Perinuclear PGL-1 Allows Quantification of Germ Cell Deaths.

ced-1(e1735) adult hermaphrodite gonad co-immunostained with αPGL-1 (green), αNPP-9 (red), and DAPI (blue). Cell deaths can be identified as nuclei with NPP-9 at nuclear rim but little to no perinuclear PGL-1 (arrows indicate several examples).

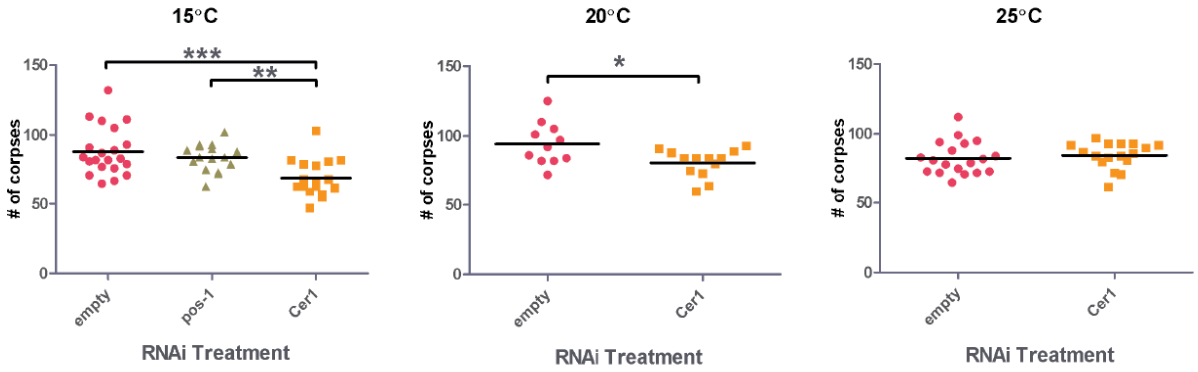

Figure 3.3. Cer1 Removal by RNAi Decreases the Number of Germ Cell Deaths.
Animals were raised on RNAi feeding bacteria strains expressing dsRNA targeting either Cer1, *pos-1*, or an empty vector control and assayed 48 hours post-L4 (15°C and 20°C) or 40 hours post-L4 (25°C). The number of cell deaths was quantified by identifying nuclei that lacked perinuclear PGL-1. Black line indicates mean. *** $p<0.001$, ** $p<0.01$, *$p<0.05$ unpaired Student's t-test.

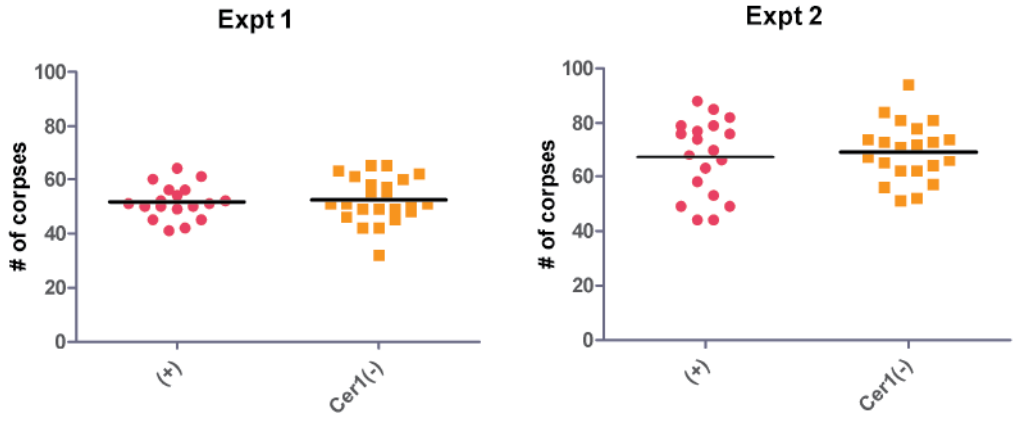

Figure 3.4. Cer1 Knock-out Has No Change in Amount of Germ Cell Death at 48 Hours Post-L4.

Animals deficient in corpse engulfment (*ced-1(e1735)*) containing either a full-length copy of Cer1 (+) or lacking it (Cer1(-)) were analyzed for number of germ cell deaths at 48 hours post-L4 at 15°C. The number of cell deaths was quantified by identifying nuclei that lacked perinuclear PGL-1. Black line indicates mean. There was no difference in the mean number of corpses at this timepoint in either of 2 independent experiments.

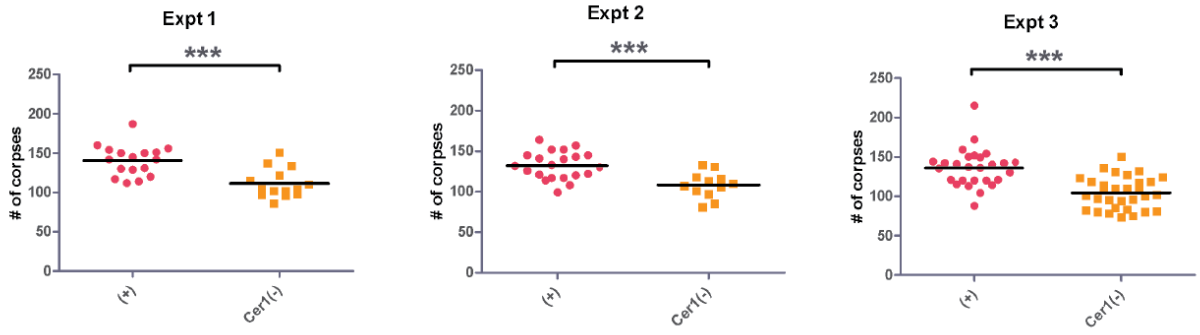

Figure 3.5. Cer1 Knock-out Has Decreased Amount of Germ Cell Death at 72 Hours Post-L4.

Animals deficient in corpse engulfment (*ced-1(e1735)*) containing either a full-length copy of Cer1 (+) or lacking it (Cer1(-)) were analyzed for number of germ cell deaths at 72 hours post-L4 at 15°C. The number of cell deaths was quantified by identifying nuclei that lacked perinuclear PGL-1. Black line indicates mean. There was a significant decrease in the mean number of corpses at this timepoint in 3 independent experiments. *** $p<0.001$ unpaired Student's t-test.

Chapter 4: Discussion, Conclusions and Future Directions

In the work described in this thesis, we have shown that there are abundant Virus-like Particles (VLPs) in the germline of the laboratory wild-type strain of *Caenorhabditis elegans* as well as 3 additional wild isolates of *C. elegans* and one strain of *Caenorhabditis japonica*. We identified these VLPs in *C. elegans* as the product of the LTR retrotransposon Cer1, which is abundantly expressed in the hermaphrodite germline. This expression is temperature and age-dependent and does not seem to be restricted by small RNA silencing pathways. Furthermore, we found that Cer1 capsids associate with microtubules, which may allow them to resist cytoplasmic flow and probe for P granule-free nuclear pores to allow easier access to the nucleus. Finally, we showed that Cer1 causes increased programmed cell death in the germline. The work presented here represents an exciting starting point for future studies of host/pathogen interactions. In this chapter I will describe some future directions and unanswered questions arising from the results in chapters 2 and 3.

CER1 EXPRESSION

In Chapter 2 we showed that Cer1 exhibits temperature-dependent expression. This expression difference could be seen at the RNA level by *in situ* hybridization as well as Northern blot analysis. By Northern a full-length transcript is present at 15°C but not 25°C, while a smaller spliced transcript containing the 3' ORF is present at both temperatures. One big remaining question is what the function of this terminal ORF might be. It is found 3' to the pol gene, which is where

envelope-encoding proteins are found in retroviruses. We found no similarity to known envelope genes, and did not observe enveloped particles via electron microscopy. However, these proteins are quite diverse, and by EM we may have simply missed the presence of enveloped particles if they were outside of the gonad or in very scarce abundance. So it remains possible that Cer1 does produce an envelope with the terminal ORF. As mentioned in the discussion of chapter 2, this ORF could alternatively serve as an export factor for the full-length, unspliced RNA that must exit the nucleus in order for Cer1 to replicate. Another intriguing possibility is that this terminal ORF could have a role in allowing Cer1 to evade silencing, possibly by directly inhibiting host defense mechanisms. One approach to elucidating the function of this ORF could be the production of full-length Cer1 transgenes with mutations to determine what role this terminal ORF plays in Cer1 function.

IS CER1 AN ACTIVE ELEMENT?

In laboratory studies of *C. elegans* no retrotransposition events of Cer1 or any other element have been observed, and we therefore have no conclusive proof that it is still competent of retrotransposition. There are several ways this can be assessed, including expressing Cer1 in a heterologous system, such as yeast, to test for its ability to replicate[153]. However, a new screen for new insertion events might also be fruitful, as previous studies searching for transposition events did not use conditions, such as low temperature, where Cer1 was abundant. Since Cer1 causes PCD it is possible that Cer1 integration events are removed by this process,

so screening for Cer1 insertions should be done in PCD mutants. This will be an exciting avenue of future research and could determine if PCD is indeed functioning as a genome defense mechanism in the *C. elegans* germline.

SMALL RNA PATHWAY REGULATION OF CER1

In Chapter 2 we disrupted small RNA pathways, with the expectation that small RNAs might be involved in restricting Cer1 expression. We were expecting to find small RNA pathway mutations that increased the amount of VLPs we could detect by EM. In only one of the mutants surveyed did we detect a reproducible increase. This was an *alg-2* mutant with *alg-1* knocked down by RNAi. These are the argonaute proteins required for the microRNA pathway; *alg-1* and *alg-2* have partially redundant roles and together are required for all known microRNA function[148]. We did some preliminary experiments looking at Cer1 protein expression using the anti-GAG antibody, and did not see a large difference with the *alg-1;alg-2* knock-down. This could mean that *alg-1;alg-2* are regulating a different retrotransposon, or simply that our immunofluorescence studies were not assessed quantitatively as our EM ones were. These will have to be repeated more rigorously, and other retrotransposons assessed, to determine why VLP numbers are increasing in the microRNA mutants. *alg-1* and *alg-2* mutants should also be assessed independently in order to determine which is having the effect. In addition, there are many microRNA mutants available, and the ones expressed in or near the gonad can be tested to narrow down which are specifically responsible for the effect we see[154]. While it is possible that microRNAs directly regulate Cer1 at the RNA level,

another distinct possibility is that the changes in germ cell biology that occur in the absence of microRNAs contribute to changes in retrotransposon expression. It is known, for example, that *alg-1* mutants enter meiosis earlier than wild-type animals[155]. The difference we see could therefore be the result of an increased zone of Cer1 expression due to early meiotic progression.

Another interesting result from our small RNA pathway studies was the lack of VLPs detected in the *prg-1;prg-2* mutants. We were expecting an increase in VLP numbers if the piRNA pathway was restricting Cer1 as it restricts Tc3 in *C. elegans,* and as the *Drosophila* piwi pathway restricts the related *gypsy* retrotransposon. Instead we saw a decrease in VLPs, detecting none by EM. This mutant was additionally negative for α-GAG staining by immunofluorescence. There are several possibilities for Piwi regulation of Cer1. The *prg* mutants have defects in fertility at high temperature, it is possible that even at low temperatures there are disruptions to the transcription profile of the mutant animals that may decrease Cer1 expression directly or indirectly. If there is an indirect effect of *prg* mutants on Cer1 expression, then it remains possible that there is an additional role of the PRG proteins in silencing Cer1. The expression of Cer1 should be more thoroughly characterized in these mutants at the RNA level, and *prg-1* and *prg-2* mutants should be independently assessed. The intersection of the piwi pathway and control of Cer1 expression could provide insight into the temperature-sensitive control of Cer1 expression. If the cause of the Cer1 decrease in *prg* mutants is indeed indirect and can be bypassed in the lab, then any direct roles of *prg-1* and *prg-2* in silencing *C. elegans* retrotransposons at low temperatures can be assessed.

CER1 CAUSES PROGRAMMED CELL DEATH

Chapter 3 results indicate that Cer1 is causing significant programmed cell death in the N2 hermaphrodite germline. This has implications for anyone studying germ cell death in *C. elegans*, especially if they are doing so at low temperatures where Cer1 is abundant. There are many remaining questions about this increased cell death, primarily what the mechanism is for the induction of PCD by Cer1. The initial steps towards elucidating this mechanism should be the determination of which known genetic components these cell deaths require, such as *egl-1* and *cep-1*. The co-suppression and RNAi pathway component *rde-2* should also be assessed as a step towards determining if the silencing-induced PCD pathway is involved.

In addition to mechanism, the question remains of what function Cer1-induced PCD has. Previous studies showed a role for PCD in maintaining the quality of oocytes in aging animals[67]. It is possible that one cause of the decrease in quality could be the activity of Cer1. This can be determined by comparing PCD pathway mutants, such as *ced-3*, in the presence and absence of Cer1. I would expect a further decrease in the quality of aging oocytes when Cer1 is present if Cer1 is indeed damaging oocytes.

These initial studies have provided key information about Cer1 replication, opening the door to a realm of exciting future studies using the *C. elegans* germline as a model for retrotransposon restriction.

Bibliography

1. Bowen NJ, McDonald JF (1999) Genomic analysis of *Caenorhabditis elegans* reveals ancient families of retroviral-like elements. Genome Res 9: 924-935.
2. Coffin JM, Hughes SH, Varmus H (1997) Retroviruses. Plainview, N.Y.: Cold Spring Harbor Laboratory Press. xv, 843 p. p.
3. Bessereau, JL (January 18, 2006) Transposons in *C. elegans, Wormbook* In: The *C. elegans* Research Community, editors. WormBook.
4. O'Donnell KA, Boeke JD (2007) Mighty Piwis defend the germline against genome intruders. Cell 129: 37-44.
5. Sarot E, Payen-Groschene G, Bucheton A, Pelisson A (2004) Evidence for a piwi-dependent RNA silencing of the gypsy endogenous retrovirus by the Drosophila melanogaster flamenco gene. Genetics 166: 1313-1321.
6. Saito K, Nishida KM, Mori T, Kawamura Y, Miyoshi K, et al. (2006) Specific association of Piwi with rasiRNAs derived from retrotransposon and heterochromatic regions in the Drosophila genome. Genes Dev 20: 2214-2222.
7. Brennecke J, Aravin AA, Stark A, Dus M, Kellis M, et al. (2007) Discrete small RNA-generating loci as master regulators of transposon activity in *Drosophila*. Cell 128: 1089-1103.
8. Tan CH, Lee TC, Weeraratne SD, Korzh V, Lim TM, et al. (2002) Ziwi, the zebrafish homologue of the Drosophila piwi: co-localization with vasa at the embryonic genital ridge and gonad-specific expression in the adults. Mech Dev 119 Suppl 1: S221-224.
9. Aravin AA, Sachidanandam R, Girard A, Fejes-Toth K, Hannon GJ (2007) Developmentally regulated piRNA clusters implicate MILI in transposon control. Science 316: 744-747.
10. Pfeffer S, Zavolan M, Grasser FA, Chien M, Russo JJ, et al. (2004) Identification of virus-encoded microRNAs. Science 304: 734-736.
11. Cullen BR (2009) Viral and cellular messenger RNA targets of viral microRNAs. Nature 457: 421-425.
12. Triboulet R, Mari B, Lin YL, Chable-Bessia C, Bennasser Y, et al. (2007) Suppression of microRNA-silencing pathway by HIV-1 during virus replication. Science 315: 1579-1582.
13. Jopling CL, Yi M, Lancaster AM, Lemon SM, Sarnow P (2005) Modulation of hepatitis C virus RNA abundance by a liver-specific MicroRNA. Science 309: 1577-1581.
14. Marques JT, Carthew RW (2007) A call to arms: coevolution of animal viruses and host innate immune responses. Trends Genet 23: 359-364.
15. Siomi H, Siomi MC (2009) On the road to reading the RNA-interference code. Nature 457: 396-404.
16. Carthew RW, Sontheimer EJ (2009) Origins and Mechanisms of miRNAs and siRNAs. Cell 136: 642-655.

17. Batista PJ, Ruby JG, Claycomb JM, Chiang R, Fahlgren N, et al. (2008) PRG-1 and 21U-RNAs interact to form the piRNA complex required for fertility in C. elegans. Mol Cell 31: 67-78.
18. Das PP, Bagijn MP, Goldstein LD, Woolford JR, Lehrbach NJ, et al. (2008) Piwi and piRNAs act upstream of an endogenous siRNA pathway to suppress Tc3 transposon mobility in the *Caenorhabditis elegans* germline. Mol Cell 31: 79-90.
19. Collins J, Saari B, Anderson P (1987) Activation of a transposable element in the germ line but not the soma of Caenorhabditis elegans. Nature 328: 726-728.
20. Emmons SW, Yesner L (1984) High-frequency excision of transposable element Tc 1 in the nematode Caenorhabditis elegans is limited to somatic cells. Cell 36: 599-605.
21. Vastenhouw NL, Fischer SE, Robert VJ, Thijssen KL, Fraser AG, et al. (2003) A genome-wide screen identifies 27 genes involved in transposon silencing in C. elegans. Curr Biol 13: 1311-1316.
22. Ketting RF, Haverkamp TH, van Luenen HG, Plasterk RH (1999) Mut-7 of C. elegans, required for transposon silencing and RNA interference, is a homolog of Werner syndrome helicase and RNaseD. Cell 99: 133-141.
23. Tabara H, Sarkissian M, Kelly WG, Fleenor J, Grishok A, et al. (1999) The rde-1 gene, RNA interference, and transposon silencing in C. elegans. Cell 99: 123-132.
24. Sijen T, Fleenor J, Simmer F, Thijssen KL, Parrish S, et al. (2001) On the role of RNA amplification in dsRNA-triggered gene silencing. Cell 107: 465-476.
25. Smardon A, Spoerke JM, Stacey SC, Klein ME, Mackin N, et al. (2000) EGO-1 is related to RNA-directed RNA polymerase and functions in germ-line development and RNA interference in C. elegans. Curr Biol 10: 169-178.
26. Cox DN, Chao A, Baker J, Chang L, Qiao D, et al. (1998) A novel class of evolutionarily conserved genes defined by piwi are essential for stem cell self-renewal. Genes Dev 12: 3715-3727.
27. Cox DN, Chao A, Lin H (2000) piwi encodes a nucleoplasmic factor whose activity modulates the number and division rate of germline stem cells. Development 127: 503-514.
28. Malone CD, Brennecke J, Dus M, Stark A, McCombie WR, et al. (2009) Specialized piRNA pathways act in germline and somatic tissues of the Drosophila ovary. Cell 137: 522-535.
29. Aravin AA, Sachidanandam R, Bourc'his D, Schaefer C, Pezic D, et al. (2008) A piRNA pathway primed by individual transposons is linked to de novo DNA methylation in mice. Mol Cell 31: 785-799.
30. Carmell MA, Girard A, van de Kant HJ, Bourc'his D, Bestor TH, et al. (2007) MIWI2 is essential for spermatogenesis and repression of transposons in the mouse male germline. Dev Cell 12: 503-514.
31. Felix MA, Ashe A, Piffaretti J, Wu G, Nuez I, et al. (2011) Natural and experimental infection of *Caenorhabditis* nematodes by novel viruses related to nodaviruses. PLoS Biol 9: e1000586.

32. Liu WH, Lin YL, Wang JP, Liou W, Hou RF, et al. (2006) Restriction of vaccinia virus replication by a *ced-3* and *ced-4*-dependent pathway in *Caenorhabditis elegans*. Proc Natl Acad Sci U S A 103: 4174-4179.
33. Lu R, Maduro M, Li F, Li HW, Broitman-Maduro G, et al. (2005) Animal virus replication and RNAi-mediated antiviral silencing in *Caenorhabditis elegans*. Nature 436: 1040-1043.
34. Lu R, Yigit E, Li WX, Ding SW (2009) An RIG-I-Like RNA helicase mediates antiviral RNAi downstream of viral siRNA biogenesis in Caenorhabditis elegans. PLoS Pathog 5: e1000286.
35. Wilkins C, Dishongh R, Moore SC, Whitt MA, Chow M, et al. (2005) RNA interference is an antiviral defence mechanism in *Caenorhabditis elegans*. Nature 436: 1044-1047.
36. Schott DH, Cureton DK, Whelan SP, Hunter CP (2005) An antiviral role for the RNA interference machinery in *Caenorhabditis elegans*. Proc Natl Acad Sci U S A 102: 18420-18424.
37. Eddy EM (1975) Germ plasm and the differentiation of the germ cell line. Int Rev Cytol 43: 229-280.
38. Gu W, Shirayama M, Conte D, Jr., Vasale J, Batista PJ, et al. (2009) Distinct argonaute-mediated 22G-RNA pathways direct genome surveillance in the C. elegans germline. Mol Cell 36: 231-244.
39. Claycomb JM, Batista PJ, Pang KM, Gu W, Vasale JJ, et al. (2009) The Argonaute CSR-1 and its 22G-RNA cofactors are required for holocentric chromosome segregation. Cell 139: 123-134.
40. Lim AK, Tao L, Kai T (2009) piRNAs mediate posttranscriptional retroelement silencing and localization to pi-bodies in the Drosophila germline. J Cell Biol 186: 333-342.
41. Aravin AA, van der Heijden GW, Castaneda J, Vagin VV, Hannon GJ, et al. (2009) Cytoplasmic compartmentalization of the fetal piRNA pathway in mice. PLoS Genet 5: e1000764.
42. Chuma S, Hosokawa M, Tanaka T, Nakatsuji N (2009) Ultrastructural characterization of spermatogenesis and its evolutionary conservation in the germline: germinal granules in mammals. Mol Cell Endocrinol 306: 17-23.
43. Pitt JN, Schisa JA, Priess JR (2000) P granules in the germ cells of *Caenorhabditis elegans* adults are associated with clusters of nuclear pores and contain RNA. Dev Biol 219: 315-333.
44. Eulalio A, Behm-Ansmant I, Izaurralde E (2007) P bodies: at the crossroads of post-transcriptional pathways. Nat Rev Mol Cell Biol 8: 9-22.
45. Balagopal V, Parker R (2009) Stm1 modulates mRNA decay and Dhh1 function in Saccharomyces cerevisiae. Genetics 181: 93-103.
46. Buchan JR, Muhlrad D, Parker R (2008) P bodies promote stress granule assembly in Saccharomyces cerevisiae. J Cell Biol 183: 441-455.
47. Decker CJ, Teixeira D, Parker R (2007) Edc3p and a glutamine/asparagine-rich domain of Lsm4p function in processing body assembly in Saccharomyces cerevisiae. J Cell Biol 179: 437-449.

48. Sheth U, Pitt J, Dennis S, Priess JR (2010) Perinuclear P granules are the principal sites of mRNA export in adult *C. elegans* germ cells. Development 137: 1305-1314.
49. Dennis S, Sheth U, Feldman JL, English KA, Priess JR (2012) C. elegans Germ Cells Show Temperature and Age-Dependent Expression of Cer1, a Gypsy/Ty3-Related Retrotransposon. PLoS Pathog 8: e1002591.
50. Zakeri ZF, Quaglino D, Latham T, Lockshin RA (1993) Delayed internucleosomal DNA fragmentation in programmed cell death. FASEB J 7: 470-478.
51. Conradt B, Xue D (2005) Programmed cell death. WormBook: 1-13.
52. Ellis HM, Horvitz HR (1986) Genetic control of programmed cell death in the nematode C. elegans. Cell 44: 817-829.
53. Hengartner MO, Ellis RE, Horvitz HR (1992) Caenorhabditis elegans gene ced-9 protects cells from programmed cell death. Nature 356: 494-499.
54. Sulston JE, Schierenberg E, White JG, Thomson JN (1983) The embryonic cell lineage of the nematode *Caenorhabditis elegans*. Dev Biol 100: 64-119.
55. Conradt B, Horvitz HR (1998) The C. elegans protein EGL-1 is required for programmed cell death and interacts with the Bcl-2-like protein CED-9. Cell 93: 519-529.
56. Jiang X, Wang X (2004) Cytochrome C-mediated apoptosis. Annu Rev Biochem 73: 87-106.
57. Liu X, Kim CN, Yang J, Jemmerson R, Wang X (1996) Induction of apoptotic program in cell-free extracts: requirement for dATP and cytochrome c. Cell 86: 147-157.
58. Jagasia R, Grote P, Westermann B, Conradt B (2005) DRP-1-mediated mitochondrial fragmentation during EGL-1-induced cell death in C. elegans. Nature 433: 754-760.
59. Wang X, Yang C, Chai J, Shi Y, Xue D (2002) Mechanisms of AIF-mediated apoptotic DNA degradation in Caenorhabditis elegans. Science 298: 1587-1592.
60. Chen F, Hersh BM, Conradt B, Zhou Z, Riemer D, et al. (2000) Translocation of C. elegans CED-4 to nuclear membranes during programmed cell death. Science 287: 1485-1489.
61. Yan N, Chai J, Lee ES, Gu L, Liu Q, et al. (2005) Structure of the CED-4-CED-9 complex provides insights into programmed cell death in Caenorhabditis elegans. Nature 437: 831-837.
62. Yang X, Chang HY, Baltimore D (1998) Essential role of CED-4 oligomerization in CED-3 activation and apoptosis. Science 281: 1355-1357.
63. Pourkarimi E, Greiss S, Gartner A (2012) Evidence that CED-9/Bcl2 and CED-4/Apaf-1 localization is not consistent with the current model for C. elegans apoptosis induction. Cell Death Differ 19: 406-415.
64. Gumienny TL, Lambie E, Hartwieg E, Horvitz HR, Hengartner MO (1999) Genetic control of programmed cell death in the Caenorhabditis elegans hermaphrodite germline. Development 126: 1011-1022.
65. Grant B, Hirsh D (1999) Receptor-mediated endocytosis in the Caenorhabditis elegans oocyte. Mol Biol Cell 10: 4311-4326.

66. Wolke U, Jezuit EA, Priess JR (2007) Actin-dependent cytoplasmic streaming in *C. elegans* oogenesis. Development 134: 2227-2236.
67. Andux S, Ellis RE (2008) Apoptosis maintains oocyte quality in aging Caenorhabditis elegans females. PLoS Genet 4: e1000295.
68. Gartner A, Milstein S, Ahmed S, Hodgkin J, Hengartner MO (2000) A conserved checkpoint pathway mediates DNA damage--induced apoptosis and cell cycle arrest in C. elegans. Mol Cell 5: 435-443.
69. Schumacher B, Schertel C, Wittenburg N, Tuck S, Mitani S, et al. (2005) C. elegans ced-13 can promote apoptosis and is induced in response to DNA damage. Cell Death Differ 12: 153-161.
70. Schumacher B, Hofmann K, Boulton S, Gartner A (2001) The C. elegans homolog of the p53 tumor suppressor is required for DNA damage-induced apoptosis. Curr Biol 11: 1722-1727.
71. Rutkowski R, Dickinson R, Stewart G, Craig A, Schimpl M, et al. (2011) Regulation of Caenorhabditis elegans p53/CEP-1-dependent germ cell apoptosis by Ras/MAPK signaling. PLoS Genet 7: e1002238.
72. Gartner A, Boag PR, Blackwell TK (2008) Germline survival and apoptosis. WormBook: 1-20.
73. Angelo G, Van Gilst MR (2009) Starvation protects germline stem cells and extends reproductive longevity in C. elegans. Science 326: 954-958.
74. O'Brien V (1998) Viruses and apoptosis. J Gen Virol 79 (Pt 8): 1833-1845.
75. Haoudi A, Semmes OJ, Mason JM, Cannon RE (2004) Retrotransposition-Competent Human LINE-1 Induces Apoptosis in Cancer Cells With Intact p53. J Biomed Biotechnol 2004: 185-194.
76. Belgnaoui SM, Gosden RG, Semmes OJ, Haoudi A (2006) Human LINE-1 retrotransposon induces DNA damage and apoptosis in cancer cells. Cancer Cell Int 6: 13.
77. Gasior SL, Wakeman TP, Xu B, Deininger PL (2006) The human LINE-1 retrotransposon creates DNA double-strand breaks. J Mol Biol 357: 1383-1393.
78. Farkash EA, Luning Prak ET (2006) DNA damage and L1 retrotransposition. J Biomed Biotechnol 2006: 37285.
79. Adamo A, Woglar A, Silva N, Penkner A, Jantsch V, et al. (2012) Transgene-mediated cosuppression and RNA interference enhance germ-line apoptosis in Caenorhabditis elegans. Proc Natl Acad Sci U S A.
80. Dernburg AF, Zalevsky J, Colaiacovo MP, Villeneuve AM (2000) Transgene-mediated cosuppression in the C. elegans germ line. Genes Dev 14: 1578-1583.
81. Siomi MC, Sato K, Pezic D, Aravin AA (2011) PIWI-interacting small RNAs: the vanguard of genome defence. Nat Rev Mol Cell Biol 12: 246-258.
82. Khurana JS, Theurkauf W (2010) piRNAs, transposon silencing, and *Drosophila* germline development. J Cell Biol 191: 905-913.
83. Houwing S, Kamminga LM, Berezikov E, Cronembold D, Girard A, et al. (2007) A role for Piwi and piRNAs in germ cell maintenance and transposon silencing in Zebrafish. Cell 129: 69-82.

84. Salinas LS, Maldonado E, Navarro RE (2006) Stress-induced germ cell apoptosis by a p53 independent pathway in Caenorhabditis elegans. Cell Death Differ 13: 2129-2139.
85. Vos JC, De Baere I, Plasterk RH (1996) Transposase is the only nematode protein required for *in vitro* transposition of Tc1. Genes Dev 10: 755-761.
86. Craig NL (2002) Mobile DNA II. Washington, D.C.: ASM Press. xviii, 1204 p.
87. Lander ES, Linton LM, Birren B, Nusbaum C, Zody MC, et al. (2001) Initial sequencing and analysis of the human genome. Nature 409: 860-921.
88. Civáň P, Švec M, Hauptvogel P (2011) On the Coevolution of Transposable Elements and Plant Genomes. Journal of Botany 2011: 1-9.
89. Zagrobelny M, Jeffares DC, Arctander P (2004) Differences in non-LTR retrotransposons within *C. elegans* and *C. briggsae* genomes. Gene 330: 61-66.
90. Ganko EW, Bhattacharjee V, Schliekelman P, McDonald JF (2003) Evidence for the contribution of LTR retrotransposons to *C. elegans* gene evolution. Mol Biol Evol 20: 1925-1931.
91. Ganko EW, Fielman KT, McDonald JF (2001) Evolutionary history of *Cer* elements and their impact on the *C. elegans* genome. Genome Res 11: 2066-2074.
92. Moerman DG, Waterston RH (1984) Spontaneous unstable *unc-22* IV mutations in *C. elegans* var. Bergerac. Genetics 108: 859-877.
93. Eide D, Anderson P (1985) The gene structures of spontaneous mutations affecting a *Caenorhabditis elegans* myosin heavy chain gene. Genetics 109: 67-79.
94. Han JS (2010) Non-long terminal repeat (non-LTR) retrotransposons: mechanisms, recent developments, and unanswered questions. Mob DNA 1: 15.
95. Suzuki Y, Craigie R (2007) The road to chromatin - nuclear entry of retroviruses. Nat Rev Microbiol 5: 187-196.
96. Konig R, Zhou Y, Elleder D, Diamond TL, Bonamy GM, et al. (2008) Global analysis of host-pathogen interactions that regulate early-stage HIV-1 replication. Cell 135: 49-60.
97. Brass AL, Dykxhoorn DM, Benita Y, Yan N, Engelman A, et al. (2008) Identification of host proteins required for HIV infection through a functional genomic screen. Science 319: 921-926.
98. Strome S, Wood WB (1982) Immunofluorescence visualization of germ-line-specific cytoplasmic granules in embryos, larvae, and adults of *Caenorhabditis elegans*. Proc Natl Acad Sci U S A 79: 1558-1562.
99. Updike D, Strome S (2010) P granule assembly and function in *Caenorhabditis elegans* germ cells. J Androl 31: 53-60.
100. Updike DL, Hachey SJ, Kreher J, Strome S (2011) P granules extend the nuclear pore complex environment in the *C. elegans* germ line. J Cell Biol 192: 939-948.
101. Schisa JA, Pitt JN, Priess JR (2001) Analysis of RNA associated with P granules in germ cells of *C. elegans* adults. Development 128: 1287-1298.

102. Schedl T (1997) Developmental Genetics of the Germ Line. In: Riddle DL, Blumenthal T, Meyer BJ, Priess JR, editors. *C elegans* II. Cold Spring Harbor, NY: Cold Spring Harbor Laboratory Press. pp. 241-269
103. Zhou K, Rolls MM, Hall DH, Malone CJ, Hanna-Rose W (2009) A ZYG-12-dynein interaction at the nuclear envelope defines cytoskeletal architecture in the *C. elegans* gonad. J Cell Biol 186: 229-241.
104. Britten RJ (1995) Active *gypsy*/Ty3 retrotransposons or retroviruses in *Caenorhabditis elegans*. Proc Natl Acad Sci U S A 92: 599-601.
105. Palopoli MF, Rockman MV, TinMaung A, Ramsay C, Curwen S, et al. (2008) Molecular basis of the copulatory plug polymorphism in *Caenorhabditis elegans*. Nature 454: 1019-1022.
106. Arkhipova IR, Mazo AM, Cherkasova VA, Gorelova TV, Schuppe NG, et al. (1986) The steps of reverse transcription of *Drosophila* mobile dispersed genetic elements and U3-R-U5 structure of their LTRs. Cell 44: 555-563.
107. Chan PP, Lowe TM (2009) GtRNAdb: a database of transfer RNA genes detected in genomic sequence. Nucleic Acids Res 37: D93-97.
108. Chi W, Reinke V (2006) Promotion of oogenesis and embryogenesis in the *C. elegans* gonad by EFL-1/DPL-1 (E2F) does not require LIN-35 (pRB). Development 133: 3147-3157.
109. Hajdu-Cronin YM, Chen WJ, Sternberg PW (2004) The L-type cyclin CYL-1 and the heat-shock-factor HSF-1 are required for heat-shock-induced protein expression in *Caenorhabditis elegans*. Genetics 168: 1937-1949.
110. Simonetta SH, Romanowski A, Minniti AN, Inestrosa NC, Golombek DA (2008) Circadian stress tolerance in adult *Caenorhabditis elegans*. J Comp Physiol A Neuroethol Sens Neural Behav Physiol 194: 821-828.
111. Krause M, Hirsh D (1987) A *trans*-spliced leader sequence on actin mRNA in *C. elegans*. Cell 49: 753-761.
112. Riddle DL, Blumenthal T, Meyer BJ, Priess JR (1997) *C. elegans* II. Cold Spring Harbor, NY: Cold Spring Harbor Laboratory Press. 1222 p.
113. Page BD, Guedes S, Waring D, Priess JR (2001) The *C. elegans* E2F- and DP-related proteins are required for embryonic asymmetry and negatively regulate Ras/MAPK signaling. Mol Cell 7: 451-460.
114. Bembenek JN, Richie CT, Squirrell JM, Campbell JM, Eliceiri KW, et al. (2007) Cortical granule exocytosis in *C. elegans* is regulated by cell cycle components including separase. Development 134: 3837-3848.
115. O'Rourke SM, Dorfman MD, Carter JC, Bowerman B (2007) Dynein modifiers in *C. elegans*: light chains suppress conditional heavy chain mutants. PLoS Genet 3: e128.
116. Vogel BE, Hedgecock EM (2001) Hemicentin, a conserved extracellular member of the immunoglobulin superfamily, organizes epithelial and other cell attachments into oriented line-shaped junctions. Development 128: 883-894.
117. Harris JE, Govindan JA, Yamamoto I, Schwartz J, Kaverina I, et al. (2006) Major sperm protein signaling promotes oocyte microtubule reorganization prior to fertilization in *Caenorhabditis elegans*. Dev Biol 299: 105-121.
118. Saito K, Siomi MC (2010) Small RNA-mediated quiescence of transposable elements in animals. Dev Cell 19: 687-697.

119. Zheng DHJ, E.R; Running, S. (1993) A daily soil temperature model based on air temperature and precipitation for continental applications. Climate Res 2: 183-191.
120. Neville M, Stutz F, Lee L, Davis LI, Rosbash M (1997) The importin-beta family member Crm1p bridges the interaction between Rev and the nuclear pore complex during nuclear export. Curr Biol 7: 767-775.
121. Fornerod M, Ohno M, Yoshida M, Mattaj IW (1997) CRM1 is an export receptor for leucine-rich nuclear export signals. Cell 90: 1051-1060.
122. Polager S, Ginsberg D (2009) p53 and E2f: partners in life and death. Nat Rev Cancer 9: 738-748.
123. Wang T, Zeng J, Lowe CB, Sellers RG, Salama SR, et al. (2007) Species-specific endogenous retroviruses shape the transcriptional network of the human tumor suppressor protein p53. Proc Natl Acad Sci U S A 104: 18613-18618.
124. Crittenden SL, Leonhard KA, Byrd DT, Kimble J (2006) Cellular analyses of the mitotic region in the *Caenorhabditis elegans* adult germ line. Mol Biol Cell 17: 3051-3061.
125. Hird SN, White JG (1993) Cortical and cytoplasmic flow polarity in early embryonic cells of *Caenorhabditis elegans*. J Cell Biol 121: 1343-1355.
126. Beyer U, Moll-Rocek J, Moll UM, Dobbelstein M (2011) Endogenous retrovirus drives hitherto unknown proapoptotic p63 isoforms in the male germ line of humans and great apes. Proc Natl Acad Sci U S A 108: 3624-3629.
127. Verkman AS (2002) Solute and macromolecule diffusion in cellular aqueous compartments. Trends Biochem Sci 27: 27-33.
128. Leopold PL, Pfister KK (2006) Viral strategies for intracellular trafficking: motors and microtubules. Traffic 7: 516-523.
129. Dodding MP, Way M (2011) Coupling viruses to dynein and kinesin-1. EMBO J 30: 3527-3539.
130. Schulze E, Kirschner M (1987) Dynamic and stable populations of microtubules in cells. J Cell Biol 104: 277-288.
131. Ausubel FM, R. Brent, R.E. Kingston, D.D. Moore, J.G. Seidman, et al. (1987) Current Protocols in Molecular Biology. New York: Greene Publishing Associates/Wiley Interscience.
132. Kamath RS, Fraser AG, Dong Y, Poulin G, Durbin R, et al. (2003) Systematic functional analysis of the *Caenorhabditis elegans* genome using RNAi. Nature 421: 231-237.
133. Timmons L, Fire A (1998) Specific interference by ingested dsRNA. Nature 395: 854.
134. Kawasaki I, Shim YH, Kirchner J, Kaminker J, Wood WB, et al. (1998) PGL-1, a predicted RNA-binding component of germ granules, is essential for fertility in *C. elegans*. Cell 94: 635-645.
135. Dong C, Muriel JM, Ramirez S, Hutter H, Hedgecock EM, et al. (2006) Hemicentin assembly in the extracellular matrix is mediated by distinct structural modules. J Biol Chem 281: 23606-23610.
136. Wayner EA, Carter WG (1987) Identification of multiple cell adhesion receptors for collagen and fibronectin in human fibrosarcoma cells possessing unique alpha and common beta subunits. J Cell Biol 105: 1873-1884.

137. Brenner S (1974) The genetics of *Caenorhabditis elegans*. Genetics 77: 71-94.
138. Berod A, Hartman BK, Pujol JF (1981) Importance of fixation in immunohistochemistry: use of formaldehyde solutions at variable pH for the localization of tyrosine hydroxylase. J Histochem Cytochem 29: 844-850.
139. McCarter J, Bartlett B, Dang T, Schedl T (1999) On the control of oocyte meiotic maturation and ovulation in *Caenorhabditis elegans*. Dev Biol 205: 111-128.
140. Walker AK, Boag PR, Blackwell TK (2007) Transcription reactivation steps stimulated by oocyte maturation in *C. elegans*. Dev Biol 304: 382-393.
141. Greenstein D (2005) Control of oocyte meiotic maturation and fertilization. WormBook: 1-12.
142. Ewen KA, Koopman P (2010) Mouse germ cell development: from specification to sex determination. Mol Cell Endocrinol 323: 76-93.
143. Tonkin LA, Bass BL (2003) Mutations in RNAi rescue aberrant chemotaxis of ADAR mutants. Science 302: 1725.
144. Knight SW, Bass BL (2001) A role for the RNase III enzyme DCR-1 in RNA interference and germ line development in *Caenorhabditis elegans*. Science 293: 2269-2271.
145. Tijsterman M, Okihara KL, Thijssen K, Plasterk RH (2002) PPW-1, a PAZ/PIWI protein required for efficient germline RNAi, is defective in a natural isolate of *C. elegans*. Curr Biol 12: 1535-1540.
146. Wang G, Reinke V (2008) A *C. elegans* Piwi, PRG-1, regulates 21U-RNAs during spermatogenesis. Curr Biol 18: 861-867.
147. Orsborn AM, Li W, McEwen TJ, Mizuno T, Kuzmin E, et al. (2007) GLH-1, the *C. elegans* P granule protein, is controlled by the JNK KGB-1 and by the COP9 subunit CSN-5. Development 134: 3383-3392.
148. Tops BB, Plasterk RH, Ketting RF (2006) The *Caenorhabditis elegans* Argonautes ALG-1 and ALG-2: almost identical yet different. Cold Spring Harb Symp Quant Biol 71: 189-194.
149. Yigit E, Batista PJ, Bei Y, Pang KM, Chen CC, et al. (2006) Analysis of the *C. elegans* Argonaute family reveals that distinct Argonautes act sequentially during RNAi. Cell 127: 747-757.
150. Schwartz MS, Benci JL, Selote DS, Sharma AK, Chen AG, et al. (2010) Detoxification of multiple heavy metals by a half-molecule ABC transporter, HMT-1, and coelomocytes of *Caenorhabditis elegans*. PLoS One 5: e9564.
151. Vaux DL, Strasser A (1996) The molecular biology of apoptosis. Proc Natl Acad Sci U S A 93: 2239-2244.
152. Oldstone MB (1997) How viruses escape from cytotoxic T lymphocytes: molecular parameters and players. Virology 234: 179-185.
153. Mathias SL, Scott AF, Kazazian HH, Jr., Boeke JD, Gabriel A (1991) Reverse transcriptase encoded by a human transposable element. Science 254: 1808-1810.
154. Miska EA, Alvarez-Saavedra E, Abbott AL, Lau NC, Hellman AB, et al. (2007) Most *Caenorhabditis elegans* microRNAs are individually not essential for development or viability. PLoS Genet 3: e215.

155. Bukhari SI, Vasquez-Rifo A, Gagne D, Paquet ER, Zetka M, et al. (2012) The microRNA pathway controls germ cell proliferation and differentiation in *C. elegans*. Cell Res.

Curriculum Vitae
Shannon M. Dennis

Former Name: Shannon M. McGonagle

Education:

UNIVERSITY OF WASHINGTON AND FRED HUTCHINSON CANCER RESEARCH CENTER, Seattle, WA
Doctor of Philosophy in Molecular and Cellular Biology
Advisor: James R. Priess
June 2012

LEWIS AND CLARK COLLEGE, Portland, OR
Bachelor of Arts in Biology,
cum laude, GPA 3.74
May 2004

Research Experience:

-Graduate Research Assistant (04/2007-06/2012).
Advisor: Dr. James Priess, Fred Hutchinson Cancer Research Center.
Research Project: "Repetitive DNA Silencing and Germline Defense Against Retrotransposons in *C. elegans.*"

-Graduate Research Rotation (1/2007-3/2007).
Advisor: Dr. David Parichy, University of Washington.
Research Project: "Gene expression studies in zebrafish pigmentation development mutants."

-Graduate Research Rotation (9/2006-12/2006).
Advisor: Dr. Cecilia Moens, Fred Hutchinson Cancer Research Center.
Research Projects: "Characterization of a hox transformation mutant and a non-canonical Wnt ligand in zebrafish."

-Research Technician I, (6/2004-8/2006).
Research Project: Targeted gene knockouts in *C. elegans*, with a focus on microRNAs.
Dr. Robert Horvitz, MIT/HHMI.

-Undergraduate research (12/2003-5/2004)
Advisor: Dr. Greg Hermann, Lewis and Clark College.
Research Project: "Investigating apoptosis in *C. elegans*"

-Undergraduate research (9/2003-12/2003)

Advisors: Dr. Ken Clifton and Dr. Greg Hermann, Lewis and Clark College.
Research Project: "Seaweed zygote development"

-Rogers Summer Research Program (5/2002-7/2003)
Advisor: Dr. Kellar Autumn, Lewis and Clark College.
Research Project: "Rough surface adhesion of gecko setal arrays."

Teaching Experience:

-Graduate Teaching Assistant, (4/2008-6/2008).
Biology 355, Foundations in Molecular Cell Biology,
Course Instructor: Dr. Alison Crowe, University of Washington.

-Graduate Teaching Assistant, (1/2008-3/2008).
Genome 371, Introductory Genetics,
Course Instructors: Dr. Carol Sibley and Dr. James Thomas, University of Washington.

Leadership Experience:

-Co-chair, Student/Postdoc Advisory Committee, 2011-2012
-Member, Student/Postdoc Advisory Committee, 2009-2011
-Molecular and Cellular Biology Symposium Planning Committee, 2009
-Molecular and Cellular Biology Program Recruitment Coordinator, 2007

Honors/Awards/Grants:

-Predoctoral Trainee, National Institutes of Health, Developmental Biology Training Grant, University of Washington, 2009-2012
-ARCS (Achievement Rewards for College Scientists) Foundation and Washington Research Foundation Fellow, 2006-2009
-National Science Foundation Graduate Research Fellowship, honorable mention, 2008
-National Science Foundation Graduate Research Fellowship, honorable mention, 2007
-Biology Prize, Lewis and Clark College, 2004
-Phi Beta Kappa, Lewis and Clark College, 2004
-Barry M. Goldwater Scholarship nominee, Lewis and Clark College, 2003
-Dean's scholarship, Lewis and Clark College, 2000-2004
-Templeton National Merit Scholarship, Lewis and Clark College, 2000-2004
-National Merit Scholar, 2000

Meetings:

-June 2011, **Shannon M. Dennis**, Ujwal Sheth, Jessica L. Feldman, Jeff N. Molk, James R. Priess. "*C. elegans* Germline Defense Against Retroelements." 18th International *C. elegans* Meeting, Los Angeles, CA. Platform Presentation.

-March 2011, **Shannon M. Dennis**, Ujwal Sheth, James R. Priess. "*C. elegans* Germline Defense Against Retroelements." Society for Developmental Biology Northwest Meeting. Poster Presentation*.

-June 2009, **Shannon M .Dennis** and James R Priess. "Analysis of Viruslike Particles in the *C. elegans* Germline." 17th International *C. elegans* Meeting, Los Angeles, CA. Poster Presentation*.

*Awarded best graduate student poster of section or night.

Publications:

-**Dennis S.**, U. Sheth, J.L. Feldman, K.A. English, and J.R. Priess, *C. elegans germ cells show temperature and age-dependent expression of Cer1, a Gypsy/Ty3-related retrotransposon*. PLoS Pathog, 2012. **8**(3): e1002591. doi:10.1371/journal.ppat.1002591

-Sheth U., J. Pitt, **S.M. Dennis**, and J.R. Priess, *P granules are principal sites of mRNA export in the adult C. elegans germline.* Development, 2010. **137**(8): p. 1305-14. PMCID: PMC2847466

-Miska, E.A., E. Alvarez-Saavedra, A.L. Abbott, N.C. Lau, A.B. Hellman**, S.M. McGonagle**, D.P. Bartel, V.R. Ambros, and H.R. Horvitz, *Most Caenorhabditis elegans microRNAs are individually not essential for development or viability.* PLoS Genet, 2007. **3**(12): p. e215. PMCID: PMC2134938

Membership in Professional Societies:

-Society for Developmental Biology
-Genetics Society of America
-National Postdoc Association